

MASS TRANSFER WITH CHEMICAL
REACTION FROM SINGLE SPHERES

MASS TRANSFER WITH CHEMICAL
REACTION FROM SINGLE SPHERES

by

WILLIAM T. HOUGHTON

A Thesis

Submitted to the Faculty of Graduate Studies
in Partial Fulfilment of the Requirements
for the Degree
Doctor of Philosophy

McMaster University

October, 1966

DOCTOR OF PHILOSOPHY (1966)
(Chemical Engineering)

McMaster University
Hamilton, Ontario.

TITLE : Mass Transfer with Chemical Reaction
From Single Spheres

AUTHOR : William T. Houghton B.Eng. (McGill)
M.Ch.E. (Delaware)

SUPERVISORS : Professors A.I. Johnson and A.E. Hamielec

NUMBER OF PAGES : xvi, 192

SCOPE AND CONTENTS:

Forced convection mass transfer rates from single gas bubbles, with accompanying chemical reaction, were determined experimentally in the intermediate Reynolds number range. The reacting system carbon dioxide-monoethanolamine was chosen for this study.

A mathematical model, describing forced convection mass transfer from a single sphere with accompanying first or second order reaction, was developed and solved using finite-difference techniques. Hydrodynamic conditions in the intermediate Reynolds number region were described using Kawaguti-type velocity profiles.

The numerical solutions of the model have been compared with the experimental results of this study as well as with previous theoretical and experimental results.

ACKNOWLEDGEMENTS

The author is grateful to Dr. A.I. Johnson and Dr. A.E. Hamielec for their guidance and encouragement throughout this study.

The author is indebted to Dr. D.J. Kenworthy for his advice on various aspects of the numerical procedures employed.

The assistance of M.W. Wilson in obtaining experimental data is greatly appreciated.

Financial assistance was obtained through the Dow Chemical Company of Canada Limited and the National Research Council

TABLE OF CONTENTS

	PAGE
1. INTRODUCTION	1
1.1 General	1
1.2 Flow Around Spheres	2
1.3 Experimental Studies of Heat and Mass Transfer from Spheres	5
1.3.1 Mass Transfer	5
1.3.2 Heat Transfer	9
1.4 Experimental Studies of Mass Transfer with Chemical Reaction	10
1.5 Solution of Penetration Theory Equations	13
1.6 Theoretical Studies of Mass Transfer from Single Spheres	15
1.6.1 Low Reynolds Number Region ($Re < 1$)	15
1.6.2 Intermediate Reynolds Number Region ($1 < Re < 200$)	17
1.6.3 High Reynolds Number Region ($Re > 200$)	19
1.7 Mass Transfer in Disperse Systems	20
1.8 Effect of Surfactants and Interfacial Turbulence on Mass Transfer	22
 2. SCOPE	 24
 3. THEORETICAL TREATMENT	 27
3.1 Formulation of Model	27
3.1.1 First Order Chemical Reaction	28
3.1.2 Second Order Chemical Reaction	31
3.1.3 Velocity Profiles	32
3.2 Solution of Mathematical Model	35
3.2.1 First Order Chemical Reaction	39
3.2.2 Second Order Chemical Reaction	47
3.3 Results and Discussion	54
3.3.1 Convergence Tests and Asymptotic Solutions	55
3.3.2 Transfer from Circulating Gas Bubbles and Penetration Theory	61
3.3.3 Transfer from Rigid Spheres	67
3.3.4 Conclusions	74
 4. EXPERIMENTAL	 77
4.1 Introduction	77
4.2 System and Reaction Mechanism	78
4.3 Apparatus	79
4.4 Operating Procedure	81

	PAGE
5. RESULTS AND DISCUSSION	86
5.1 Absorption Rates from Single Gas Bubbles	86
5.2 Calculation Procedure	90
5.3 Results	92
5.4 Auxiliary Studies	101
5.5 Comparison of Theoretical and Experimental Results	102
5.5.1 Preliminary Comparisons	102
5.5.2 Convergence Tests	106
5.5.3 Effect of Diffusivity and Reaction Rate	108
5.5.4 General Conclusions	109
6. CONCLUSIONS AND RECOMMENDATIONS	115
6.1 Conclusions	115
6.2 Recommendations	115
APPENDICES	117
A. Solution of Elliptic Equation for First Order Reaction	118
B. Finite-Difference Approximations	120
C. Diffusion from a Sphere with Second Order Reaction	122
D. Polynomial Representation of Boundary Condition $\partial C_B / \partial r = 0$ at $r = 1$	125
E. Physical Data	126
F. Measurement of Bubble Surface Area	132
G. Measurement of Gas Leakage	137
H. Sample Calculation	142
I. Auxiliary Experimental Studies	144
J. Solution of Navier-Stokes Equation	154
K. Program Listings and Procedure Outlines	160
(i) Diffusion from a Sphere into a Stagnant Fluid with Second Order Reaction	160

	PAGE
(ii) Mass Transfer from a Circulating or Non-circulating Sphere with First Order Chemical Reaction	164
(iii) Mass Transfer from a Circulating or Non-circulating Sphere with Second Order Chemical Reaction	171
L. Experimental Data and Correlations	181
BIBLIOGRAPHY	185

LIST OF TABLES

TABLE		PAGE
1.1	Summary of Experimental Correlations	7
3.1	Comparison of Numerical Solutions with Analytical Solutions for a Stagnant Fluid-Transfer from Solid Spheres.	57
3.2	Convergence Tests - Transfer from a Solid Sphere with First Order Reaction	58
3.3	Convergence Tests - Transfer from Circulating Bubbles and Solid Spheres with Second Order Reaction	59
3.4	Comparison of Finite-Difference and Boussinesq Solutions	62
3.5	Mass Transfer from Circulating Gas Bubbles - First Order Reaction	65
3.6	Mass Transfer from Circulating Gas Bubbles - Second Order Reaction	66
3.7	Mass Transfer from Frontal Stagnation Point	75
5.1	Physical Properties at 25.0°C	93
5.2	Experimental Results - Absorption from Carbon Dioxide Bubbles into Monoethanolamine Solutions	94
5.3	Theoretical Results - Mass Transfer from a Non-Circulating Gas Bubble with Second Order Reaction	104
5.4	Convergence Tests - Transfer from a Solid Sphere with Second Order Reaction	107
5.5	Effect of Monoethanolamine Diffusivity on Calculated Sherwood Numbers	110
5.6	Effect of Reaction Rate Constant on Calculated Sherwood Numbers	111
F.1	Measurements from Bubble Photographs	135
G.1	Measurement of Carbon Dioxide Leakage Rate	139
I.1	Absorption Rate Results - Cylindrically Shaped Bubble Support	146

TABLE		PAGE
I.2	Effect of Dissolved Metals on Rate of Absorption of Carbon Dioxide into Monoethanolamine Solutions	151
I.3	Effect of Contact Time Between Monoethanolamine and Water-Tunnel Materials - Absorption of Carbon Dioxide	152
L.1	Experimental Data - Absorption of Carbon Dioxide into Monoethanolamine Solutions	182
L.2	Experimental Correlations	184

LIST OF FIGURES

FIGURE		PAGE
1	Spherical Volume Element	29
2	Boundary Conditions for Mass Transfer with Second Order Reaction	33
3a	Streamlines around a Circulating Sphere	36
3b	Streamlines around a Rigid Sphere	36
4	Finite-Difference Mesh System	38
5	Effect of Zero-Slope Criterion at $\theta=0^\circ$ on Calculated Sherwood Numbers	45
6a	Concentration Profile - First Order Reaction	60
6b	Concentration Profiles- Second Order Reaction	60
7	Comparison of This Work with Penetration Theory	64
8	Comparison of Finite-Difference Results with Analytical Solution of Baird and Hamielec	68
9	Comparison of Numerical Solutions with Experimental Correlations - Transfer to Liquids	71
10	Comparison of Numerical Solutions with Experimental Correlations - Transfer to Air	72
11	Schematic of Water-Tunnel Apparatus	80
12	Details of Gas Feeding Apparatus	82
13	Details of Gas Syringe	83
14	Bubble Holder Details	84
15	Single Gas Bubble Results - Absorption Rate vs. Time	87
16	Experimental Results	96
17	Comparison Between Theoretical and Experimental Results	105

FIGURE	PAGE
18 Concentration Profiles for Conditions Approaching Infinitely Fast Second Order Reaction	112
19 Viscosity of Monoethanolamine Solutions	127
20 Rotameter Calibration Curves	128
21 Index of Refraction of Monoethanolamine Solutions	129
22 Photographs of Gas Bubble	133
23 Distance Measured on Bubble Photographs	134
24 Equipment Arrangement - Determination of Leakage Rate from Gas Syringe	138
25 Leakage Rates - Applied to Experiments with Cylindrical Bubble Support	141
26 Schematic of Tapered and Cylindrical Bubble Supports	145
27 Vertically Elongated Gas Bubble	148
28 Glass Water-Tunnel Used for Preliminary Experiments	150
29 Finite-Difference Mesh System - Solution of Navier-Stokes Equation	155

NOMENCLATURE

a	bubble dimension (Appendix F)
$a_1, a_2, a_3,$ a_4, a_5, a_6	coefficients in finite-difference equation (Appendix A)
A	lattice spacing in z-direction (Appendix J)
A_b	surface area of bubble, cm^2
A_1, A_2, A_3, A_4	velocity profile coefficients (Equations 3.6, 3.7)
$A_{i,j}$	concentration of material A at mesh point location (i,j), dimensionless
b	bubble dimension (Appendix F)
b_1, b_2, b_3, b_4	coefficients in finite-difference equation (Appendix A)
B	lattice spacing in θ -direction (Appendix J)
B_1, B_2, B_3, B_4	velocity profile coefficients (Equations 3.6, 3.7)
$B_{i,j}$	concentration of material B at mesh point location (i,j), dimensionless
c	bubble dimension (Appendix F)
c	concentration of diffusing material (Equation 1.1), moles/liter
c^s	concentration at gas-liquid interface (Equation 1.1), moles/liter

c_A	concentration of material being transferred from sphere, dimensionless or moles/liter
c_A^s	concentration of material A at interface, moles/liter
c_B	concentration of reactant in liquid phase, dimensionless
c_B^o	concentration of reactant in bulk of liquid phase, moles/liter
$c_{i,j}$	concentration at mesh point location (i,j)
c_∞	concentration of diffusing material at some distance from gas-liquid interface, moles/liter
d	equivalent diameter of gas bubble, cm
D_A	diffusivity of material A in liquid phase, cm^2/sec .
D_B	diffusivity of material B in liquid phase, cm^2/sec .
D_{CO_2}	diffusivity of carbon dioxide in water, cm^2/sec .
E^2	differential operator (Appendix J)
F	quantity in finite-difference equation (Appendix J)
g	acceleration due to gravity
G	quantity in finite-difference equation (Appendix J)
Gr	$\rho g d^3 \Delta \rho / \mu^2$, Grashof number

h	constant greater than unity (Equation 3.16)
k	$k_1 R^2 / D_A$, dimensionless rate constant for first order reaction
k_A	$k_2 R^2 c_B^0 / D_A$, dimensionless rate constant for second order reaction
k_B	$k_2 R^2 c_A^S / D_B$, dimensionless rate constant for second order reaction
k_L	liquid phase mass transfer coefficient, cm/sec.
k_1	rate constant for first order reaction, sec. ⁻¹
k_2	rate constant for second order reaction, liter/mole-sec.
$l_1, l_2, l_3,$ l_4, l_5, l_6	coefficients in finite-difference equation (Equation 3.23)
\sqrt{M}	$2\sqrt{k} / \overline{Sh}^*$ for first order reaction, $2\sqrt{k_A} / \overline{Sh}^*$ for second order reaction
N_{CO_2}	absorption rate of carbon dioxide, gm.-moles/sec.
Nu	Nusselt number
Pe_A	$2RU / D_A$, Peclet number, material A
Pe_B	$2RU / D_B$, Peclet number, material B
Pr	Prandtl number

r	radial distance, dimensionless or cm.
R	radius of sphere, cm.
Re	$2RU\rho/\mu$, Reynolds number
Sc, Sc_A	$\mu/\rho D_A$, Schmidt number of material being transferred from the sphere
Sc_B	$\mu/\rho D_B$, Schmidt number of liquid phase reactant
Sh	$2Rk_L/D_A$, Sherwood number, local or average value
\overline{Sh}	Sherwood number for chemical reaction, averaged over sphere surface
\overline{Sh}^*	Sherwood number for physical mass transfer, averaged over sphere surface
t	time (Equation 1.1)
U	main stream or centerline velocity, cm/sec.
V_r	radial velocity component, dimensionless or cm/sec.
V_θ	angular velocity component, dimensionless or cm/sec.
W, WW	relaxation factors (Appendix J)

x	penetration depth (Equation 1.1)
X	viscosity ratio, disperse to continuous phase
\bar{x}_1, \bar{x}_2	mean values (Appendix I)
y	dummy integration variable (Appendix F)
Z	radial distance variable (Appendix J)
$\Delta\theta$	angular increment, radians
Δr_0	size of first radial step, dimensionless
ζ	vorticity (Appendix J)
θ	angle, radians
μ	viscosity, poise
ν	μ/ρ , kinematic viscosity
Π	3.1416 radians
ρ	density, gm./cc
ϕ	$\overline{Sh}/\overline{Sh}^*$, enhancement factor
ϕ_a	limiting enhancement factor (Equation 3.46)
$\phi(c)$	source term (Equation 1.1)

Ψ stream function (Appendix J)

ω relaxation factor (Appendix A)

INTRODUCTION

1.1 General

Operations involving mass transfer from gas bubbles, liquid drops or solid spheres have been of considerable interest for some time. Of particular importance industrially are processes which involve a chemical reaction between an absorbed gas and a reactant in the liquid phase. Such industrial applications include chlorinations, oxidations and removal of products such as hydrogen-sulphide and carbon-dioxide from gas streams. This work was initiated by an examination of the chlorohydrin process for the manufacture of ethylene glycol. This process involves the reaction of ethylene bubbles in aqueous chlorine solutions (A2). Of particular interest was the investigation of the effect on the gas absorption rate of a chemical reaction between the absorbed gas and a liquid phase reactant. Since the concentration of the gas molecules in the liquid will be decreased due to the reaction, it would be expected that the concentration gradients near the bubble surface would be increased. This results in increased mass transfer rates ("enhancement" effect) over the rate which would be expected for physical mass transfer. The hydrodynamic effect was also of interest since an increase in liquid flow rate should enable the removal of absorbed gas from near the surface more quickly and cause an additional increase in absorption rates.

Previous work in this area of mass or heat transfer from spheres has been confined to studies of physical transfer alone.

Investigations which have involved reacting systems have been confined to geometries other than the spherical, mainly in order to prevent the accompanying theoretical analyses from becoming too complex.

The study of transfer, where the resistance in the dispersed phase is significant, *into* single spheres involves fundamental differences in both the theoretical and experimental approach to the problem. No attempt will be made to review the literature in this area. For surveys of this field the interested reader is referred to publications by Harriot (H6) and Wellek (W3).

1.2 Flow Around Spheres

Any theoretical study of forced convection transfer from spheres would be simplified appreciably if accurate descriptions of the flow field were available from previous studies.

The Stokes (S9) velocity profiles provide a description of the hydrodynamics for flow around solid spheres at $Re < 1$. The Hadamard-Rybczynski (H1, R8) velocity profiles apply for flow around fluid spheres which may have internal circulation due to the transmission of viscous forces across the interface. These also apply only for $Re < 1$. The "potential flow" solutions of the Navier-Stokes equation, obtained after assuming irrotational fluid behaviour, provide a reasonable description of the flow around circulating gas bubbles at high Reynolds numbers, say $Re \geq 200$. This solution is an exact one of the complete Navier-Stokes equation. Fortunately it satisfies the boundary conditions which closely approximate those for a fully circulating sphere.

The solution of the Navier-Stokes equation by analytical techniques for other flow situations is not possible at present, due to the extreme non-linearity of the equation. Approximate solutions, using the "boundary layer" approach, have been obtained by several workers. This technique involves an order of magnitude analysis on the momentum and continuity equations, assuming that inertial and viscous effects are concentrated within a thin boundary layer near the surface. An example of this approach, as applied to flow around solid spheres, is contained in the work of Frossling (F5). Unfortunately any boundary layer technique does not allow for the description of the flow beyond the point at which flow separation occurs. The vortex region which forms beyond the "separation point" begins to appear near Reynolds number of 20 (T1).

Alternative methods involving error-distribution techniques such as the Galerkin method (C7) have been used to obtain approximate solutions to the Navier-Stokes equation. The method involves the assumption of trial stream functions. These are made to satisfy approximately the Navier-Stokes equation using an orthogonality principle and to satisfy the boundary conditions exactly. Initial work in this area was carried out by Kawaguti (K1) for solid spheres. This was extended by Hamielec and co-workers (H2, H3) to higher Reynolds numbers and flow around circulating drops and bubbles as well as solid spheres. Solutions of this nature are available in convenient polynomial form. They are a significant improvement on boundary layer solutions in that they allow for a complete description of the flow field, including

the vortex region. Solutions have been obtained covering a wide range of Reynolds numbers. However, in the solid sphere case these are applicable only up to Reynolds numbers of about 500, since the wake becomes unstable (T1) at higher values.

Recently more accurate solutions of the Navier-Stokes equation have been obtained using numerical techniques. Jenson (J2), employing a "relaxation" method, has obtained solutions for flow around solid spheres for Reynolds numbers up to 40. This work has been extended by Hamielec and co-workers (H4, H5) to higher Reynolds numbers and includes flow around circulating gas bubbles as well as solid spheres. An outline of this work is given in Appendix J. The study by Hamielec has included an investigation of the effect on the velocity profiles of a non-zero surface flux (H5). These finite-difference solutions indicate the Kawaguti-type velocity profiles are accurate up to the separation point, but are less satisfactory in the vortex region, especially at $Re > 200$.

Since velocity profiles are available which adequately describe the flow field at $Re < 500$, it would seem reasonable to confine any theoretical study of transfer from spheres to this region, at least initially. A study at higher Reynolds numbers would necessarily consider the transient behaviour of the wake and the effect of main stream turbulence. In this study the complex problem of turbulence effects will not be considered theoretically. Any experimental study will be carried out under laminar conditions. A review of turbulence effects has been given by Torobin and Gauvin (T1).

1.3 Experimental Studies of Heat and Mass Transfer from Spheres.

Heat or mass transfer from single spheres has been the subject of many investigations. Recent publications by Rowe et al (R4) and by Ross (R3) contain detailed reviews of previous studies. Some of the more important ones which contain a substantial portion of their results in the region $Re < 1000$ will be discussed here. Correlations obtained by the various workers are listed in Table 1.1.

1.3.1 Mass Transfer

One of the earliest mass transfer studies was carried out by Frossling (F4) who investigated transfer rates from spheres of naphthalene, aniline, water and nitrobenzene into an air stream. The work has been criticized (R4) because diffusivities were not measured but were calculated from the observed mass transfer rates at zero air velocity. Use was then made of the theoretical relationship that the Sherwood number is 2 under these conditions. Ross (R3), however, states that, for the sphere sizes used in Frossling's study, natural convection effects should have been negligible. Thus the use of the theoretical relationship was justified.

Aksel'rud (A3) measured transfer rates from spheres of sodium chloride and potassium nitrate into water over the range $200 < Re < 4000$.

Garner and co-workers (G4, G5, G6) as well as Linton and Sutherland (L7) have investigated forced convection transfer from benzoic acid spheres into water. There is a considerable discrepancy in the results reported by the two groups. In general it may be said that the results of Garner and co-workers are higher than the majority

of other workers in this field (see Table 1.1). Linton and Sutherland (L7) have noted that the screens used to obtain a uniform velocity profile in (G4) and (G5) were placed too close to the test sphere. They suggest that gross turbulence may have resulted causing abnormally high mass transfer rates. In the study by Garner and Key (G6), a parabolic velocity profile was used. The results were correlated using the average rather than the centerline velocity. As stated by Key and Glen (K2), "It is thus tempting to suggest a factor of maximum value $\sqrt{2}$ arises between these workers and those who... set out to maintain a parabolic velocity distribution". If the experimental set-up were such that the sphere diameter was only a small percentage of the pipe diameter (it was <15% of the pipe diameter in (G6)) then the centerline velocity, rather than the average velocity, of the parabolic velocity profile would be a more realistic quantity to use for correlation purposes. In fact, if the centerline velocity had been used the results of Garner and Key (G6) would be in reasonable agreement with the results of Linton and Sutherland (L7). Incidentally, in the latter study a flat velocity profile was obtained in the test sphere region using a specially designed inlet section. Thus there was no question regarding the choice of velocity to be employed for correlation purposes.

Studies of mass transfer from stationary and falling liquid drops at $Re < 20$ have been carried out by Ward et al (W1). Appreciable natural convection effects were noted as might be expected in this low Reynolds number region. Griffith (G9) carried out a study of

TABLE 1.1 SUMMARY OF EXPERIMENTAL CORRELATIONS

Author	ref.	System	Reynolds Number	Sphere Diameter (cm.)	Correlation
Frossling	F4	naphthalene, aniline, water	2 - 1300	0.01 - 0.20	$Sh = 2 + 0.552 Re^{1/2} Sc^{1/3}$
Aksel'rud	A3	sodium chloride, potassium nitrate into water	200 - 4000		$Sh = 0.82 Re^{1/2} Sc^{1/3}$
Garner and co-workers	G4 G5 G6	benzoic acid into water	20 - 1000	1.3 - 1.9	$Sh = 0.94 Re^{1/2} Sc^{1/3}$
Linton and Sutherland	L7	benzoic acid into water	500 - 8000	1.0	$Sh = 2 + 0.65 Re^{1/2} Sc^{1/3}$
Steinberger and Treybal	S7	benzoic acid into water	27 - 16,900	1.3 - 2.5	$Sh = 2 + 1.00 Re^{1/2} Sc^{1/3}$
Rowe et al	R4	benzoic acid into water	226 - 1150	1.3 - 3.8	$Sh = 2 + 0.73 Re^{1/2} Sc^{1/3}$
		naphthalene into air	96 - 1050	1.6 - 3.8	$Sh = 2 + 0.68 Re^{1/2} Sc^{1/3}$
Griffith	G9	organic liquid drops into water; gas bubbles into water			$Sh = 2 + 0.63 Re^{1/2} Sc^{1/3}$
Ranz and Marshall	R1	water and benzene into air	2 - 200	0.1	$Sh = 2 + 0.60 Re^{1/2} Sc^{1/3}$
Kramers	K3	heat to air, water, oil	0.4 - 2000	0.7 - 1.3	$Nu = 2 + 1.3 Pr^{0.15} + 0.66 Re^{1/2} Sc^{1/3}$
Yuge	Y3	heat to air	10 - 1800	0.1 - 6.0	$Nu = 2 + 0.49 Re^{1/2} Pr^{1/3}$
Tsubouchi & Masuda	T3	heat to air, oil	1 - 2400	0.06 - 0.24	$Nu = 2 + 0.57 Re^{1/2} Pr^{1/3}$
Rowe et al	R4	heat to water	40 - 1000	1.3 - 3.8	$Nu = 2 + 0.79 Re^{1/2} Pr^{1/3}$
		heat to air	65 - 1750	1.3 - 3.8	$Nu = 2 + 0.69 Re^{1/2} Pr^{1/3}$

transfer from drops of ethyl acetate, iso-butanol and cyclohexanol, as well as from gas bubbles, including oxygen, nitrogen, and carbon dioxide, into water at $Re < 150$. The effect of the presence of surfactants on the mass transfer rate was also included in Griffith's work. As sufficient surfactant was usually added to prevent internal circulation, the liquid drop or gas bubble then behaved as a rigid sphere.

The work of Steinberger and Treybal (S7) has been criticized (R3) since their study was undoubtedly influenced by a "blockage effect" due to sphere-to-tube diameter ratio being as high as 0.5. Richardson, among others, has noted (V2) that a large blockage causes an increase in mass transfer in the region beyond the separation point. The choice of suitable correlation velocities, under high blockage conditions, is also rendered more difficult (G6).

A recent study by Rowe et al (R4) has included results for mass transfer from benzoic acid spheres into water, and from naphthalene spheres into air over the range $30 < Re < 1750$. At the same time an analogous heat transfer study was carried out using both water and air streams. Their results are slightly higher than those of other workers. Ross (R3) has suggested that, at least for the results in air, turbulence may have been a factor since wind tunnel Reynolds numbers used were as high as 13,000. This does not offer a complete explanation for the results of Rowe et al as their values for transfer to water, obtained under laminar conditions, were also high.

1.3.2. Heat Transfer

Extensive reviews of the available literature on heat transfer from spheres have been written by Rowe et al (R4) and by Ross (R3). These reviewers have noted that the accuracy of experimental correlations is not sufficient to draw definite conclusions regarding the analogy of heat and mass transfer, but that the results "tend" to confirm the analogy.

The work of Kramers (K3) considers heat transfer from metal spheres to air, water and oil. His results have been questioned (R4) because of the large blockage effect, the tube diameter being only 2.7 times the sphere diameter. Further, an additional term was required in his correlation (see Table 1.1) in order to bring all the data for oil, water, and air into line. Rowe et al (R4) have suggested that the results may have been affected by the method of heating the sphere. An induction technique was used which may have caused disturbances in the oil flow field. In addition, these workers noted that natural convection effects may have been appreciable for part of the study as the properties of the oil employed were very temperature dependent.

Experiments concerned with heat transfer from spheres into air streams have been carried out by Yuge and co-workers (Y3) and Tsubouchi and Masuda (T3). In the latter study thermistor beads were used as the test spheres and both air and oils of various viscosities were used as the transfer medium. In the opinion of the author the correlations of these workers are among the most reliable in the

literature.

The study of Ranz and Marshall (R1), dealing with the evaporation of liquid drops into air, involved both heat and mass transfer. The investigation was carried out over the range $2 < Re < 200$. This work is generally considered as one of the more reliable correlations. It has, however, been criticized recently by Ross on the grounds that turbulence may not have been negligible, and internal droplet circulation may have been induced by the droplet feeding method.

Evaporation of water droplets into a steam medium was the subject of a recent study by Ross (R3). The droplet was subjected to a high radiant heat load and the main object of the work was the investigation of the surface flux - forced convection interaction.

1.4 Experimental Studies of Mass Transfer with Chemical Reaction

Up to the present time apparently no experimental studies of mass transfer with chemical reaction from single spheres have been reported. Investigations which have been concerned with reacting systems have generally been confined to the simple geometries found in laminar liquid jets, falling films, films formed on a rotating cylinder, and plane interfaces.

The advantages offered by apparatus such as those mentioned above are that the gas-liquid contact time can be obtained with good accuracy, and that the mass transfer area can be easily determined. The experimental results are usually interpreted in terms of the

"penetration theory". The essential assumption of this theory is that the diffusion time of the absorbed material is short enough to prevent the material from reaching the other boundary of the fluid. The absorption process can then be described in terms of the equations for unsteady diffusion, with or without chemical reaction, into a semi-infinite medium. These equations can be handled readily and some of the available solutions will be discussed later.

Nijsing et al (N1) carried out studies on the absorption of carbon dioxide into laminar jets and laminar falling films of aqueous solutions of sodium, potassium and lithium hydroxides. Conditions were varied so the absorption could be carried out accompanied by either pseudo first order or second order reaction.

Danckwerts and co-workers (D3, R2, S2) have carried out a series of studies on the absorption of carbon dioxide into alkaline solution with a variety of interfacial geometries. Danckwerts and Kennedy (D3) utilized a rotating drum on which a thin film of the absorbing medium could be formed continuously. The contact time between the gas and the liquid was controlled by varying the speed of rotation. They studied absorption into sodium hydroxide solutions and buffer solutions of sodium carbonate-sodium bicarbonate. The buffer solution results could be interpreted by a first order reaction mechanism. The reaction between the carbon dioxide and caustic solutions was found to be second order for the gas-liquid contact times employed. Roberts and Danckwerts (R2) utilized a wetted wall column to study absorption of carbon dioxide into the same solutions as in (D3) but

also included a study of the effect of arsenite catalyst on the reaction rate. Sharma and Danckwerts (S2) expanded the catalyst study by evaluating the effect of formaldehyde and hypochlorite as well as arsenite, this time with a laminar jet apparatus. They also studied absorption of carbon dioxide into monoisopropanolamine solutions and found that these results could be interpreted according to second order kinetics.

The carbon dioxide - monoethanolamine system has been the subject of many investigations, notably those by Emmert and Pigford (E1), Astarita (A5, A6) and Clarke (C6). The work of Emmert and Pigford utilized a laminar liquid jet apparatus. Contact times were of sufficient duration to allow the interpretation of the data in terms of penetration theory for a very fast second order reaction. Clarke, on the other hand, used very short contact times (also with a laminar jet apparatus) and could show that under these conditions the reaction was pseudo first order. When the shorter contact times are utilized there is no depletion of monoethanolamine in the liquid phase near the gas liquid interface. Whereas, for the longer contact times, depletion does take place. Astarita has conducted investigations with many different types of apparatus including laminar jets, packed beds, and wetted wall columns. In the laminar jet study (A5) the data were found to be between those predicted from penetration theory for first order and infinitely fast second order reaction kinetics. The main objective of the second study (A6) was to investigate the effect on absorption rates of the monoethanolamine concentration level and of the "carbonation ratio"

(moles of CO_2 /moles of MEA in liquid). It was possible to confirm from the experimental results that the reaction was pseudo first order if the carbonation ratio was >0.5 and second order if the ratio was <0.5 .

Many studies of mass transfer with chemical reaction in stirred vessels have been reported (A2, M1, P1, V1). These have been concerned with a variety of reacting systems. Both film and penetration theories have been employed to interpret the experimental results.

1.5 Solution of Penetration Theory Equations

The absorption of a material at a plane interface and its unsteady diffusion into a semi-infinite medium can be described by

$$\frac{\partial c}{\partial t} = D \frac{\partial^2 c}{\partial x^2} - \phi(c) \quad (1.1)$$

with initial and boundary conditions of

$$t = 0, \quad c = 0 \quad \text{at} \quad x > 0$$

$$t > 0, \quad c = c^s \quad \text{at} \quad x = 0$$

$$t \geq 0, \quad c \rightarrow 0 \quad \text{as} \quad x \rightarrow \infty$$

These conditions describe the situation where equilibrium exists at the interface, where there is no absorbed material in the fluid medium initially and where the concentration decreases to zero as x , the distance from the interface, increases. The $\phi(c)$ would be $k_1 c$ for first order reaction and zero for simple diffusion with no reaction. Similar equations may be written for the case of diffusion with second order reaction or for a bi-molecular reaction of general order.

An analytic solution for the first order reaction situation (equation 1.1 with $\phi(c) = k_1 c$) was first obtained by Danckwerts (D1)

and has been used extensively in the interpretation of experimental data. For the case of an infinitely fast second order reaction, solutions have been obtained by Danckwerts (D2) and by Sherwood and Pigford (S3).

Initial studies on the solution of the equations describing a second order reaction for any reaction rate level were carried out by Perry and Pigford (P3). They were able to obtain solutions over a fairly narrow range of parameter values using numerical techniques. More recently, with the aid of the much faster digital computers now available, this work was greatly extended by Brian and co-workers to cover a wider range of values for the second order case (B9), to solve the equations for a bi-molecular reaction of general order (B10), and to treat the case of a two-step second order reaction involving a transient intermediate product (B12). Most of the results of these studies are available in graphical form. They should be of considerable use in the interpretation of experimental data obtained under conditions where the penetration theory would be expected to apply.

Approximate analytic solutions for a general order bi-molecular reaction have been obtained by Hikita and Asai (H8) who used a linearizing technique similar to that employed by Brian and co-workers. The results of the two approaches are in reasonable agreement.

Pearson (P2) has shown how analytic solutions may be obtained for the second order reaction case under some extreme conditions such as very short contact times, pseudo first order behaviour, and infinitely fast second order reaction. Some numerical results in

the intermediate regions were also presented and were in agreement with the work of Brian et al (B9).

Recent studies have extended penetration theory solutions to account for some non-ideal behaviour. Brian et al (B11) have studied the effect of the presence of ionic species in a system with mass transfer and simultaneous second order chemical reaction. Since ions, because of their electrical charge, obey a different law of diffusion than molecular species, it was found that in many cases the predicted mass transfer rates were markedly different from those expected in molecular systems. Duda and Vrentas (D7) have considered the case of unsteady diffusion (no chemical reaction) into an infinite medium with both volume change on mixing and a concentration dependent diffusivity. Their approach is somewhat unique since it involves the transformation of the equations to obtain an ordinary differential equation. The equation is then solved using asymptotic solutions and standard forward integration techniques.

1.6 Theoretical Studies of Mass Transfer from Single Spheres

1.6.1 Low Reynolds Number Region ($Re < 1$)

In this region of creeping flow around a sphere it is possible to obtain analytic solutions describing physical mass (or heat) transfer. A review of the available solutions has been given by Acrivos and Taylor (A1). These authors note that the earlier solutions obtained by Kronig and Bruijsten (K4) and by Breiman (B8) for the low Peclet number region are not in agreement despite the use of identical

mathematical models. The methods of solution differed in the two cases, and perhaps this is the source of the discrepancy. Acrivos and Taylor (A1) have developed perhaps the most accurate solution available for the low Peclet number region using a perturbation technique.

Solutions covering the entire Peclet number range have been obtained by Friedlander (F2) and Yuge (Y2). Friedlander's method involved the assumption of a concentration profile and the conversion of the mass transfer equation into integral form. Yuge on the other hand, has developed a method utilizing successive power series approximations for the concentrations. This makes it possible to reduce the partial differential equation to a small number of ordinary differential equations. Yuge's method was extended by Johnson and Akehata (J3) to include mass transfer with a first order chemical reaction from both solid spheres and gas bubbles. These authors investigated other methods of solution including finite-difference techniques and published the only work to date which has considered mass transfer from a sphere with simultaneous chemical reaction.

Analytic solutions have been obtained for the case of very high Peclet numbers. Levich (L5) and Friedlander (F3) have obtained identical relationships after assuming that concentration changes could be confined within a thin boundary layer.

The integral method (e.g. F2), assuming a polynomial form for the concentration profile, has been extended by Bowman et al (B5)

to include transfer from both circulating and non-circulating spheres. These workers were able to predict mass transfer rates which agreed with their experimental results (W1) up to Reynolds numbers of around 10, despite the fact that the Stokes and Hadamard velocity profiles (strictly applicable only for $Re < 1$) were used to describe the hydrodynamics.

1.6.2 Intermediate Reynolds Number Region ($1 < Re < 200$)

As mentioned earlier in this review different methods are used to obtain descriptions of the flow field at $Re > 1$. These include the boundary layer approach (F5, L7), variational techniques (K1, H2, H3), and finite-difference methods (J2, H4, H5). Such descriptions of the hydrodynamics are essential to any theoretical study of mass transfer from spheres.

The thin concentration boundary layer approach (L5, F3) has been employed by Baird and Hamielec (B1) to obtain analytic solutions for transfer from both circulating and non-circulating spheres. Even with the use of Kawaguti-type velocity profiles (K1, H2, H3), which adequately describe the flow field, it was not possible, in the case of solid spheres, to obtain transfer rates in the vortex region without making one further assumption. These authors assumed that "fresh fluid" entered the vortex region continuously along a line through the rear stagnation point. As a result they were able to obtain local transfer rates in this region. The values obtained are undoubtedly high as the vortex region will in fact contain little "fresh fluid", but rather may be almost saturated with the material being transferred.

The same disadvantage, the inability to predict mass transfer

rates in the vortex region, also exists with the integral boundary layer techniques as used by Frossling (F5), Aksel'rud (A3), Linton and Sutherland (L7) and more recently by Ruckenstein (R5).

The investigation into wake transfer by Lee and Barrow (L3) was mainly experimental, but a preliminary theoretical analysis was also presented. The agreement with experimental values is not very satisfactory. It is actually best in the region $Re > 500$ where the vortex ring becomes unstable and is subject to periodic shedding and reforming.

An integral method utilizing an assumed polynomial for the concentration profile, coupled with the use of Kawaguti-type velocity profiles, has been used by Ross (3). The solutions predict reasonable average mass transfer rates, but it is doubtful whether local mass transfer rates obtained beyond the separation point are meaningful.

Theoretical studies by Garner and Keey (G6) and by Grafton (G8) claim the ability to predict physical mass transfer rates in the vortex region. The methods involve the assumption of suitable polynomials for both the velocity and concentration profiles along with a relationship, due to Levich (L5), between the hydrodynamic and boundary layer thicknesses. Finally, in the method of Grafton (G8), a knowledge of the shape of the vortex region is required. The theoretically predicted mass transfer rates of these workers are in reasonable agreement with the experimental results of Garner and co-workers (G4, G5, G6). However, it has been previously pointed out in this review that the results of (G4) and (G5) were most likely affected by the presence of turbulence in the transfer medium. In the work of (G6), the unrealistic choice

of the average, rather than the centerline velocity, was used for correlating purposes. In view of the fact that the theoretical results are in agreement only with doubtful experimental data, the confirmation of the applicability of these methods must await further careful evaluation by workers in the field.

The inability of all the above theories to deal satisfactorily with the problem of transfer in the vortex region is a severe limitation when considering transfer from solid spheres. The area covered by the wake may reach as high as 40% of the total surface area at Reynolds numbers of the order of 400. Therefore, accurate prediction of overall mass transfer rates is very difficult without a knowledge of wake transfer rates. There is no flow separation, and thus no vortex region, when the flow is around fully circulating drops or bubbles. Thus, some of the theories discussed should allow for the prediction of overall physical mass transfer ratio under these conditions.

1.6.3 High Reynolds Number Region ($Re > 200$)

Attempts to predict flow behaviour and mass transfer rates theoretically in this region have proven difficult and unsatisfactory. The velocity profiles developed by Hamielec (H2, H3) are available in this region for flow around solid spheres. However it has been shown by comparison with experimental studies (G8) and with recent numerical solutions (H4, H5), that the predicted shape of the vortex ring is unrealistic. Also, it has been noted that the vortex ring becomes unstable beyond Reynolds numbers of 500. Theoretical profiles cannot account for the transient nature of the wake and therefore are of

questionable value in this region.

For flow around circulating gas bubbles at high Reynolds numbers the potential flow velocity profiles provide a reasonable description of the flow field. The use of these profiles and penetration theory leads to a theoretical relationship (B3, H7, S6) which has found wide application in predicting absorption rates from gas bubbles. Typical of this use is the work of Bowman (B4) and Calderbank and Lochiel (C5). These workers found reasonable agreement between the predicted transfer rates and those observed with carbon dioxide bubbles rising through distilled water. A more recent study by Yau (Y1), with a single orifice bubble column, has shown that accurate prediction of mass transfer rates is possible up to the point where bubble deformation becomes significant. Although this work was with a reacting system, the oxidation of acetaldehyde, the reaction rate was slow and consequently did not cause a significant enhancement of mass transfer.

Any theoretical studies which would attempt to account for oscillation and deformation of drops and bubbles, and for the presence of turbulence in the boundary layer, would involve mathematical complexities of another order of magnitude and are beyond the scope of the present study.

1.7 Mass Transfer in Disperse Systems

Hopefully, the results of any theoretical study of mass transfer from a single sphere would be applicable to disperse systems, providing the interaction between particles was small. Yau (Y1), in a recent

study using the ideal situation of a single orifice bubble column, has indicated that it is possible to extend the theoretical results for a single bubble to the prediction of average transfer rates for a number of bubbles formed consecutively. In the particular column used by Yau interaction between bubbles was probably negligible.

Typical of the extensive experimental studies which have been carried out in disperse systems is the work of Calderbank and co-workers (C1 -C4). The studies include investigations of interfacial areas generated in sieve trays and bubble cap plates, and measurements of mass transfer coefficients and interfacial areas with and without mechanical agitation. Some recent experimental studies by Westerterp et al (W4) and by Gal-Or and Resnick (G1) have been concerned with mass transfer in agitated vessels where the transfer was accompanied by a first order chemical reaction.

A fundamental theoretical study of mass transfer from bubble swarms has recently been developed by Gal-Or and co-workers (G1, G2, G3). The model deals with bubble swarms in agitated vessels where the bubble velocity relative to the fluid cannot be readily obtained. In view of this difficulty, an average residence time approach was developed where a gas bubble is assumed to be in contact with a certain volume of liquid for a suitable contact time. Penetration theory equations are then used to describe the mass transfer during the contact period. The model allows for a distribution of contact times to be considered as well as a certain amount of interaction between bubbles. It is also possible to predict the effect of a first order

chemical reaction. Initial comparisons between predicted and experimentally observed values have been encouraging.

1.8 Effect of Surfactants and Interfacial Instability on Mass Transfer

The effect of the presence of surface active impurities on mass transfer has been the subject of investigations for some time. Many of these studies have attempted to determine whether a resistance to mass transfer was added when surfactant material was present at the transfer interface. Most investigators have concluded that interfacial resistance is very small (W2, W5), and often could not be easily detected because of the accompanying hydrodynamic effect (e.g. G7). In the case of drops or bubbles, for example, several authors (B6, B7, W5) have shown that surfactants may slow down or completely prevent internal circulation. This effect, solely hydrodynamic, would cause a marked decrease in absorption rates. It therefore was difficult to detect any interfacial resistance which may have been added by the surfactant film. The reduction of internal circulation is the result of the accumulation of surfactant which establishes surface tension gradients opposing the external shear forces.

A recent experimental study by Plevan and Quinn (P4) investigated the effect of a mono-molecular film on the rate of absorption into a quiescent liquid. They were able to detect interfacial resistance effects only for very soluble gases, such as sulfur dioxide.

In the absence of surfactants, interfacial instability effects have been observed in many mass transfer studies (L6, O1, S1, S4). This

interfacial activity, the Marangoni effect, is set up as a result of changes in interfacial tension caused by local concentration variations. The effect can therefore be expected to be larger when the interfacial tension is very concentration dependent. Sherwood and Wei (S4) observed that interfacial activity did not occur in pure systems, i.e., when no solute was present in either phase.

Sternling and Scriven (S8) were apparently the first to formulate a theoretical model describing interfacial activity at plane interfaces. Ruckenstein and Berbente (R7) have extended this to include the effect of a first order chemical reaction. The latter workers conclude that even a slow first order reaction may cause instabilities in an otherwise stable system.

The Sternling and Scriven approach for plane interfaces has been extended by Ruckenstein (R6) to mass transfer from a single drop or bubble with accompanying interfacial turbulence effects. The theory, which is confined to $Re < 1$, allows the conclusion that Marangoni effects should be a factor only in transfer from small drops or bubbles.

2. SCOPE

A review of the available literature has indicated that no suitable theoretical treatment of mass transfer from single spheres with simultaneous first or second order reaction has been developed. It would be advantageous to carry out any such theoretical development in the intermediate Reynolds number region where relationships adequately describing the flow field are available.

The development of a theory which could successfully describe the behaviour of single spheres, either circulating or rigid, in the intermediate Reynolds number region, and, at the same time, predict the effect of a first or second order reaction, would be a valuable addition to bubble reactor design fundamentals. Present design procedures are based on empirical techniques and, as a result, scale-up difficulties are unavoidable. The successful description of single bubble mass transfer behaviour would bring design based on sound fundamental principles one step closer. Further theoretical developments could then consider the problems of bubble oscillation and interaction.

Experimental studies of mass transfer from single spheres have not considered reacting systems. Because of its industrial significance, data on mass transfer accompanied by a chemical reaction would be of considerable interest.

Workers dealing with transfer from single spheres have invariably carried out such studies in a wind-tunnel (or water-tunnel)

where the flow of the transfer medium past the test sphere could be easily controlled. Whether or not special precautions are taken to obtain a flat or a parabolic velocity profile, in the region of the test sphere, is of no great importance, provided care is taken in the choice of the correlating velocity.

Reacting systems suitable for experimental study include many gas-liquid systems. Systems consisting of carbon dioxide as the gas and either caustic, buffer, or monoethanolamine solutions, have been studied extensively. There is reasonable agreement among the authors with regard to the reaction mechanisms. The carbon dioxide-buffer system can be described according to first order kinetics. The remaining two systems exhibit second order behaviour except under some extreme conditions such as very short gas-liquid contact times, where they may behave according to pseudo first order kinetics. The latter two systems are especially attractive as they show markedly increased transfer rates for relatively modest additions of reactant to the liquid phase. This would facilitate experimental measurements of the increased mass transfer while, at the same time, allowing the use of fairly dilute solutions.

In view of the above it was decided that the scope of this study would include:

(i) the attempted development and solution, by whatever method is most suitable, of a mathematical model describing mass transfer, with simultaneous first or second order reaction, from single circulating or non-circulating spheres. The study was to be confined to the intermediate Reynolds number region where the flow field may be adequately described

by existing relationships.

(ii) the measurement of mass transfer rates from single gas bubbles in a water-tunnel apparatus. After a consideration of the water-tunnel construction materials, it was apparent that the carbon dioxide - monoethanolamine system would be suitable for this study.

(iii) the evaluation of the model solutions through comparisons with previous theoretical and experimental results, as well as with the experimental data of this study.

3. THEORETICAL TREATMENT

3.1 Formulation of Model

In deriving the equations which describe mass transfer from a single sphere, with or without accompanying chemical reaction, it was first necessary to make several assumptions. These assumptions permit the mathematical analysis to be discussed, and do not invalidate the application of the analysis results to physical situations.

The following conditions were assumed:

- (i) Steady state conditions exist. Essentially steady state conditions were obtained in the experimental work to be discussed. In commercial reactors, however, a bubble may be in transient behaviour. The implications of this assumption in considering bubble reactors will be discussed later, but transient conditions are beyond the scope of the present study.
- (ii) The system is isothermal and the heat of reaction is negligible. In the absence of this assumption it would be necessary to solve the energy equation as well as the mass transfer equation.
- (iii) Density, viscosity and diffusivities are constant.
- (iv) The fluid is Newtonian and the flow is axisymmetric.
- (v) The particles are spherical and behave as either fully circulating gas bubbles or drops, or as non-circulating, rigid spheres. The latter situation can occur in gas-liquid systems as a result of the accumulation of surfactant material at the interface (B6, B7).
- (vi) The liquid phase is non-volatile, i.e., there is no transfer

from the continuous phase into the sphere.

(vii) All resistance to mass transfer is in the continuous phase.

This not only allowed for the assumption of equilibrium at the interface, but also eliminated the necessity of solving, simultaneously, a second equation describing concentration changes *within* the sphere.

(viii) Mass transfer rates are small so that the radial velocity component at the interface can be assumed to be zero. Hamielec et al (H5) have shown that for radial velocities at the interface of less than 1% of the main stream velocity the hydrodynamics are not significantly changed from the zero surface flux case.

(ix) Chemical reactions considered are either first or second order; although the method used for the second order case should be applicable to higher orders.

(x) Natural convection effects are negligible.

3.1.1 First Order Chemical Reaction

A mass balance was carried out on a spherical volume element (Figure 1) as in the work of Johnson and Akehata (J3, see also B2).

The following equation was obtained (quantities are defined in Nomenclature):

$$v_r \frac{\partial c_A}{\partial r} + \frac{v_\theta}{r} \frac{\partial c_A}{\partial \theta} = D_A \left[\frac{\partial^2 c_A}{\partial r^2} + \frac{2}{r} \frac{\partial c_A}{\partial r} + \frac{1}{r^2} \frac{\partial^2 c_A}{\partial \theta^2} + \frac{\cot \theta}{r^2} \frac{\partial c_A}{\partial \theta} \right] - k_1 c_A \quad (3.1)$$

with boundary conditions

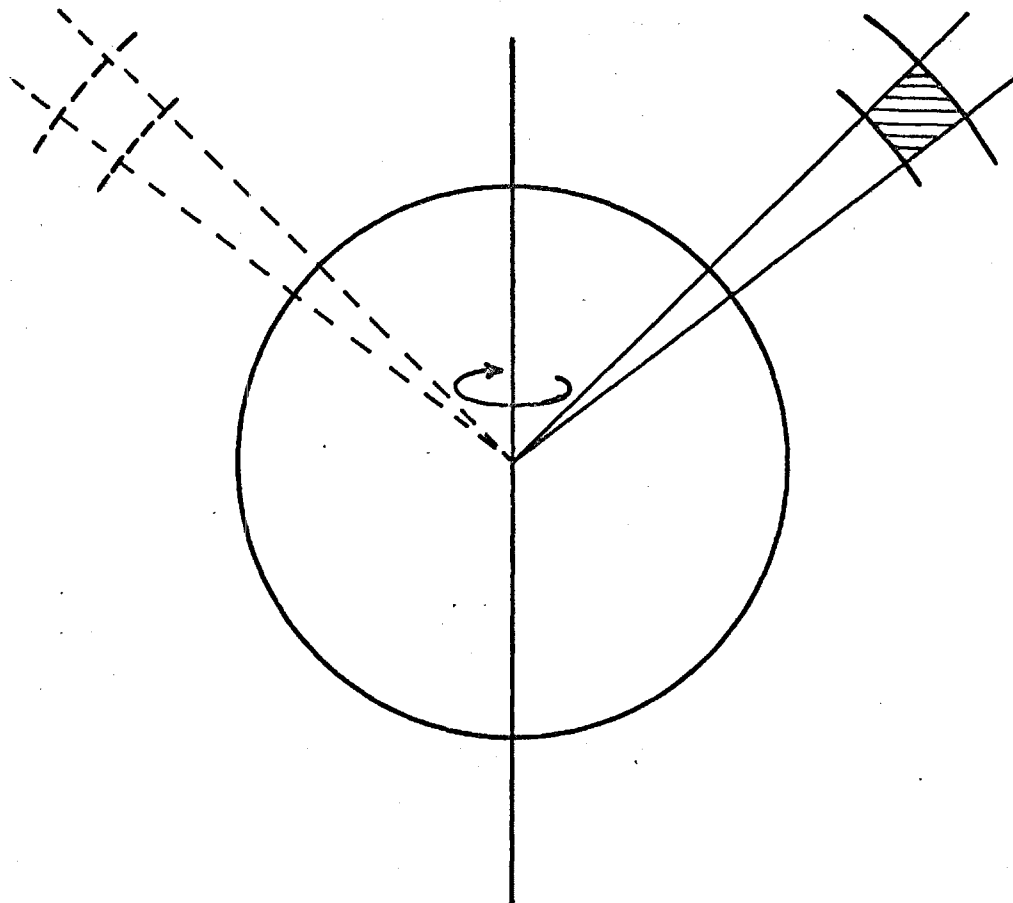


FIGURE 1. - SPHERICAL VOLUME ELEMENT

$$c_A = c_A^S \quad \text{at} \quad r = R$$

$$c_A = 0 \quad \text{as} \quad r \rightarrow \infty$$

and as a result of the assumption of axisymmetric flow conditions

$$\frac{\partial c_A}{\partial \theta} = 0 \quad \text{at} \quad \theta = 0, \pi$$

Equation (3.1) could be converted into dimensionless form by making the following definitions:

$$V_r' = V_r/U \quad ; \quad V_\theta' = V_\theta/U \quad ; \quad c_A' = c_A/c_A^S$$

$$r' = r/R \quad ; \quad Pe_A = 2RU/D_A \quad ; \quad k' = k_1 R^2/D_A$$

Using these definitions and dropping the primes equation (3.1) becomes

$$V_r \frac{\partial c}{\partial r} + \frac{V_\theta}{r} \frac{\partial c_A}{\partial \theta} = \frac{2}{Pe_A} \left[\frac{\partial^2 c_A}{\partial r^2} + \frac{2}{r} \frac{\partial c_A}{\partial r} + \frac{1}{r^2} \frac{\partial^2 c_A}{\partial \theta^2} + \frac{\cot \theta}{r^2} \frac{\partial c_A}{\partial \theta} - k c_A \right] \quad (3.2)$$

The case of purely physical mass transfer can be obtained simply by setting $k = 0$ in the above equation.

Equation (3.2) as it now stands is of elliptic form. In the examination by Johnson and Akehata (J3) of transfer at $Re < 1$ it was found that solutions of this equation via finite-difference techniques became unstable for any $Pe > 10^2$. Further study of this work confirmed that these instabilities were also present for $Re > 1$. Since the Peclet numbers associated with transfer at intermediate Reynolds

numbers are much greater than 10^2 (especially true of transfer into a liquid), no useful results could be obtained from the elliptic equation. The details of the solution methods attempted and an examination of the causes of the instabilities are given in Appendix A. This examination has revealed that the instabilities could have been suppressed only by employing impractically small angular and radial step sizes (finite-difference approximations were used). Storage capacities much larger than available in present-day digital computers would have been required.

In order to circumvent the difficulties associated with the elliptic equation, it was necessary to assume that molecular diffusion in the angular direction was negligible. This assumption made it possible to drop the terms $-\frac{1}{r^2} \frac{\partial^2 c_A}{\partial \theta^2}$, $\frac{\cot \theta}{r^2} \frac{\partial c_A}{\partial \theta}$, from equation (3.2). The remaining terms formed a parabolic equation:

$$V_r \frac{\partial c_A}{\partial r} + \frac{V_\theta}{r} \frac{\partial c_A}{\partial \theta} = \frac{2}{Pe_A} \left[\frac{\partial^2 c_A}{\partial r^2} + \frac{2}{r} \frac{\partial c_A}{\partial r} - k c_A \right] \quad (3.3)$$

where the boundary conditions remained unchanged, no difficulties of a stability nature were encountered by Johnson and Akehata (J3) in dealing with this equation at $Re < 1$. Further discussion of the mathematical model will deal only with equation (3.3). The disadvantages of using this equation to describe the mass transfer will be dealt with in detail in subsequent sections.

3.1.2 Second Order Chemical Reaction

A mass balance was carried out as before on a spherical volume element. Neglecting molecular diffusion in the angular direction, the

following two dimensionless equations of parabolic form were obtained:

$$V_r \frac{\partial c_A}{\partial r} + \frac{V_\theta}{r} \frac{\partial c_A}{\partial \theta} = \frac{2}{Pe_A} \left[\frac{\partial^2 c_A}{\partial r^2} + \frac{2}{r} \frac{\partial c_A}{\partial r} - k_A c_A c_B \right] \quad (3.4)$$

$$V_r \frac{\partial c_B}{\partial r} + \frac{V_\theta}{r} \frac{\partial c_B}{\partial \theta} = \frac{2}{Pe_B} \left[\frac{\partial^2 c_B}{\partial r^2} + \frac{2}{r} \frac{\partial c_B}{\partial r} - k_B c_A c_B \right] \quad (3.5)$$

with boundary conditions (see Figure 2)

$$c_A = 1, \quad \frac{\partial c_B}{\partial r} = 0 \quad \text{at} \quad r = 1$$

$$c_A = 0, \quad c_B = 1 \quad \text{as} \quad r \rightarrow \infty$$

$$\frac{\partial c_A}{\partial \theta} = \frac{\partial c_B}{\partial \theta} = 0 \quad \text{at} \quad \theta = 0, \pi$$

Since these equations contain a nonlinear source term, $k_A c_A c_B$ or $k_B c_A c_B$, it was anticipated that the solution technique would differ somewhat from that required for equation (3.3).

3.1.3 Velocity Profiles

Before any consideration can be given to the solutions of the mass transfer equations (3.3, 3.4, 3.5), values of both velocity components, V_r and V_θ , must be available as a function of radial and angular position. Johnson and Akehata (J3) in their study at $Re < 1$ used the Stokes (S9) or Hadamard-Rybczynski (H1, R8) velocity profiles. In the intermediate Reynolds number region, of interest here, the results of Kawaguti (K1) and Hamielec et al (H2, H3) were available in polynomial form. The recent results of Jenson (J2) and Hamielec and co-workers (H4, H5) consist of tabulations of values of

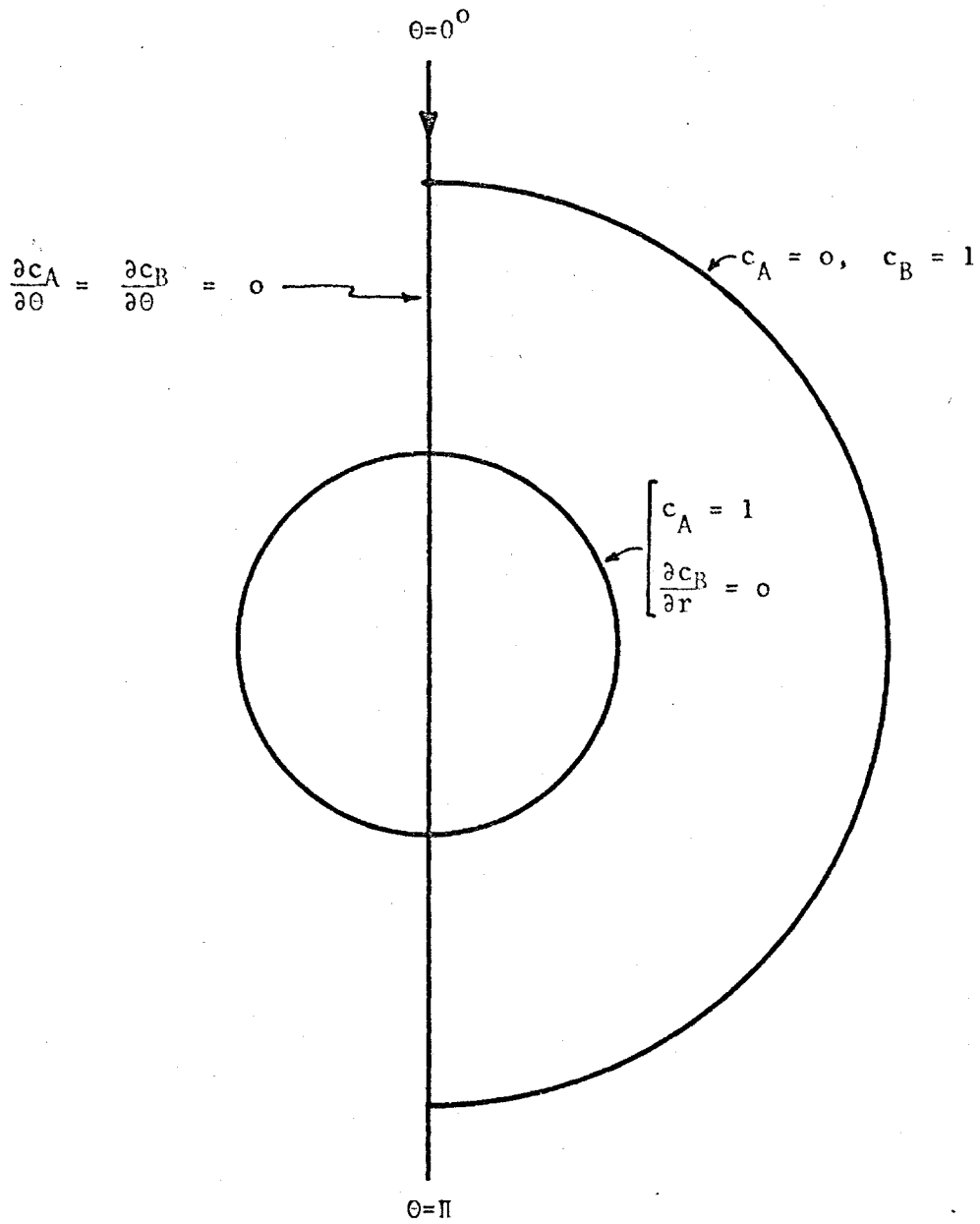


FIGURE 2. - BOUNDARY CONDITIONS FOR MASS TRANSFER WITH SECOND ORDER REACTION

the vorticity and stream function. A recent comparison of vorticity and stream function values obtained by the two procedures, error-distribution and finite-difference techniques, has indicated that the polynomial representations are in good agreement with the more accurate numerical solutions. In the case of flow around a rigid sphere this agreement is good up to the point of flow separation. However, the polynomial relationships give a less accurate description of flow in the vortex region. The polynomial forms developed by Hamielec et al (H2, H3) were used to describe the flow field in this study. These relationships were much more convenient for computer usage than the numerical results of (H4, H5) which had become available only during the latter stages of this investigation.

The velocity profiles from (H2, H3) may be written:

$$V_{\theta} = \left[1 - \frac{A_1}{r^3} - \frac{2A_2}{r^4} - \frac{3A_3}{r^5} - \frac{4A_4}{r^6} \right] \sin \theta + \left[-\frac{B_1}{r^3} - \frac{2B_2}{r^4} - \frac{3B_3}{r^5} - \frac{4B_4}{r^6} \right] \sin \theta \cos \theta \quad (3.6)$$

$$V_r = \left[-1 + \frac{2A_1}{r^3} + \frac{2A_2}{r^4} + \frac{2A_3}{r^5} + \frac{2A_4}{r^6} \right] \cos \theta - \left[\frac{B_1}{r^3} + \frac{B_2}{r^4} + \frac{B_3}{r^5} + \frac{B_4}{r^6} \right] (2\cos^2 \theta - \sin^2 \theta) \quad (3.7)$$

where

$$A_2 = \frac{-125 - 120X}{60 + 29X} + \left(\frac{-140 - 75X}{60 + 29X} \right) A_1 \quad (3.8)$$

$$A_3 = \frac{135 + 153X}{60 + 29X} + \left(\frac{108 + 63X}{60 + 29X} \right) A_1 \quad (3.9)$$

$$A_4 = \frac{-40 - 47.5X}{60 + 29X} + \left(\frac{-28 - 17X}{60 + 29X} \right) A_1 \quad (3.10)$$

$$B_2 = \left(\frac{-140 - 69X}{60 + 27X} \right) B_1 \quad (3.11)$$

$$B_3 = \left(\frac{108 + 57X}{60 + 27X} \right) B_1 \quad (3.12)$$

$$B_4 = \left(\frac{-28 - 15X}{60 + 27X} \right) B_1 \quad (3.13)$$

X is the ratio of the viscosity of the disperse phase to that of the continuous phase. Values of A_1 and B_1 have been tabulated at several Reynolds numbers (II2, II3).

Typical flow patterns are shown in Figure 3 for a fully circulating sphere.

3.2 Solution of Mathematical Model

Solutions to the first and second order reaction models were required in the form $c_A = f(r, \theta)$. Local Sherwood numbers could be calculated from the relationship

$$Sh = \frac{2Rk_L}{D_A} = -2 \left[\frac{\partial c_A}{\partial r} \right]_{r=1} \quad (3.14)$$

The average Sherwood number over the entire sphere surface could be obtained from

$$\overline{Sh} = \frac{\int_0^\pi Sh \sin\theta d\theta}{\int_0^\pi \sin\theta d\theta} \quad (3.15)$$

The mathematical models developed (equations (3.3, 3.4 and 3.5)) are second order parabolic partial differential equations, and in the case of equations (3.4) and (3.5) are nonlinear. These relationships are somewhat complex and are not amenable to solution by normal

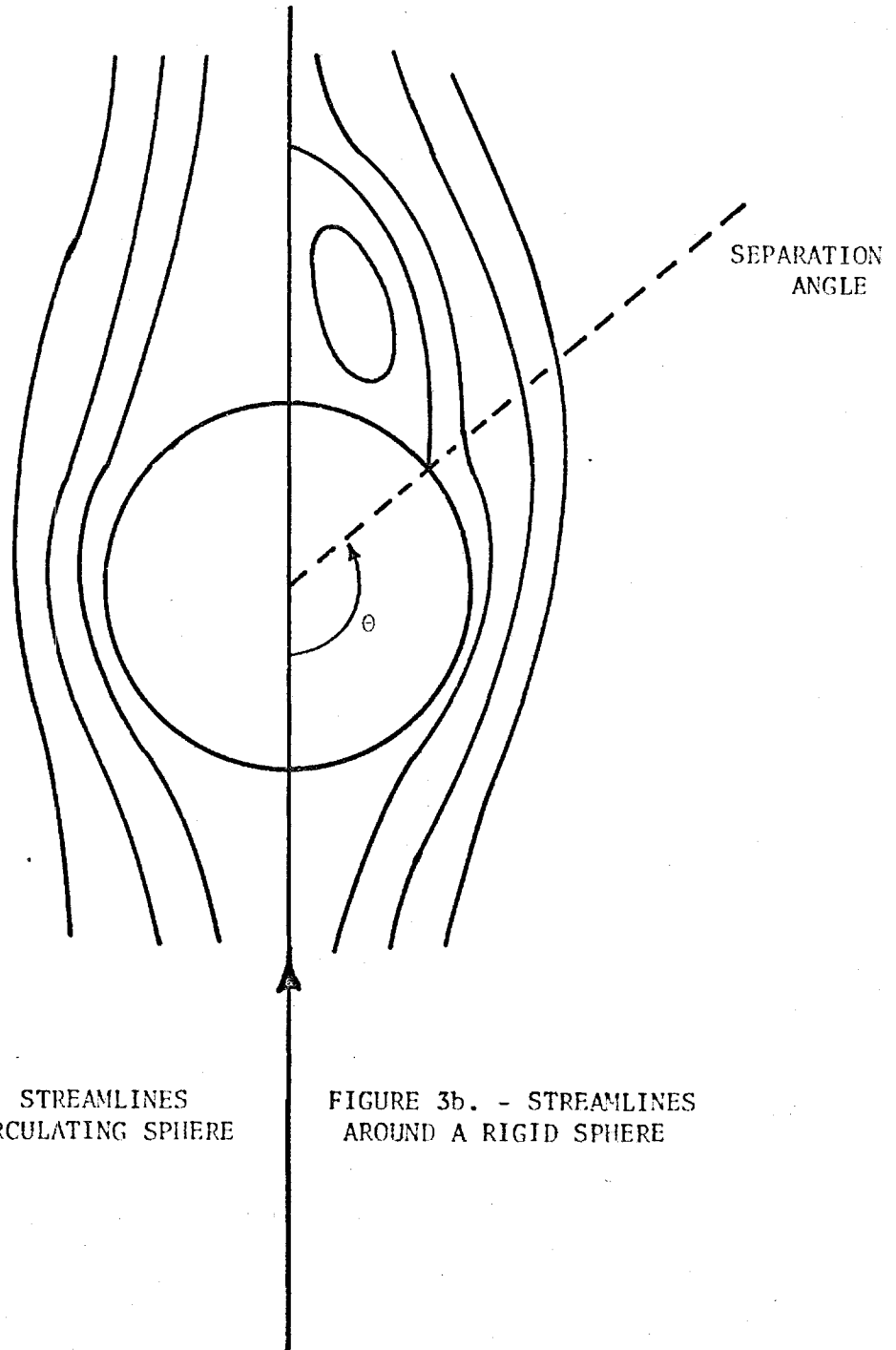


FIGURE 3a. - STREAMLINES
AROUND A CIRCULATING SPHERE

FIGURE 3b. - STREAMLINES
AROUND A RIGID SPHERE

exact analytical methods. The most obvious alternative method for equations of this type are finite-difference techniques. In this procedure finite-difference approximations are substituted for the partial derivatives, with the result that the partial differential equations are replaced by a set of algebraic equations. These can usually be handled with ease by present-day digital computers.

The finite-difference mesh system used in this work is shown in Figure 4 where the mesh point locations are labelled. A variable step size in the radial direction, identical with that employed in the earlier study (J3), was used throughout. With this particular formula the distance to the i^{th} step position is given by

$$r_i = 1 + \Delta r_0 \left[\frac{h^{i-1} - 1}{h - 1} \right] \quad (3.16)$$

where Δr_0 is the value of the first radial step and h is a constant greater than unity. The larger the value of h the more rapid the increase in step size as i increases. Although other forms were tried, equation (3.16) was the most flexible and convenient from a computation standpoint. As an example, transfer into a liquid at high Reynolds numbers, with accompanying chemical reaction, required a large number of mesh points very near the sphere surface where the concentration gradient was large. On the other hand, a relatively small number of mesh points was required at some distance from the surface. This sort of variation was readily handled by equation (3.16) simply by choosing a small value for Δr_0 with a large h value. A constant step size was used in the angular direction

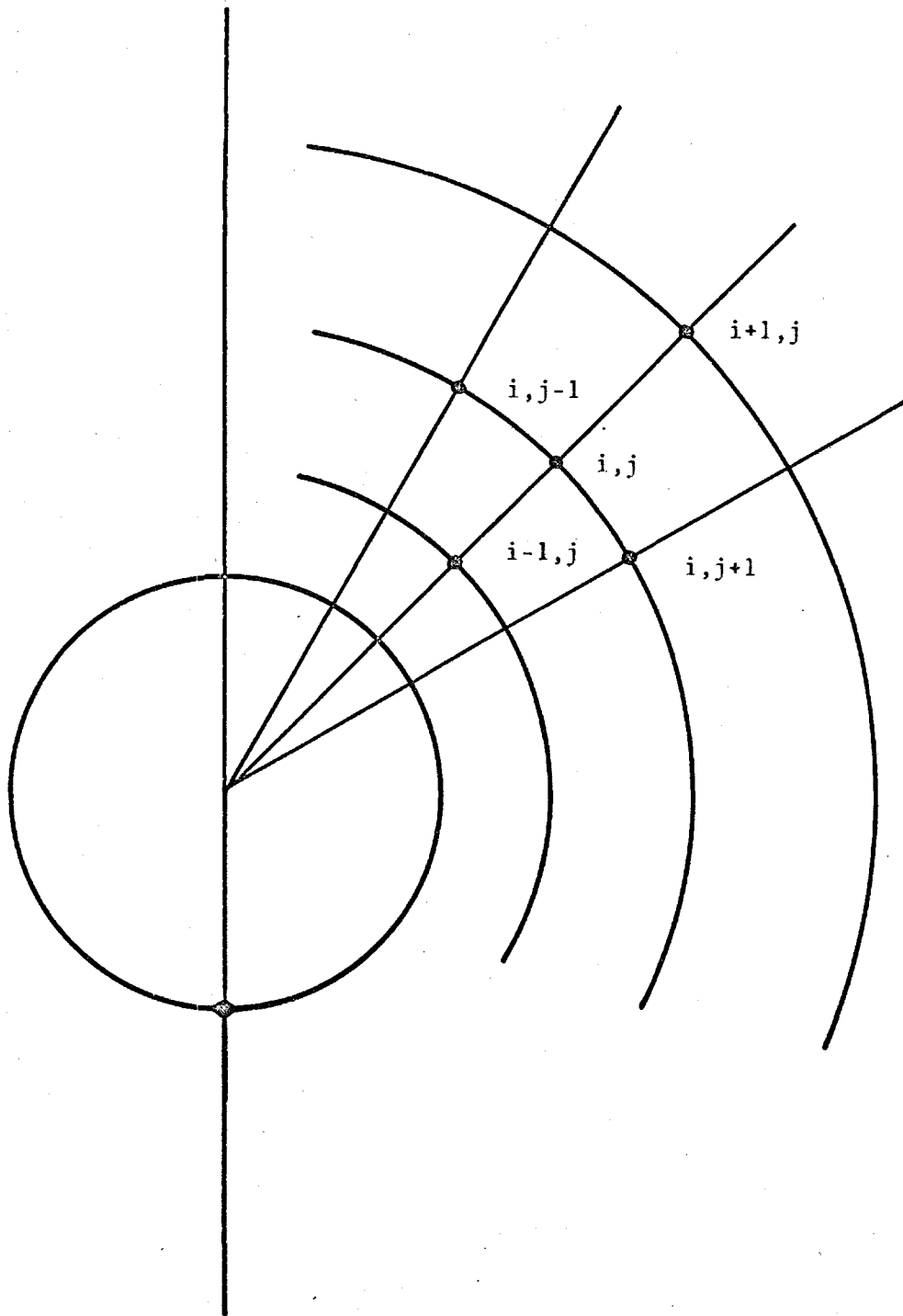


FIGURE 4. - FINITE-DIFFERENCE MESH SYSTEM

except for the first angular increment at $\theta = 0^{\circ}$. This increment was usually further subdivided into a number of equal steps for reasons to be discussed later.

After deciding to solve the model equations using finite-difference techniques, the choice between explicit and implicit procedures remained. The explicit methods allow the solution to proceed directly, solving explicitly for one unknown value at a time. In the implicit technique, a set of simultaneous algebraic equations must be solved at each step (L1). The difficulty with the explicit procedures is that usually very small steps must be taken in the "marching" direction (the angular direction in this problem). Otherwise instability problems arise. Implicit methods, on the other hand, are stable even with relatively large steps. Since the handling of large sets of simultaneous equations by matrix techniques is not a problem with modern computers, implicit methods are usually employed. They were the only ones considered for this study.

3.2.1 First Order Chemical Reaction

(i) General Method: The Crank-Nicholson implicit method (L1) was utilized to solve equation (3.3). This part of the study was simply an extension to the region $Re > 1$ of the earlier examination of the problem for $Re < 1$ by Johnson and Akehata (J3). For this problem, the procedure consisted of replacing the derivative in the angular direction by a forward difference approximation. The radial derivations were averaged over the j^{th} and $(j+1)^{st}$ angular increments.

The derivatives required can be written in general form, replacing c_A by A in the finite difference approximations, as

$$\frac{\partial c_A}{\partial \theta} = \frac{A_{i,j+1} - A_{i,j}}{\Delta \theta} \quad (3.17)$$

$$\frac{\partial c_A}{\partial r} = \frac{1}{2} \left[\frac{\partial c_A}{\partial r} \Big|_{i,j} + \frac{\partial c_A}{\partial r} \Big|_{i,j+1} \right] \quad (3.18)$$

$$= \frac{1}{2} \left[\frac{A_{i+1,j} - A_{i-1,j}}{r_{i+1} - r_{i-1}} + \frac{A_{i+1,j+1} - A_{i-1,j+1}}{r_{i+1} - r_{i-1}} \right] \quad (3.19)$$

$$\frac{\partial^2 c_A}{\partial r^2} = \frac{1}{2} \left[\frac{\partial^2 c_A}{\partial r^2} \Big|_{i,j} + \frac{\partial^2 c_A}{\partial r^2} \Big|_{i,j+1} \right] \quad (3.20)$$

$$= \frac{1}{2} \left[\frac{2A_{i+1,j}}{(r_{i+1}-r_i)(r_{i+1}-r_{i-1})} - \frac{2A_{i,j}}{(r_i-r_{i-1})(r_{i+1}-r_i)} + \frac{2A_{i-1,j}}{(r_i-r_{i-1})(r_{i+1}-r_{i-1})} \right. \\ \left. + \frac{2A_{i+1,j+1}}{(r_{i+1}-r_i)(r_{i+1}-r_{i-1})} - \frac{2A_{i,j+1}}{(r_i-r_{i-1})(r_{i+1}-r_i)} + \frac{2A_{i-1,j+1}}{(r_i-r_{i-1})(r_{i+1}-r_{i-1})} \right] \quad (3.21)$$

These approximations were developed from the usual Taylor series approach and are written here in terms of radial positions. This was done simply for programming convenience, since any variable radial step size, in addition to the form shown by equation (3.16), could be evaluated with a minimum number of program changes. The details of the development of the relationship for $\partial^2 c_A / \partial r^2$ are given in Appendix B. The use of a uniform radial step size would result in the more familiar form for the second derivative, i.e., if $(r_{i+1}-r_i) = (r_i-r_{i-1}) = \Delta r$ then

$$\frac{\partial^2 c_A}{\partial r^2} \Big|_{i,j} = \frac{A_{i+1,j} - 2A_{i,j} + A_{i-1,j}}{\Delta r^2} \quad (3.22)$$

When the finite-difference approximations were substituted for the partial derivatives in equation (3.3), and the r_i replaced by equation (3.16), the following finite-difference equation was obtained.

$$\begin{aligned} & A_{i+1,j}^* \left[\ell_1 - \ell_2 - \ell_3 \right] + A_{i-1,j}^* \left[-\ell_1 - h\ell_2 + \ell_3 \right] \\ & + A_{i+1,j+1} \left[\ell_1 - \ell_2 - \ell_3 \right] + A_{i-1,j+1} \left[-\ell_1 - h\ell_2 + \ell_3 \right] \\ & + A_{i,j+1} \left[\ell_4 + \ell_5 + \ell_6 \right] + A_{i,j}^* \left[-\ell_4 + \ell_5 + \ell_6 \right] = 0 \end{aligned} \quad (3.23)$$

where

$$\ell_1 = V_r / (2h^{i-1} \Delta r_o (1+1/h)) \quad (3.24)$$

$$\ell_2 = 2 / (h^{i-1} \Delta r_o)^2 (1+1/h) Pe_A \quad (3.25)$$

$$\ell_3 = 2 / (h^{i-1} \Delta r_o) (1+1/h) r_i Pe_A \quad (3.26)$$

$$\ell_4 = V_\theta / r_i \Delta \theta \quad (3.27)$$

$$\ell_5 = 2(1+h) / (h^{i-1} \Delta r)^2 (1+1/h) Pe_A \quad (3.28)$$

$$\ell_6 = k / Pe_A \quad (3.29)$$

and the starred quantities are known values.

Initially the unknown values along the radial vector through θ_{j+1} were obtained using a relaxation factor and an iterative procedure

as illustrated in (J3). Later solutions, however, were obtained more rapidly by inverting the matrix, which was of tridiagonal form, at each angular increment. The latter method was far superior to the iterative procedure and resulted in a great saving in computer time.

(ii) Boundary Condition at $\theta=0^\circ$: The boundary condition along the radial vector through the frontal stagnation point specifies only that the angular gradient in concentration is zero, but does not specify the concentrations along this line. In the early stages of this study, estimates of the concentration were inserted at $\theta=0^\circ$ and no attempt was made to satisfy the zero slope criterion. The solution was allowed to proceed, step by step, without regard for this fact. This resulted in oscillating values of the local Sherwood numbers over the first 10 to 15 degrees. At angles beyond this region the solutions obtained behaved in the expected manner, i.e., the local Sherwood numbers decreased in a regular fashion as θ increased. In an attempt to reduce these fluctuations more quickly, the first angular increment was further subdivided into 10 to 20 equal increments. This did in fact dampen out the oscillating values more quickly, but fluctuations in local Sherwood numbers still occurred over the first 5 to 10 degrees. Since this was unsatisfactory, a method was developed which allowed the zero slope condition to be satisfied. The procedure consisted of inserting initial estimates along the zero angle line, and then utilizing an iterative procedure until the zero slope criterion was satisfied. The initial estimates were taken from the solution of the equation describing diffusion from a sphere into a stagnant medium. The equation may be

written as

$$\frac{d^2 c_A}{dr^2} + \frac{2}{r} \frac{dc_A}{dr} - kc_A = 0 \quad (3.30)$$

This has an analytic solution given by

$$c_A = \frac{e}{r} \sqrt{k} (1-r) \quad (3.31)$$

In the earlier stages, where the boundary condition had been avoided, the values given by (3.31) were inserted along the zero angle line and assumed to be correct values. The iterative procedure developed to satisfy the boundary condition used the concentration of (3.31) as initial estimates only. From these, new concentration values at $\theta = \Delta\theta$ were calculated. These new values were then compared with the initial estimates to see whether $\partial c_A / \partial \theta$ equaled zero. If not, the new values at $\theta = \Delta\theta$ were assumed to be better estimates of the values at $\theta = 0^\circ$, and replaced the initial estimates of (3.31). This procedure was repeated as many times as was necessary to satisfy $\partial c_A / \partial \theta = 0$ within a specified tolerance. The practice of subdividing the first angular increment, employed initially to dampen out fluctuating values, was continued when employing the iterative procedure. The use of a small initial $\Delta\theta$ reduced the number of iterations required to satisfy the zero slope condition.

Once the boundary condition had been fulfilled, the solution proceeded in the normal manner through one angular increment after another. The local Sherwood numbers obtained in this case were well behaved and showed none of the fluctuating characteristics of the earlier results. A comparison of the local Sherwood number values.

obtained in the two cases is shown in Figure 5. It is interesting to note that beyond the first 15° there is very little difference in the local values. Since the area associated with the first 15° was a very small percentage of the total surface area, the average Sherwood numbers differed by less than 3%. In the cases reported here this boundary condition was always satisfied. The values obtained for transfer at the frontal stagnation point should therefore be suitable for comparison with theoretically predicted values (F5, L7, S5).

(iii) Mesh Details: Angular step sizes were usually 3° , with the first increment subdivided into ten steps of 0.3° . Thirty radial mesh points were employed. The position of the outer boundary was normally 1.44 dimensionless radii from the sphere center. The effect of choice of step sizes and position of the outer boundary will be discussed in a later section.

Computation times on an IBM-7040 were about 2 minutes for a typical case involving 70 angular, and 30 radial mesh locations.

(iv) Disadvantages of Parabolic Equation: As discussed previously, it was necessary to simplify equation (3.2) by neglecting the angular diffusion terms in order to obtain the equation in a form which could be solved by standard numerical techniques. The parabolic equation (equation (3.3)) which resulted, although readily solved with no stability difficulties, has the disadvantage that it does not everywhere describe the physical situation accurately. For transfer from circulating gas bubbles or liquid drops (Figure 3a), the neglected diffusion terms are important only in a very small region near the frontal and rear stagnation points.

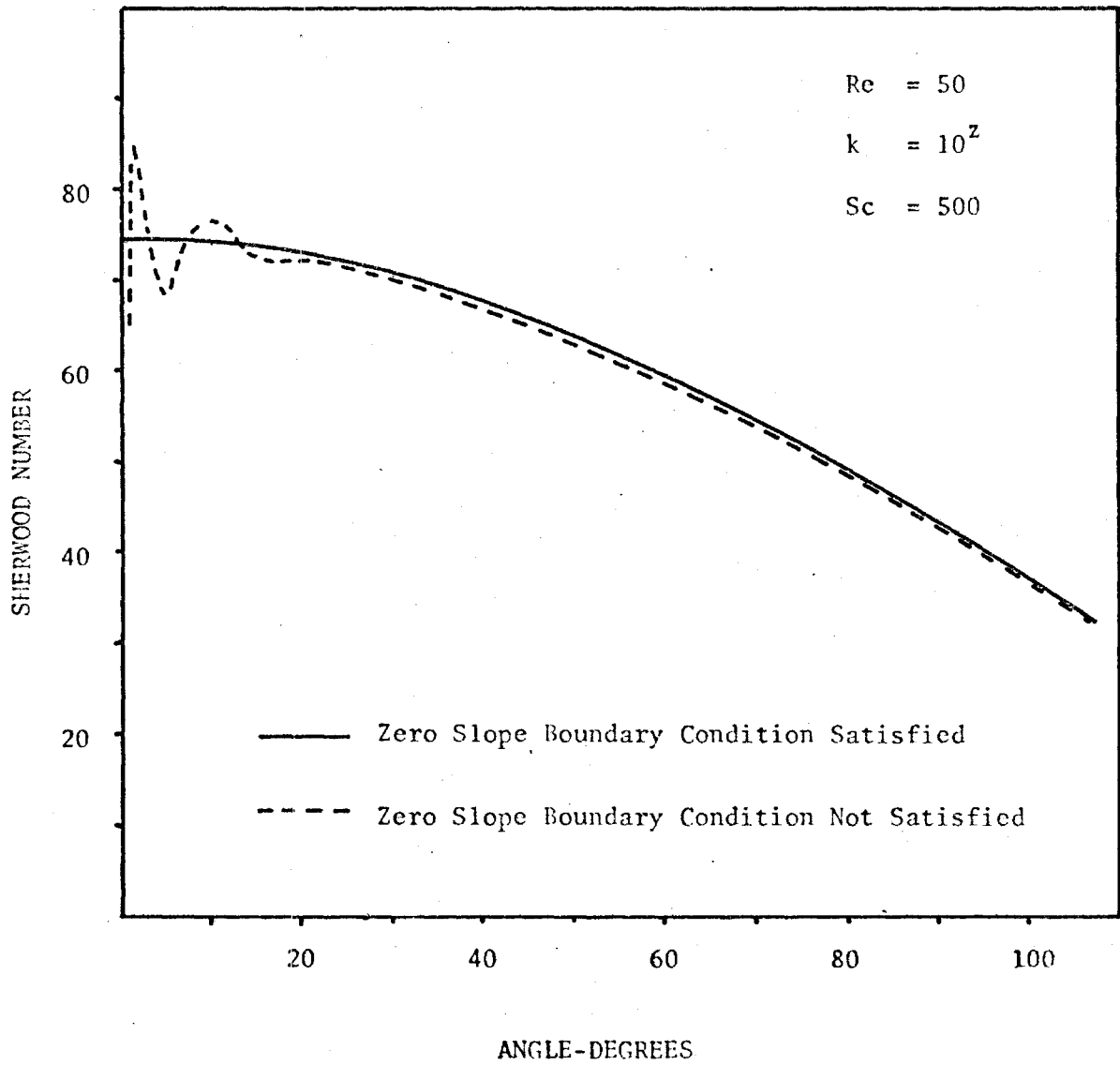


FIGURE 5. - EFFECT OF ZERO-SLOPE CRITERION AT $\theta=0^\circ$
ON CALCULATED SHERWOOD NUMBERS

This presented no computation difficulties. It was always possible to obtain solutions over the entire surface of the circulating sphere. For transfer from rigid spheres the neglected angular diffusion terms become extremely important at the point of flow separation and beyond (see Figure 3b). In this region the parabolic equation no longer adequately describes the physical situation and the numerical procedures, as should be expected, break down. Therefore, the present numerical method suffers from the same disadvantage as the previous theoretical treatments discussed in Section 1.6.2, i.e, it does not allow for the prediction of local mass transfer rates in the vortex region. The description of transfer in the vortex region would require the solution of the elliptic equation (equation 3.2) for which standard numerical techniques have proven unsuccessful. However, it has been possible to obtain transfer rates in the vortex region for one extreme case, that of a very fast first order reaction. Under these conditions it was found that the mass transfer rate was independent of angle, and the results obtained were in good agreement with the stagnant fluid solutions (See Table 3.1). It is doubtful, however, whether these local values are meaningful. The existence, at steady state, of a bi-molecular first order reaction would be unlikely under conditions present in the vortex region. The extremely fast reaction would be expected to consume quickly most of the liquid phase reactant, thus resulting in depletion near the reaction zone and a second order, not first order, reaction situation. These high reaction rate results, although useful for comparing with the stagnant fluid solutions, are not considered to be the descriptions of transfer in the vortex region.

for any real situation.

3.2.2 Second Order Chemical Reaction

Since the two parabolic equations (equations (3.4) and (3.5)) developed for the second order case are nonlinear, a straightforward Crank-Nicholson method is not applicable. It would seem desirable that the procedure used should involve only linear algebraic equations, since nonlinear equations would require normally less efficient iterative methods. A linearizing technique, involving only linear finite-difference equations, has been developed by Douglas (D5) for parabolic equations of this type. The method has been used by Brian and co-workers (B9, B10) in solving the penetration theory equations which describe unsteady diffusion, with a simultaneous bi-molecular reaction of general order, into a stagnant fluid. The procedure, as outlined in (B9), has been followed here with only slight variations dictated by numerical stability requirements.

(i) Outline of Solution Procedure

1. Equation (3.5) was approximated by the explicit finite-difference equation (where the c_B were replaced by B) written as

$$\begin{aligned}
 & B_{i+1,j} \left[\frac{l_1}{2} - 2l_2 - 2l_3 \right] + B_{i,j} \left[\frac{l_4}{2} - \frac{l_5}{2} + \frac{2k_B A_{i,j}}{Pe_B} \right] \\
 & + B_{i-1,j} \left[\frac{-l_1}{2} - 2hl_2 + 2l_3 \right] + B_{i,j-1} \left[\frac{-l_4}{2} - \frac{l_5}{2} \right] \\
 & + B_{i,j+\frac{1}{2}} \left[l_4 - l_5 \right] = 0
 \end{aligned} \tag{3.32}$$

A forward difference was used for the angular derivative; a central difference for the first derivative in the radial direction; and a DuFort-Frankel approximation (F1), rather than the normal central difference, for the second derivative in r . The DuFort-Frankel form for a variable radial step size may be written as

$$\frac{\partial^2 c_B}{\partial r^2} = \frac{2B_{i+1,j}}{(r_{i+1}-r_i)(r_{i+1}-r_{i-1})} - \frac{B_{i,j-1} + B_{i,j+1}}{(r_i-r_{i-1})(r_{i+1}-r_i)} + \frac{2B_{i-1,j}}{(r_i-r_{i-1})(r_{i+1}-r_{i-1})} \quad (3.33)$$

Whereas the "standard" form is given by equation (3.21).

The same variable radial step size, equation (3.16), was used for both first and second order reaction studies.

It was found that if the DuFort-Frankel form was not used in the *explicit* step, errors were introduced which quickly swamped the true solution. The difficulty was traced to a point in the calculations where it became necessary to subtract two very large numbers of the same order of magnitude. In some cases the first non-zero residual occurred in the eighth column, and since the IBM-7040 carried only 8 figures in normal operation, the results quickly became meaningless. The use of the DuFort-Frankel form for the second derivative in r enabled the solution to proceed without encountering such an error-introducing calculation. This made it unnecessary to resort to "Double-Precision" computation procedures.

Equation (3.22) was solved directly for $B_{i,j+\frac{1}{2}}$ since all the

B_i values were known at angular position j .

2. Equation (3.4) was approximated using the normal Crank-Nicholson implicit procedure. The finite-difference equation which results is written (replacing c_A by A) as

$$\begin{aligned}
 & A_{i+1,j} \left[\ell_1 - \ell_2 - \ell_3 \right] + A_{i-1,j} \left[-\ell_1 - h\ell_2 - \ell_3 \right] \\
 & + A_{i+1,j+1} \left[\ell_1 - \ell_2 - \ell_3 \right] + A_{i-1,j+1} \left[-\ell_1 - h\ell_2 + \ell_3 \right] \\
 & + A_{i,j+1} \left[\ell_4 + \ell_5 + \frac{k_A B_{i,j+\frac{1}{2}}}{Pe_A} \right] \\
 & + A_{i,j} \left[-\ell_4 + \ell_5 + \frac{k_A B_{i,j+\frac{1}{2}}}{Pe_A} \right] = 0 \quad (3.35)
 \end{aligned}$$

Since all the $B_{i,j+\frac{1}{2}}$ were known from the previous step, the set of linear algebraic equations was readily solved.*

3. Values for $A_{i,j+\frac{1}{2}}$ were calculated from the following relationship:

$$A_{i,j+\frac{1}{2}} = \frac{A_{i,j+1} + A_{i,j}}{2} \quad (3.36)$$

4. Equation (3.5) was then written in finite-difference form using the Crank-Nicholson approximations.

$$\begin{aligned}
 & B_{i+1,j} \left[\ell_1 - \ell_2 - \ell_3 \right] + B_{i-1,j} \left[-\ell_1 - h\ell_2 + \ell_3 \right] \\
 & + B_{i+1,j+1} \left[\ell_1 - \ell_2 - \ell_3 \right] + B_{i-1,j+1} \left[-\ell_1 - h\ell_2 + \ell_3 \right]
 \end{aligned}$$

* A Gaussian elimination technique was employed to handle the tridiagonal matrix which resulted.

$$\begin{aligned}
& + B_{i,j+1} \left[\ell_4 + \ell_5 + \frac{k_B A_{i,j+\frac{1}{2}}}{Pe_B} \right] \\
& + B_{i,j} \left[-\ell_4 + \ell_5 + \frac{k_B A_{i,j+\frac{1}{2}}}{Pe_B} \right] = 0
\end{aligned} \tag{3.37}$$

Since the $A_{i,j+\frac{1}{2}}$ were known from (3.36), the set of algebraic equations were linear and could be solved for the $B_{i,j+1}$ by handling the tridiagonal matrix as before.

5. Over the next angular increment the procedure was reversed, with the explicit finite-difference approximation written for equation (3.4) instead of (3.5), and the $A_{i,j+\frac{1}{2}}$ solved for directly.

6. The $A_{i,j+\frac{1}{2}}$ were substituted into equation (3.37) and the $B_{i,j+1}$ obtained by matrix inversion.

7. Values for $B_{i,j+\frac{1}{2}}$ were obtained from the relationship

$$B_{i,j+\frac{1}{2}} = \frac{B_{i,j+1} + B_{i,j}}{2} \tag{3.38}$$

8. These $B_{i,j+\frac{1}{2}}$ values were then substituted into equation (3.35) and the matrix inversion step applied to give the $A_{i,j+1}$ values.

The procedure was followed through one angular increment to another. Brian et al (B9) have pointed out that the use of this implicit procedure, instead of an explicit method, results in a great saving in computer time, and avoids any stability limitations usually encountered with the latter.

(ii) Boundary Conditions: The same iterative procedure, as in the first order reaction case, was used to satisfy the zero slope condition

along the radial vector through $\theta=0^\circ$. In this case initial concentration estimates were obtained from the solutions of the equations describing diffusion from a sphere into a stagnant fluid with second order reaction.

These equations may be written as

$$\frac{d^2 c_A}{dr^2} + \frac{2}{r} \frac{dc_A}{dr} - k_A c_A c_B = 0 \quad (3.39)$$

$$\frac{d^2 c_B}{dr^2} + \frac{2}{r} \frac{dc_B}{dr} - k_B c_A c_B = 0 \quad (3.40)$$

Since analytic solutions to these equations were not available, numerical methods had to be used to obtain the required initial estimates. No difficulties were encountered in obtaining solutions when using the technique described in Appendix C.

The boundary condition $\partial c_B / \partial r = 0$ at $r=1$ was handled by writing the first derivative in terms of the first three radial locations, equating the derivative to zero, and solving for the concentration of $B_{1,j}$ at the interface. The relationship obtained may be written (details of derivation are given in Appendix D) as

$$B_{1,j} = \left[\frac{(r_3 - r_1)^2}{(r_3 - r_1)^2 - (r_2 - r_1)^2} \right] B_{2,j} - \left[\frac{(r_2 - r_1)^2}{(r_3 - r_1)^2 - (r_2 - r_1)^2} \right] B_{3,j} \quad (3.41)$$

The use of this relationship caused no difficulties. The concentration of B at the interface never appeared explicitly in the matrix but only as a function of $B_{2,j}$ and $B_{3,j}$.

(iii) Stability of Numerical Procedures: Stability difficulties, in addition to the one already noted in Step 1 of the solution procedure,

had to be resolved before results could be obtained for all conditions.

One of these stability problems arose when an attempt was made to use a finite-difference form for the first derivative in r which had a smaller truncation error than the standard form given by

$$\frac{\partial c_A}{\partial r} = \frac{A_{i+1,j} - A_{i-1,j}}{(r_{i+1} - r_{i-1})} \quad (3.42)$$

where the truncation error is of order $[(r_{i+1} - r_i)^2 - (r_{i-1} - r_i)^2] \frac{\partial^2 c_A}{\partial r^2}$.

A form having a smaller truncation error can be developed and results in the following relationship (see Appendix B for details):

$$\begin{aligned} \frac{\partial c_A}{\partial r} = & \left[\frac{(r_{i-1} - r_i)}{(r_{i+1} - r_i)(r_{i-1} - r_{i+1})} \right] A_{i+1,j} \\ & - \left[\frac{(r_{i-1} - r_i)}{(r_{i+1} - r_i)(r_{i-1} - r_{i+1})} - \frac{(r_{i+1} - r_i)}{(r_{i-1} - r_i)(r_{i-1} - r_{i+1})} \right] A_{i,j} \\ & - \left[\frac{(r_{i+1} - r_i)}{(r_{i-1} - r_i)(r_{i-1} - r_{i+1})} \right] A_{i-1,j} \end{aligned} \quad (3.43)$$

This form has truncation error of the order $(r_{i+1} - r_{i-1})^3 \frac{\partial^3 c_A}{\partial r^3}$. The

latter two equations are equivalent only if the radial step size is constant.

In this case a variable step size was used and the two relationships were

not equivalent. It had been hoped that equation (3.43), because of its

smaller truncation error, would prove more reliable. The use of

equation (3.43), however, always resulted in unstable solutions. Thus

it was necessary to use the form given by equation (3.42) which proved

to be stable under all conditions. This instability is similar to another

well known effect in parabolic systems where a central difference

representation for the marching direction derivation, in this case the θ -direction, always results in unstable solutions. Whereas the forward difference, with a larger truncation error, is stable (L2).

A further stability difficulty was encountered only when dealing with transfer from *rigid* spheres and reaction rates of $k_A > 10^4$. Instabilities occurred which could be traced to the *implicit* step calculations. The source of error was identical with the *explicit* step error previously discussed. The difficulty was circumvented once more by using the DuFort-Frankel form for the second derivative in r . Normally this derivative was replaced in the implicit step by equation (3.20), repeated here for convenience:

$$\frac{\partial^2 c_A}{\partial r^2} = \frac{1}{2} \left[\frac{\partial^2 c_A}{\partial r^2}{}_{i,j} + \frac{\partial^2 c_A}{\partial r^2}{}_{i,j+1} \right] \quad (3.20)$$

where the derivatives at (i,j) and $(i,j+1)$ were replaced by the "standard" difference formula (equation 3.21). In this case only the second derivative at $(i,j+1)$ was replaced by the "standard" form, whereas the derivative at (i,j) was replaced by the DuFort-Frankel form written as

$$\begin{aligned} \frac{\partial^2 c_A}{\partial r^2} &= \frac{2A_{i+1,j}}{(r_{i+1}-r_i)(r_{i+1}-r_{i-1})} - \frac{(A_{i,j-1}+A_{i,j+1})}{(r_i-r_{i-1})(r_{i+1}-r_i)} \\ &+ \frac{2A_{i-1,j}}{(r_i-r_{i-1})(r_{i+1}-r_{i-1})} \end{aligned} \quad (3.44)$$

The use of this modified form for the second derivative in r does not introduce any additional unknown quantities, but simply replaces $A_{i,j}$ by the known value $A_{i,j-1}$ and the unknown value $A_{i,j+1}$. The latter

unknown was already present as a result of the approximation for $\partial^2 c_A / \partial r^2$ at $(j+1)$.

For reaction rate values of $k_a \leq 10^4$ the results obtained using the standard form, equation (3.21), were identical with those using the modified form above.

It should be emphasized that no difficulties of this nature were encountered when dealing with transfer from *circulating* spheres at any reaction rate level. The difficulties were present only when considering transfer from *rigid* spheres for $k_A > 10^4$.

(iv) Disadvantages of Parabolic Equations: The disadvantages discussed for the case of first order reaction apply to the second order case as well. Once again it was not possible to obtain values of local transfer rates within the vortex region, whereas values could be obtained over the whole surface for transfer from circulating spheres.

(v) Mesh Details: As in the first order case the angular increment was normally 3° with the first increment divided into ten smaller steps. Thirty radial mesh locations were employed with the same step size variation as before (equation (3.16)). The outer boundary was usually placed 1.44 radii from the sphere center.

Computation times for a typical set of parameter values were of the order of 3 minutes on the IBM-7040.

3.3 Results and Discussion

The question of whether a numerical solution is a good approximation

of the exact analytic solution is normally a very difficult one, except in the trivial case where the analytic solution is available. In cases where general analytic solutions are not known, some indication of the "accuracy" of the numerical results may be obtained by comparing them with any available asymptotic solutions, and with experimental results obtained where the physical situation corresponds to the equation and its boundary conditions. An additional criterion very often used is the application of a convergence test, i.e., to decrease the finite-difference mesh size in order to check whether any further change of calculated values occurs. These three topics will be covered in the ensuing discussion.

3.3.1. Convergence Tests and Asymptotic Solutions

One of the tests applied in the earlier study of Johnson and Akehata (J3) was a comparison with the theoretical value for transfer into a stagnant fluid ($Sh=2$). They found that as the Peclet number approaches zero, the calculated Sherwood numbers did in fact approach the theoretical value, and were in reasonable agreement with the theoretical results of other workers.

The computer programs developed in the present study were checked initially by re-running some of the cases from (J3). Identical results were obtained as expected.

The solution available from the equation describing transfer into a stagnant fluid, equation (3.30), might be expected to supply an asymptotic solution for very high first order reaction rates. Under these conditions the concentration boundary layer will become extremely

thin, and a point should be reached where the transfer rates become independent of the hydrodynamics. Table 3.1 lists results obtained for transfer from a solid sphere with first order reaction at several Reynolds number levels. The solutions at $k=10^4$ show that there is a small effect of hydrodynamics as indicated by a slight increase in Sherwood number with increasing Reynolds number. The results obtained for $k=10^6$ are unaffected by the hydrodynamics. In both cases, the value at the lowest Reynolds number is a very reasonable approximation, within 2%, of the exact solution of equation (3.30).

Extensive convergence tests were carried out varying step size in both the radial and angular directions. Results, along with pertinent details of mesh size, are given in Table 3.2 for tests of the first order reaction equation. Results for the second order reaction equations are given in Table 3.3.

A conclusion readily drawn is that the placing of the outer boundary at a distance greater than 1.44 radii does not affect the solutions. Figures 6a and 6b indicate for one particular choice of conditions that the location of the outer boundary is a realistic approximation of the conditions $c_A=0$ and $c_B=1$ as $r \rightarrow \infty$. Care was always taken to ensure that the outer boundary was realistically located and, except in a very few cases, a distance of 1.44 was adequate.

Decreasing the angular and radial step sizes also had little effect on calculated values. In all cases, variations in Sherwood numbers were less than 2%, indicating that convergence was obtained

TABLE 3.1

Comparison of Numerical Solutions with
Analytical Solutions for a Stagnant Fluid Transfer
from Solid Spheres

$$Sc = 500$$

Type of Solution	Re	k	\bar{Sh}
Analytical	-	10^4	202
Numerical	20	10^4	202.7
Numerical	50	10^4	202.4
Numerical	100	10^4	205.7
Numerical	200	10^4	208.8
Analytical	-	10^6	2002
Numerical	20	10^6	1964
Numerical	50	10^6	1964
Numerical	100	10^6	1965
Numerical	200	10^6	1965

TABLE 3.2

Convergence Tests - Transfer from
a Solid Sphere with First Order Reaction

Re	Sc _A	k	Δr_0	No. of Radial Steps	$\Delta\theta$ (deg.)	Position of Outer Boundary	Sherwood Number			AVG. over Entire Surface
							AT 0°	AT 45°	AT 90°	
200	500	0	5×10^{-5}	30	3	1.44	167.6	143.3	73.6	72.8
			5×10^{-5}	30	3	1.59	167.9	143.4	73.6	72.8
			5×10^{-5}	30	1.5	1.44	168.7	143.3	73.6	*
			2.3×10^{-5}	60	3	1.44	168.6	143.2	73.1	72.5
			2.3×10^{-5}	60	1.5	1.44	168.9	143.2	73.6	*
50	500	10^4	5×10^{-5}	30	3	1.44	206.9	206.0	202.1	202.4
			2.3×10^{-5}	60	3	1.44	208.8	204.6	200.1	202.0
200	500	10^4	5×10^{-5}	30	3	1.44	248.0	232.7	195.9	208.8
			2.3×10^{-4}	60	3	31.3	245.9	228.8	191.9	210.3
			2.3×10^{-5}	60	3	1.44	249.6	230.9	193.8	209.9

* Solutions obtained only up to $\theta=90^\circ$

TABLE 3.3

Convergence Tests -
Transfer from Circulating Bubbles and Solid Spheres
with Second Order Reaction

Re	Sc _A	Sc _B	k _A	k _B	Δr _o	No. of Radial Steps	Δθ (deg.)	Position of Outer Boundary	Sherwood Number			AVG. over Entire Surface
									AT 0°	AT 45°	AT 90°	
(i) Circulating Gas Bubbles - Kawaguti-type Profiles												
80	100	100	10 ⁶	10 ⁶	5x10 ⁻⁵	30	3	1.44	466.0	400.9	238.5	237.4
					2.3x10 ⁻⁵	60	3	1.44	466.9	401.9	238.1	237.3
(ii) Circulating Gas Bubbles - Potential Flow Profiles												
200	100	100	10 ⁶	10 ⁶	5x10 ⁻⁵	30	3	1.44	546.6	494.6	341.9	320.1
					2.3x10 ⁻⁵	60	3	1.44	547.6	495.6	341.6	*
					5x10 ⁻⁵	60	3	7.02	546.6	491.8	338.4	317.8
					2.3x10 ⁻⁵	60	1.5	1.44	548.0	495.5	-	*
(iii) Solid Sphere - Kawaguti-type Profiles												
200	500	800	10 ⁴	10 ³	5x10 ⁻⁵	30	3	1.44	245.3	228.0	187.4	143.6
					2.3x10 ⁻⁵	60	3	1.44	244.6	227.8	186.9	143.3

* Solutions obtained only up to θ=90°

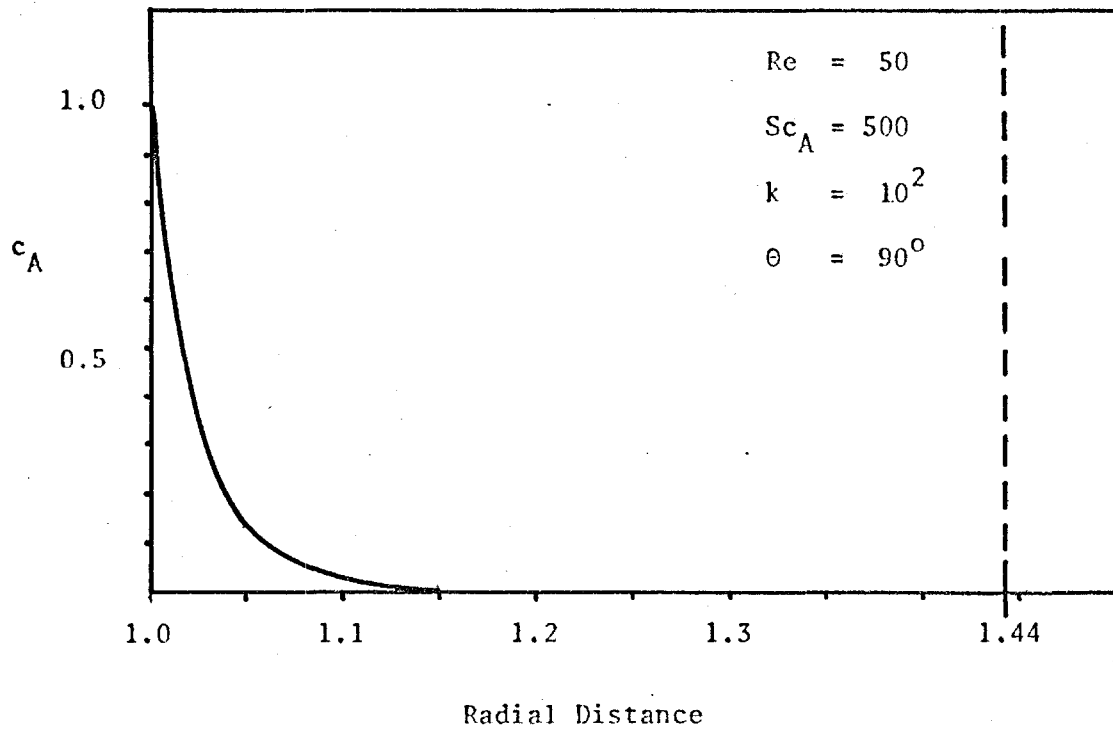


FIGURE 6a. - CONCENTRATION PROFILE - FIRST ORDER REACTION

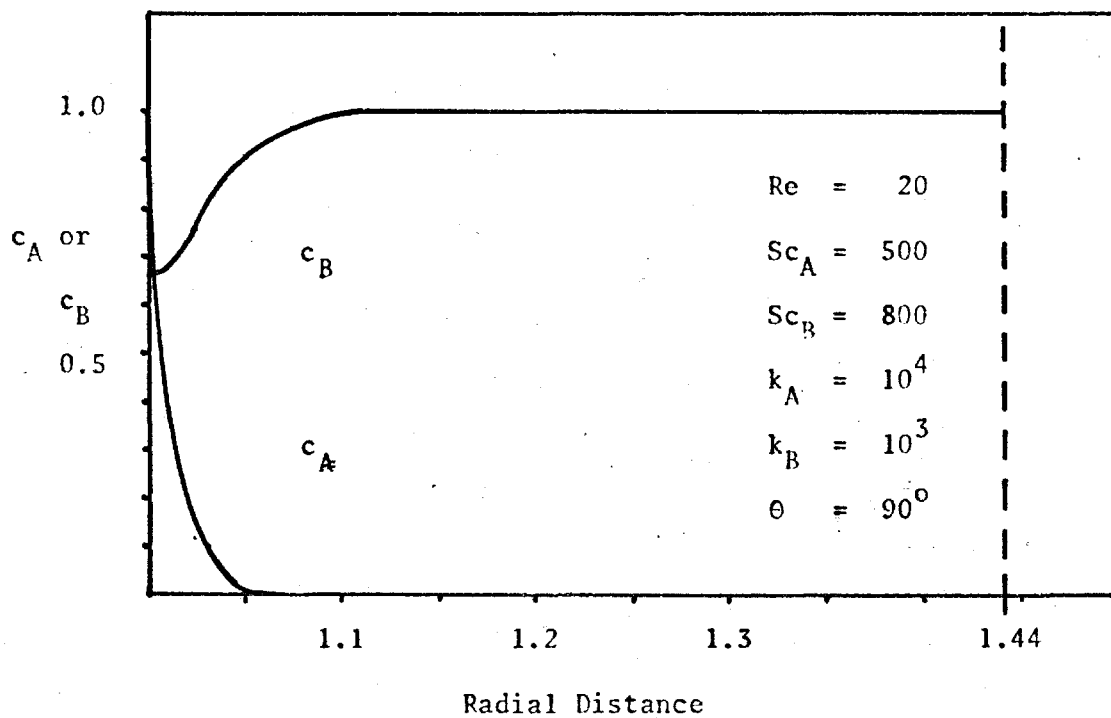


FIGURE 6b. - CONCENTRATION PROFILES - SECOND ORDER REACTION

for all practical purposes. This in itself does not prove that the numerical results obtained are accurate approximations of the exact solutions of the differential equation; convergence is a "necessary" but not a "sufficient" condition. Firm conclusions, regarding the applicability of the model, should await comparisons with previous theoretical and experimental studies.

The comparisons with previous studies is most conveniently done by dividing further discussion into sections concerned with transfer from circulating bubbles and transfer from solid spheres.

3.3.2 Transfer from Circulating Gas Bubbles and Penetration Theory

A recent article by Sideman (S6) has pointed out the equivalence of penetration and potential flow theory for physical mass transfer at high Peclet numbers. He demonstrated how the equations for transfer from circulating bubbles could be transformed into the penetration theory equation. Solutions of either equation resulted in the familiar solution (B3) for physical transfer from a sphere in a potential flow field given by

$$\overline{Sh}^* = 1.13 (Pe)^{\frac{1}{2}} \quad (3.45)$$

Solutions of equation (3.3), with $k=0$, using potential flow profiles are compared with (3.45) in Table 3.4. The agreement between equation (3.45) and the finite-difference solutions is excellent, as it should be.

Beaverstock suggested* that the results for transfer from

* Reviewer's comment on reference (J4) when submitted for publication

TABLE 3.4

Comparison of Finite Difference and
Boussinesq Solutions

Re	Sc _A	Pe _A = Re x Sc _A	\overline{Sh}^* Numerical	\overline{Sh}^* Boussinesq
200	100	2×10^4	160.6	159.8
	500	10^5	358	357
	1000	2×10^5	506	506
500	100	5×10^4	253	253
	500	25×10^4	566	565
	1000	5×10^5	800	799

circulating bubbles could be compared with penetration theory, even when the transfer was accompanied by a first or second order reaction. This reviewer pointed out that the comparison could be made most conveniently if the results of this study were expressed as a plot of "enhancement factor" versus \sqrt{M} . The enhancement factor is defined as the Sherwood number for transfer with chemical reaction divided by the Sherwood number for physical mass transfer. The quantity \sqrt{M} has been widely used (B9, B10, B12), and is a measure of the reaction rate level. Such a plot made it possible to compare the results for transfer from circulating bubbles with Danckwert's analytic solution for first order reaction (D1), as well as with the numerical solutions obtained by Brian et al for the second order case (B9). This comparison is shown in Figure 7, and the calculated values from which the curves were drawn are listed in Tables 3.5 and 3.6. The agreement between the values for transfer from circulating bubbles and penetration theory is excellent for both first and second order reaction. The second order results approach asymptotically the limiting enhancement factor for an infinitely fast second order reaction (B9) given by

$$\phi_a = 1 + \frac{c_B^0}{c_A^s} \sqrt{\frac{D_B}{D_A}} = 1 + \frac{k_A}{k_{BV}} \sqrt{\frac{Sc_B}{Sc_A}} \quad (3.46)$$

It can be concluded that mass transfer with or without chemical reaction from circulating gas bubbles can be described very well by the penetration theory. With the exception of physical transfer under potential flow conditions (S6) this equivalence had not been demonstrated previously. As a result, the penetration theory equations can be used with some confidence in future to describe transfer from circulating bubbles, making it unnecessary to deal with the more complex equations (3.3, 3.4 and 3.5) of this study.

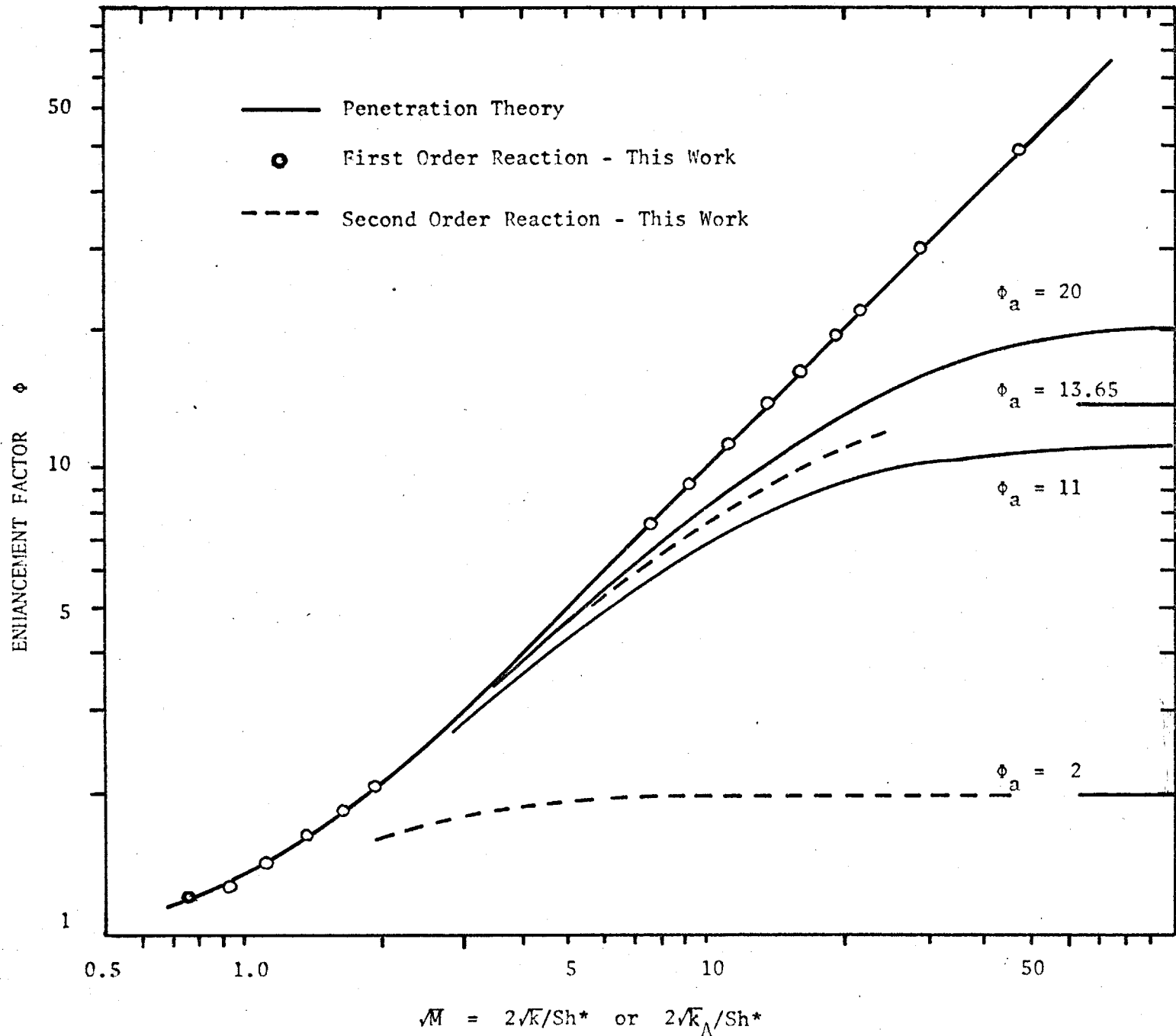


FIGURE 7. - COMPARISON OF THIS WORK WITH PENETRATION THEORY

TABLE 3.5

Mass Transfer from Circulating
Gas Bubbles - First Order Reaction

Re	k	Sc	\overline{Sh}^*	\overline{Sh}	\sqrt{M}	$\phi = \frac{Sh}{Sh^*}$ CALC.	
20 ⁺	10 ²	500	91.0	92.1	0.22	1.01	
		10 ⁴	100	41.9	203	4.8	4.8
			500	91.0	209	2.2	2.3
	10 ⁶	1000	125	222	1.6	1.8	
		10 ⁶	100	41.9	1963	47.7	47
			500	91.0	1963	22.0	22
	1000	125	1963	16.0	16		
	50 ⁺	10 ²	500	148	149	0.14	1.01
		10 ⁴	500	148	235	1.4	1.6
10 ⁶		500	148	1970	13.5	13	
80 ⁺	10 ²	500	270	271	0.07	1.00	
		10 ⁴	100	119	219	1.7	1.8
			500	270	316	0.74	1.2
	1000	372	410	0.54	1.1		
	10 ⁶	100	119	1964	16.8	17	
		500	270	1964	7.4	7.3	
		1000	372	1966	5.4	5.3	
	200 ⁺⁺	10 ⁴	100	161	241	1.2	1.5
			500	358	397	0.56	1.1
1000			506	534	0.40	1.05	
10 ⁶		100	161	1963	12.4	12	
		500	358		5.6		
		1000	506		4.0		
500 ⁺⁺	10 ⁴	100	253	307	0.79	1.2	
		500	566	590	0.35	1.04	
		1000	800	817	0.25	1.02	
	10 ⁶	100	253	1977	7.9	7.8	
		500	566		3.5		
		1000	800		2.5		

* Velocity profiles from Hamielec et al (H2, H3).

** Potential flow velocity profiles

TABLE 3.6

Mass Transfer from Circulating
Gas Bubbles - Second Order Reaction

Re	k_A	k_B	Sc_A	Sc_B	\overline{Sh}^*	\overline{Sh}	\sqrt{M}	$\phi = \frac{\overline{Sh}}{\overline{Sh}^*}$
20 ⁺	10 ⁶	10 ⁶	100	100	41.9	83.3	47.8	1.99
			500	500	91.0	180	22.5	1.98
			1000	1000	125	250	16.0	2.00
80 ⁺	10 ⁶	10 ⁶	100	100	119	237	16.8	1.99
			500	500	270	520	7.6	1.93
			1000	1000	372	717	5.4	1.93
200 ⁺⁺	10 ⁶	10 ⁶	100	100	161	321	12.4	1.99
			500	500	358	702	5.6	1.96
			1000	1000	506	955	4.0	1.89
500 ⁺⁺	10 ⁶	10 ⁶	100	100	253	502	7.9	1.99
			500	500	566	1043	3.5	1.85
			1000	1000	800	1370	2.5	1.72
20 ⁺	10 ²	10	500	800	91.0	92.1	0.22	1.01
	10 ⁴	10 ³			91.0	203	2.2	2.2
	10 ⁶	10 ⁵			91.0	1011	21.9	11.1
50 ⁺	10 ²	10	500	800	148	150	0.14	1.01
	10 ⁴	10 ³			148	232	1.4	1.6
	10 ⁶	10 ⁵			148	1314	13.5	8.9
80 ⁺	10 ²	10	500	800	270	271	0.07	1.00
	10 ⁴	10 ³			270	321	0.74	1.2
	10 ⁶	10 ⁵			270	1616	7.4	6.0

+ Velocity profiles from Hamielec et al (H2, H3).

++ Potential flow velocity profiles

3.3.3 Transfer from Rigid Spheres

(i) Work of Baird and Hamielec: Several theoretical studies of physical mass transfer from spheres, as discussed in Section 1.6, allow for the prediction of local mass transfer rates up to the separation point. In the opinion of the author, the analytic solution obtained by Baird and Hamielec (B1), via the thin concentration boundary layer assumption, is one of the most reliable. In addition, these authors employed the same velocity profiles as this study and, therefore, there should be agreement between their analytic values and those obtained by finite-difference techniques. A typical comparison is shown in Figure 8 where local Sherwood numbers are plotted against angle. The excellent agreement should serve as an additional check on the numerical procedures.

(ii) Disadvantages of Parabolic Equation: It has been previously noted that the use of the parabolic equations (3.3, 3.4 and 3.5) has limited solutions to local mass transfer rates up to the separation point. In some previous theoretical treatments assumptions were made which allowed local rates to be calculated in the vortex region. These have been reviewed in Section 1.6.2 where it was concluded that no one of these theories is exact in the vortex region. Baird and Hamielec's (B1) "fresh fluid" assumption undoubtedly leads to high values; the efforts of Lee and Barrow (L3) do not agree with experimental values; while the theories of Garner and Keey (G6) and Grafton (G8) agree only with the questionable correlations of Garner and co-workers (G4, G5, G6).

When considering purely physical mass transfer from solid spheres

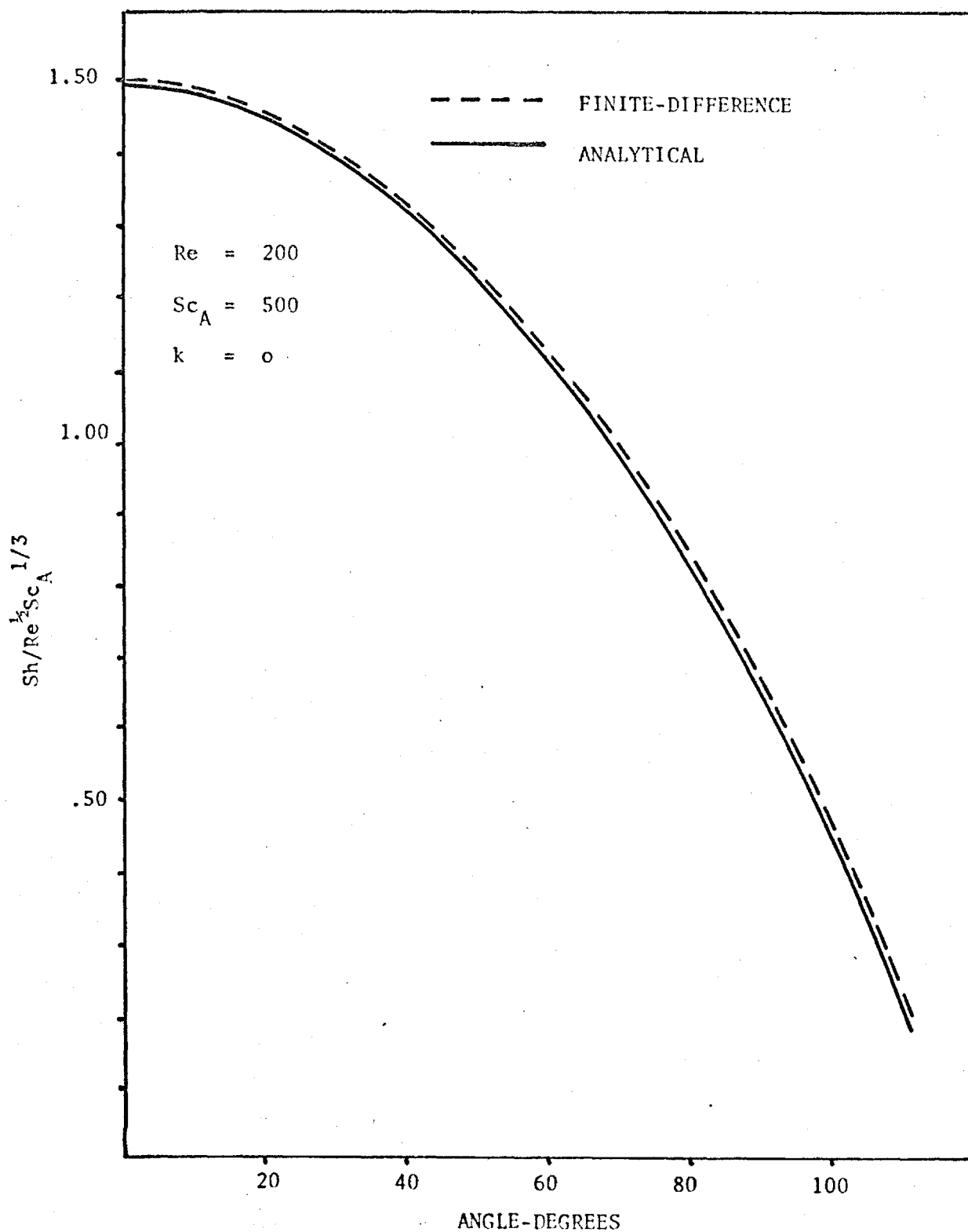


FIGURE 8. - COMPARISON OF FINITE-DIFFERENCE RESULTS WITH ANALYTICAL SOLUTION OF BAIRD & HAMIELEC

the numerical methods of this study are not an improvement on previous theoretical work, since the equations used do not describe transfer in the vortex region. The methods developed, however, do serve as a useful check on previous investigations and allow for the prediction of mass transfer with simultaneous chemical reaction, apparently for the first time. Although only solutions for the first and second order reaction cases have been obtained, the technique for second order reaction is equally applicable to higher order cases (B10).

In this work, average Sherwood numbers based on the entire surface area were calculated by assuming no transfer beyond the separation point. In calculating overall mass transfer rates zeros were inserted for any local value $\theta_j >$ the separation angle. This assumption, although somewhat arbitrary, may not be too far from reality under conditions when there is no vortex shedding. For physical mass transfer it is quite possible that the fluid circulating in the vortex will become almost saturated with transferred material, thus reducing the driving force markedly. In the reaction situation the main stream reactant would probably be rapidly depleted in the vortex, particularly for high reaction rates, and the region may once again be almost saturated with transferred material. At the lower Reynolds numbers, where there is only a small percentage of the surface area in the vortex region, the assumption of zero mass transfer will be less critical. This study has been confined to $Re < 200$, thus avoiding the problem of transient wake behaviour and at the same time keeping the effect of the zero transfer assumption to a minimum. The fact that the velocity

profiles employed here become inaccurate at $Re > 200$ is an additional factor, as previously discussed.

(iii) Comparison with Experimental Correlations: Data dealing with mass transfer and simultaneous reaction from spheres have not been reported. However, physical mass and heat transfer data are in abundance. Making the assumption of no mass transfer beyond the separation point it was possible to obtain average Sherwood numbers from the numerical solutions and to compare them with the available correlations. Results for transfer into liquids, where the Schmidt number values can be expected in the range 10^2 to 10^4 , are presented in Figure 9. The correlations for the benzoic acid-water system are taken from the paper by Rowe et al (R4) who recalculated the results of other workers using a benzoic acid diffusivity of $7.9 \times 10^{-6} \text{ cm}^2/\text{sec}$ at 20°C . This results, in some cases, in correlations which differ slightly from those contained in the original publications. The curve from the numerical procedures of this study was obtained using a Schmidt number of 456. Data obtained from transfer to air experiments are compared in Figure 10 with a numerically obtained curve for a Schmidt number of unity. Also included on this graph are the theoretical results of Ross (R3).

In view of the scatter of the various experimental correlations, a rigorous check on the correctness of the numerical values for transfer from rigid spheres is hampered. It can be concluded from a study of Figures 9 and 10 only that there is general agreement between the finite-difference solutions and the more reliable experimental correlations. The data of Garner and co-workers and of Rowe, at $Sc \approx 1$, are not included in

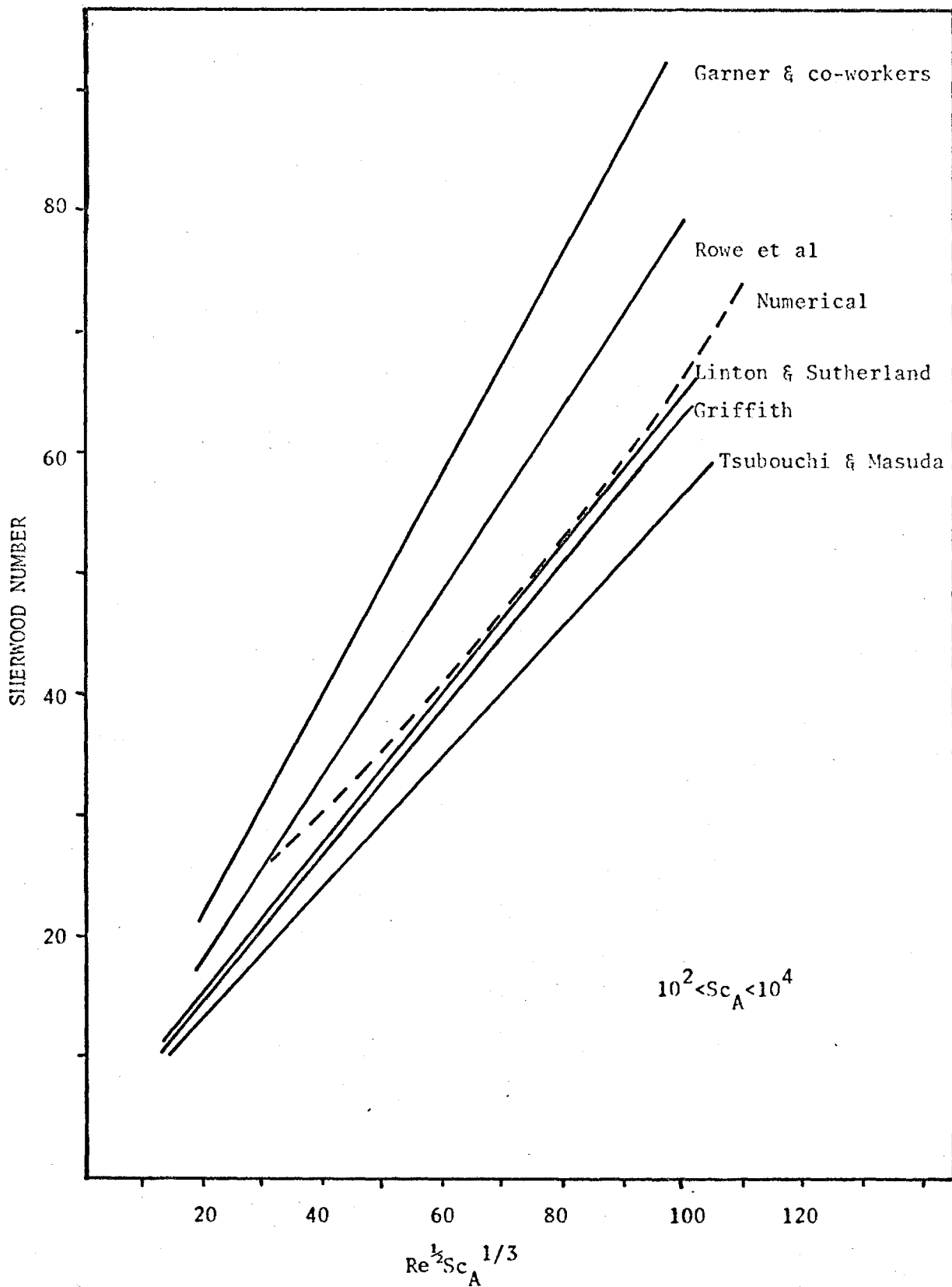


FIGURE 9. - COMPARISON OF NUMERICAL SOLUTIONS WITH EXPERIMENTAL CORRELATIONS - TRANSFER TO LIQUIDS

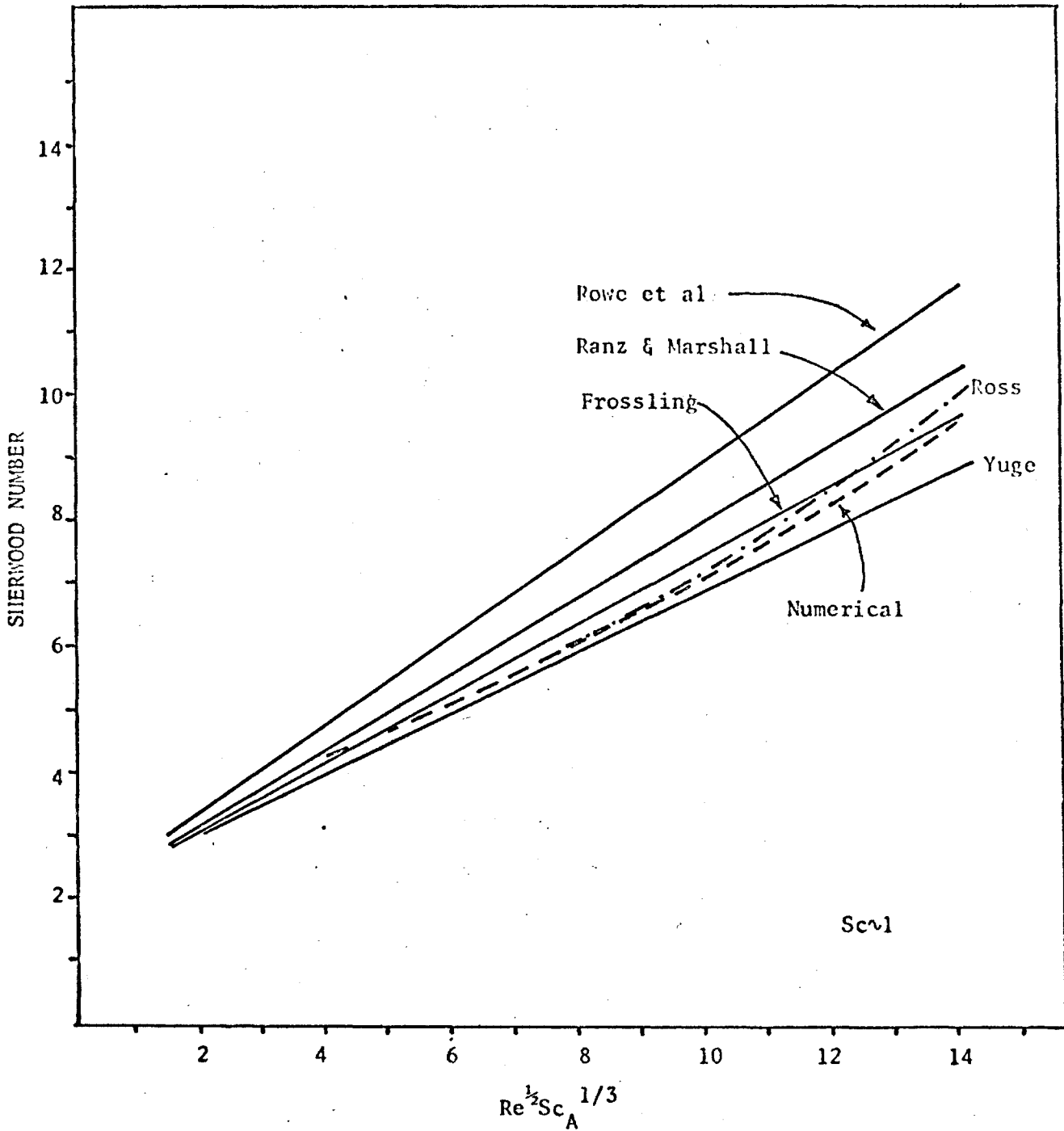


FIGURE 10. - COMPARISON OF NUMERICAL SOLUTIONS WITH EXPERIMENTAL CORRELATIONS - TRANSFER TO AIR

the latter category. The agreement with the theoretical results of Ross is good. Since the latter worker used the same velocity profiles as utilized here, but employed an integral method, this comparison serves as another useful check on the numerical procedures. In fact, it would be expected that the finite-difference technique would give more accurate predictions of mass transfer up to the separation point than an integral method, which requires the assumption of a polynomial form for the concentration profile.

It is interesting to speculate on the effect of Schmidt number on the correlation constant (e.g. constant = 0.60 for the Ranz and Marshall correlation). Correlations obtained from data for transfer into air have, on the average, lower coefficients than those for transfer into liquids. The numerical solutions obtained predict the same effect; a straight line through these solutions would have a slope of approximately 0.55 from $Sc \sim 1$, and a value of about 0.65 for $Sc \sim 500$. These observations lend support to the many discussions (K2, R4) regarding the adequacy of the simple relationship usually used for correlation purposes, i.e.

$$Sh = 2 + A Re^{1/2} Sc^{1/3} \quad (3.47)$$

It is usually concluded that equation (3.47) is not always suitable and some theories suggest that the Schmidt number exponent should depend on the Schmidt number value (K2). This work confirms that equation (3.47) is somewhat inadequate but does not allow the question to be resolved completely.

(iv) Rate of Transfer at Frontal Stagnation Point: Several boundary layer developments have considered transfer from the frontal stagnation

point of a solid sphere. Frossling (F5) has obtained the following relationship:

$$\left[\text{Sh}/\text{Re}^{1/2} \text{Sc}^{1/3} \right]_{\theta=0}^{\circ} = 1.53 - 0.190/\text{Sc}^{1/3} \quad (3.48)$$

for $0.1 < \text{Sc} < \infty$

Linton and Sutherland (L7) used the same approach to obtain

$$\left[\text{Sh}/\text{Re}^{1/2} \text{Sc}^{1/3} \right]_{\theta=0}^{\circ} = 1.478 - 0.158/\text{Sc}^{1/3} \quad (3.49)$$

for $0.5 < \text{Sc} < \infty$

Values obtained from the above equations along with the theoretical results of Ross (R3) and this worker are listed in Table 3.7. At values of $\text{Sc} \geq 1$ the agreement at the higher Reynolds numbers is excellent. That the agreement is somewhat less at the lower Reynolds number is not surprising since thin boundary layer assumptions would not be expected to hold at Reynolds numbers much below 200. The agreement among values at a Schmidt number of 500 is better overall. The improved agreement between predicted values at a Reynolds number of 100 is probably due to the thinner concentration boundary layer present under high Schmidt number conditions. At lower Schmidt numbers, the relatively thick concentration boundary layer no doubt aggravates any inaccuracy introduced by the assumption of a thin hydrodynamic boundary layer.

3.3.4 Conclusions

The proposed mathematical model has been solved via finite-difference techniques, and the results obtained have been compared with previous theoretical and experimental values.

Results for mass transfer from circulating gas bubbles with

TABLE 3.7

Mass Transfer from Frontal
Stagnation Point

Re	Sc	$\left[(\text{Sh} - 2) / \text{Re}^{1/2} \text{Sc}^{1/3} \right]_{\theta=0^\circ}$	Source
100	1.0	1.13	Ross (R3)
100	1.0	1.04	This work
200	1.0	1.33	Ross (R3)
200	1.0	1.37	This work
B.L.*	1.0	1.34	Frossling (F5)
B.L.	1.0	1.32	Linton & Sutherland(L7)
100	500	1.37	This work
200	500	1.49	This work
B.L.	500	1.51	Frossling (F5)
B.L.	500	1.45	Linton & Sutherland(L7)

* Boundary Layer theory

first or second order chemical reaction are in excellent agreement with penetration theory, when compared on an 'enhancement factor" basis.

Predicted rates of forced convection transfer from rigid spheres are in reasonable agreement with correlations obtained from heat or mass transfer experiments.

Experimental data for mass transfer with first or second order reaction from rigid spheres must be obtained in order to complete the evaluation of the model.

4. EXPERIMENTAL

4.1 Introduction

(i) Apparatus: No experimental work has been reported on mass transfer with chemical reaction from single spheres. In order to further evaluate the model developed in the previous section, it was necessary to obtain such data under forced convection conditions at intermediate Reynolds numbers. Previous studies dealing with physical transfer from single spheres have usually consisted of fixing the test sphere in a flowing liquid (G4, G5, G6, L7, R1, R3, R4, T3, Y3). A "water tunnel" apparatus suitable for the study of transfer into water was available in the Chemical Engineering Department of McMaster University. The apparatus contained copper tubing, brass flanges, and cast iron in the form of a Venturi meter. The presence of these materials limited the choice of a suitable gas-liquid reacting system.

(ii) Chemical System: The requirements of a reacting system were threefold:

1. The chemicals should not attack the water tunnel material, at least not to such an extent that the apparatus would be damaged, or the absorption or chemical reaction rates affected.
2. The gas-liquid system should have a high rate of reaction, i.e., there should be a large increase in absorption rate with increasing reactant concentration in the liquid. This was desirable since it would result in easily detectable increases in absorption rates, in spite of normal experimental scatter, while utilizing relatively

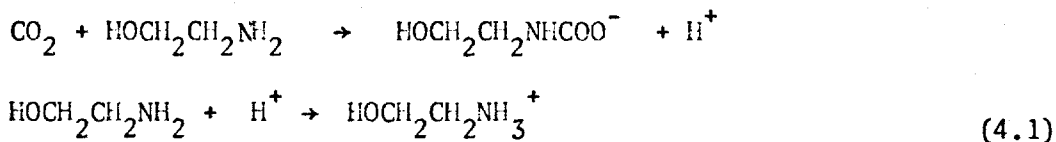
dilute solutions.

3. The kinetics of the reacting system should be readily available, thus eliminating the necessity for auxiliary kinetic studies.

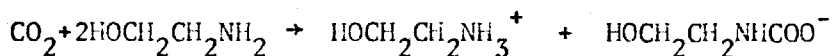
The first requirement made it impossible to consider the sodium and potassium hydroxide solutions used by other workers (D3, N1, R2) in studies with laminar liquid jets. The second requirement eliminated the buffer solutions which have been the subject of several investigations by Danckwerts and co-workers (D3, R2, S2). After a careful study of the literature and a few preliminary experiments, it was decided that the system carbon dioxide-monoethanolamine was most suitable for this study. Other carbon dioxide-amine systems have been investigated (e.g. monoisopropanolamine(S2), diethanolamine (N2)), but none so extensively as monoethanolamine (A5, A6, C6, E1).

4.2 System and Reaction Mechanism

The carbon dioxide-monoethanolamine system has been the subject of investigations by Emmert and Pigford (E1), Astarita (A5, A6), and Clarke (C6) using mainly the laminar liquid jet apparatus. The reaction mechanism has been explained by these authors in terms of the two main reactions:



Yielding the overall reaction:



The second reaction occurs instantaneously, while the first reaction,

although fast, is the limiting step (A6). The reaction rate constant for the rate controlling step has been determined by Faurholt et al (J1) as 3190 liters/mole-sec. at 18°C (C1, E2). Using an activation energy of the order of 12-13 kcal (C6), the reaction rate constant at 25°C can be estimated as 5400 liters/mole-sec as reported by Emmert and Pigford (E1). Astarita (A5), on the other hand, reports this same value but at 21.5°C. Clarke (C6) reported values around 7000 liters/mole-sec at 25°C which he states were calculated from the data of Faurholt et al (J1). Since the value used by Emmert and Pigford was obtained directly from Faurholt via a "private communication", the quantity reported by these authors was taken as the most reliable and used throughout this work. The sensitivity of the theoretical calculations to the rate constant chosen will be discussed in a subsequent section.

4.3 Apparatus

The water-tunnel used to carry out the absorption rate measurements is shown schematically in Figure 11. The constant head tank on the top level is approximately 24.5 feet above the bottom circulation tank. The connecting lines were of two inch copper tubing with streamlined fittings to reduce turbulence at the connections. The test section was constructed of lucite. The capacity of the system is approximately 55 Imperial gallons. Coarse temperature control was effected in the bottom tank where cooling water was passed through a copper coil and steam could be admitted within the vessel jacket. This coarse control coupled with the use of an ordinary laboratory Haake thermostat unit in the top tank allowed the temperature to be controlled within $\pm 0.1^\circ\text{C}$. The pump was a centrifugal type driven by

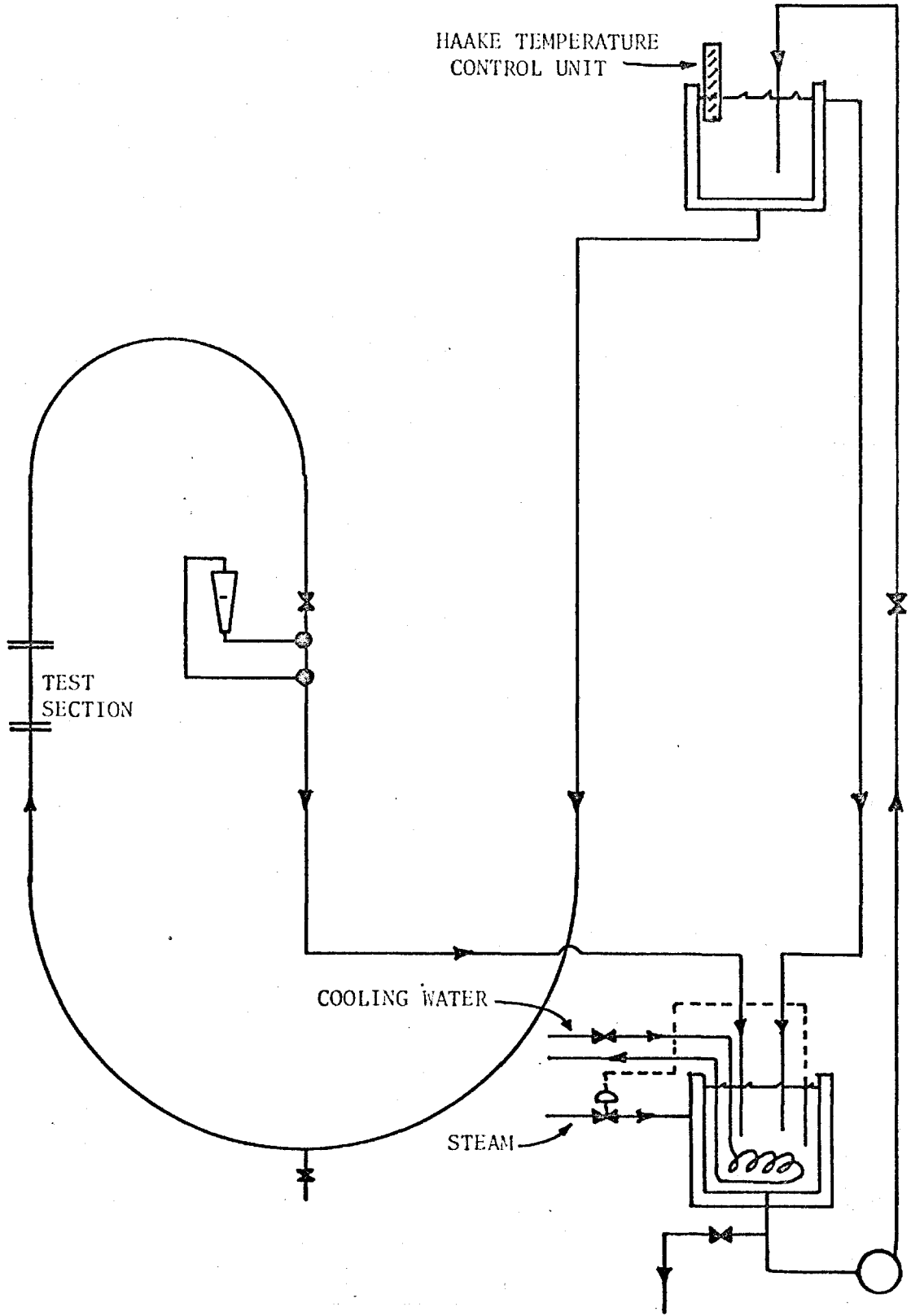


FIGURE 11. - SCHEMATIC OF WATER-TUNNEL APPARATUS

a 3 h.p. motor. Liquid flow rates were determined by means of Fisher-Porter glass rotameters equipped with stainless steel floats. Calibration curves for these rotameters are shown in Appendix E.

Details of the test section and gas feeding apparatus are given in Figure 12. The gas was fed from a gas cylinder, through a copper coil, and then bubbled through a Fisher-Milligan gas washer where it became saturated with water vapor. The constant temperature bath was maintained at the same temperature (25°C) as the liquid in the water tunnel. The syringe used to feed the gas bubble was a Manostat micropipet syringe with a 10 c.c. capacity. It was modified slightly to reduce the amount of gas leakage. Details of the gasket arrangement are shown in Figure 13.

The gas bubble was formed on a tapered Teflon tip which had been fitted over stainless steel tubing. Dimensions and particulars of the bubble support employed in this study are shown in Figure 14.

The carbon dioxide employed was Coleman grade (content of CO_2 99.99⁺%) obtained from the Matheson Gas Company. Technical grade monoethanolamine was supplied by the Dow Chemical Company of Canada Limited. Distilled water was used for all runs.

4.4 Operating Procedure

The apparatus was flushed out for 3-4 hours before each experiment with a flow of water from the regular city main. After draining, the water-tunnel was filled with distilled water. At this point a small flow of gas had to be maintained through the gas feeding apparatus sufficient to prevent the back flow of water into the syringe.

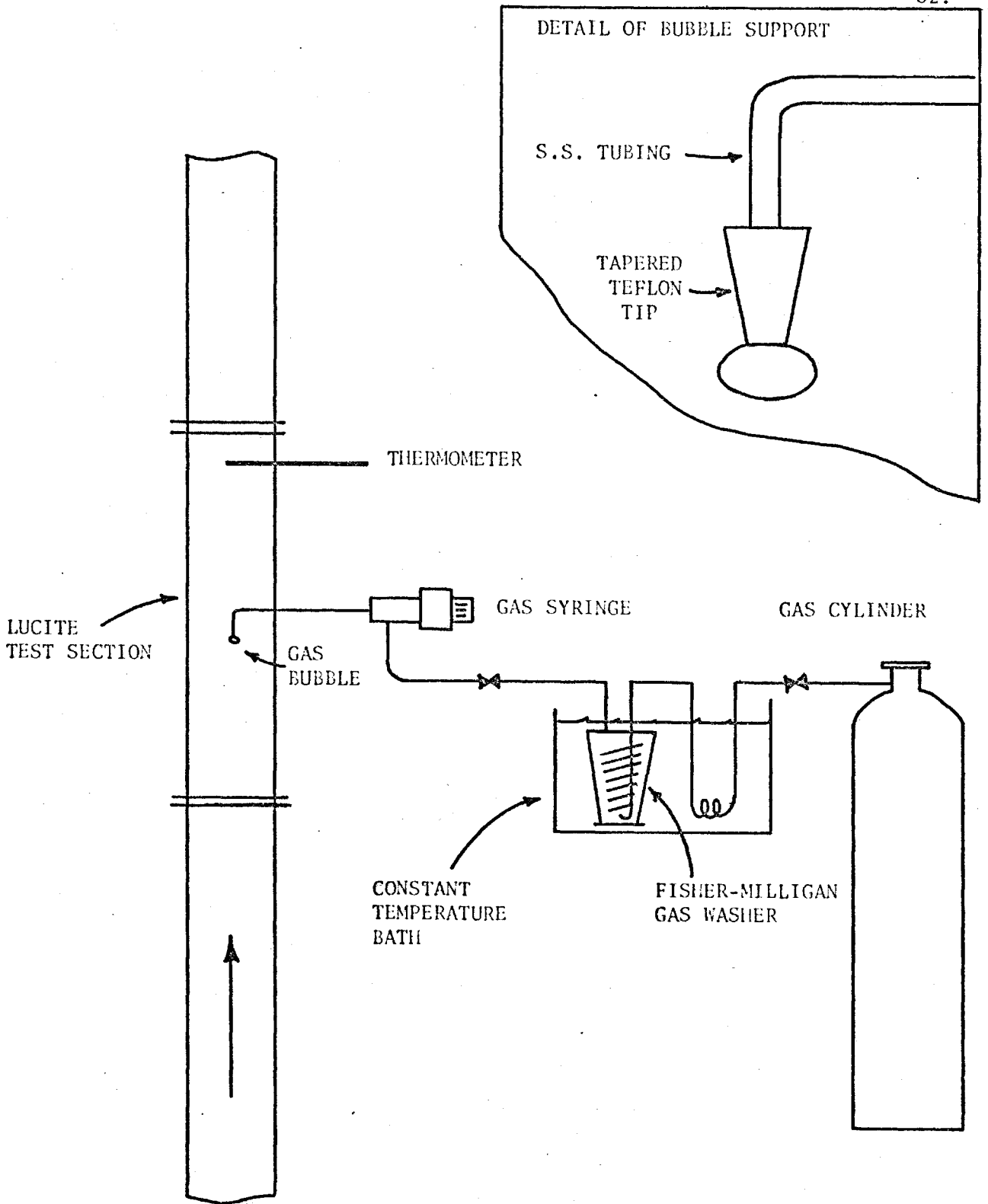


FIGURE 12. - DETAILS OF GAS FEEDING APPARATUS

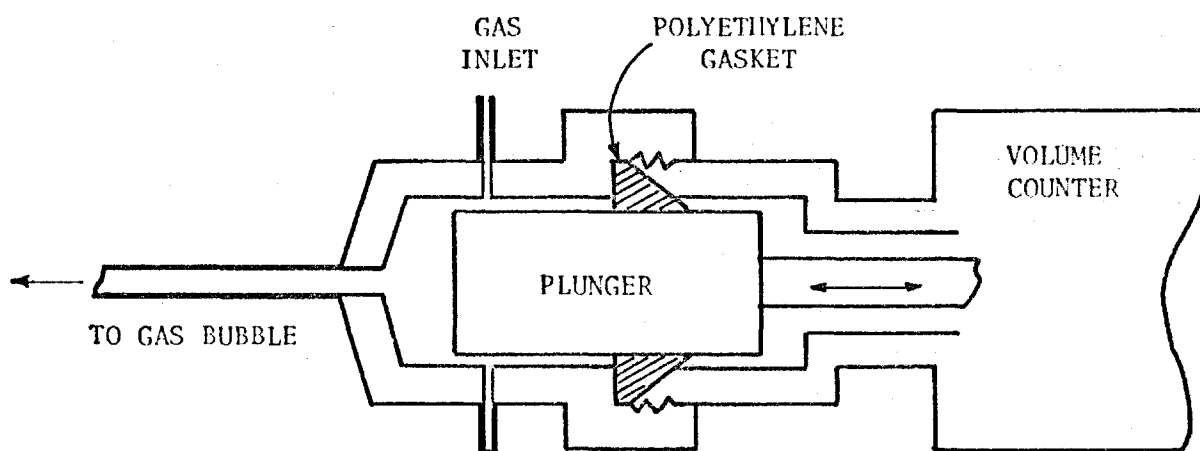


FIGURE 13. - DETAILS OF GAS SYRINGE

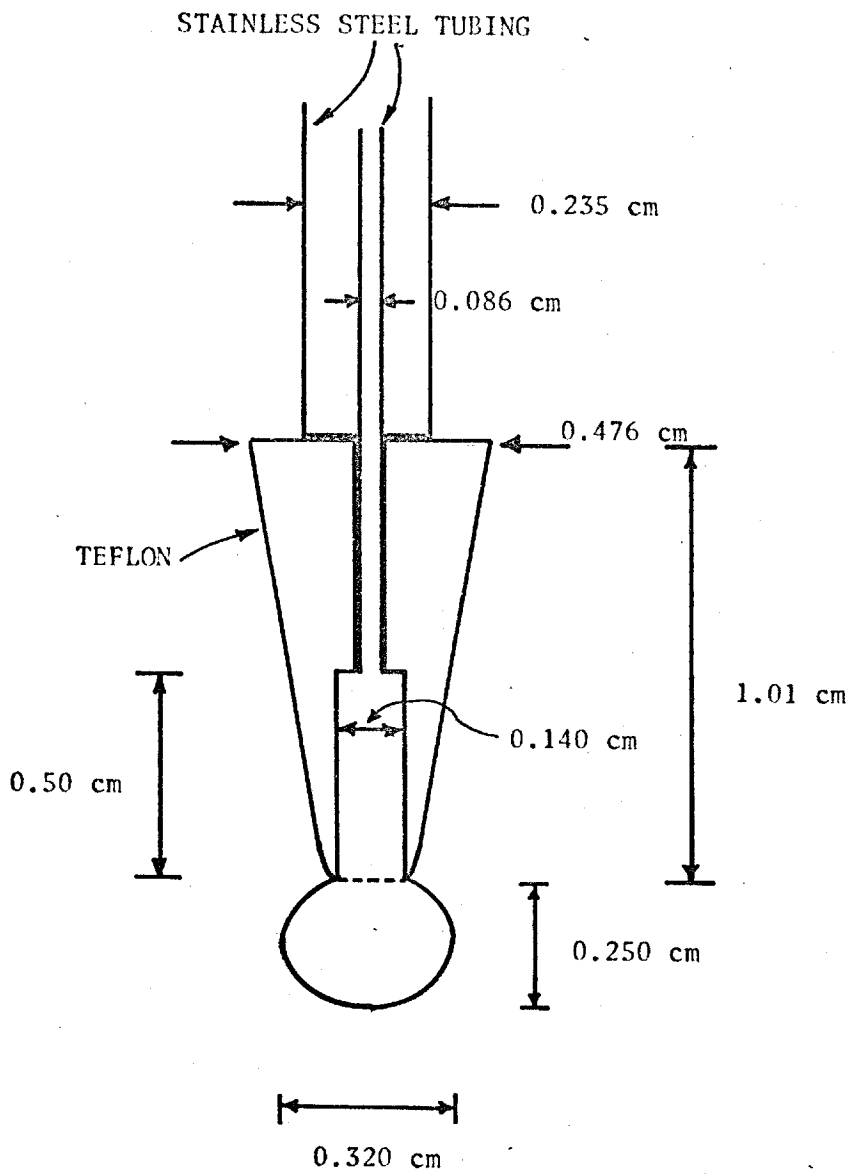


FIGURE 14. - BUBBLE HOLDER DETAILS

Once the temperature had been brought to the 25.0°C level used throughout the study, it was possible to begin absorption rate measurements.

The valve between the syringe and the gas washer was closed and a fresh bubble formed on the Teflon tip. The size was fixed by observing the bubble through a cathetometer (Griffin & George Limited, No.P.369). The top of the bubble was maintained level with the cathetometer cross-hair, a measured distance from the Teflon tip. Only one bubble size was employed in this work, measuring 2.5 mm from the bubble support to bubble top. Gas was fed manually from the syringe as required. The volume absorbed was obtained by recording syringe volume counter readings over several consecutive timed intervals. Normally the volume readings were taken every 30 seconds over a total period of from four to six minutes. Measurements were begun from the time a bubble of the proper size was formed. This formation step usually required five to ten seconds. Two persons were needed to carry out the experiments; one to maintain a bubble of fixed size, and the other to record volumes at each time interval.

5. RESULTS AND DISCUSSION

Absorption rates were determined at each of four monoethanolamine concentrations: 0.0, 0.33, 0.66 and 0.99 mole %. At higher concentrations, it proved difficult to maintain a bubble of constant size over any reasonable interval. Four liquid flow rates were studied. The centerline velocities were 1.12, 1.82, 3.68 and 5.8 cm./sec. Attempts at operation with higher centerline velocities were not successful as the bubble behaviour and observed absorption rates became quite erratic. All studies, therefore, were carried out with relatively low velocities. The corresponding pipe Reynolds numbers were always <1700. Visual observations of dye flowing through the test section offered supporting evidence that the flow was always laminar.

Duplicate runs of each of the non-zero monoethanolamine concentrations were carried out. Absorption rates for carbon dioxide into distilled water were determined a total of six times at each of the four flow rates.

Bubble size and bubble support dimensions were not varied in this study.

5.1 Absorption Rates from Single Gas Bubbles

Typical results of absorption rate versus time measurements are shown in Figure 15. The lower curve is for the absorption of carbon dioxide into distilled water, while the upper curve is for absorption into an aqueous monoethanolamine solution.

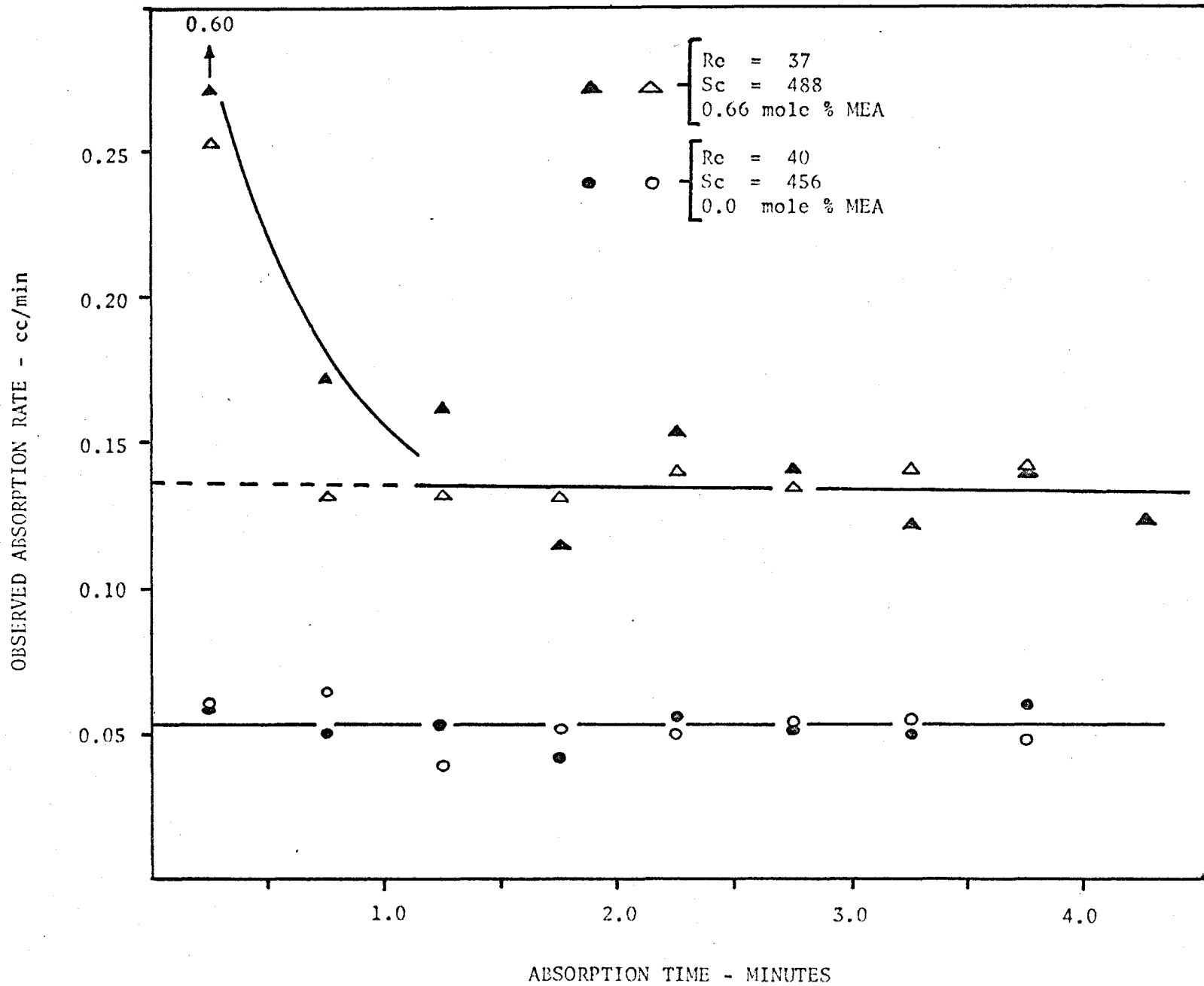


FIGURE 15. - SINGLE GAS BUBBLE RESULTS - ABSORPTION RATE VS. TIME

(i) Initial Falling Rate Period: The rapid initial decrease in rate for the reaction case was never observed for the carbon dioxide-water system. It is quite likely that such an initial period exists for this system also; however, it may be too short in duration to be detected by readings at 30 second intervals. The initial decrease is probably due to the accumulation of surfactant on the bubble surface which tends to inhibit, and finally prevent completely, any interfacial movement. Additions of surfactants, in amounts over and above that already present through normal contamination, did not appear to speed up the accumulation process. However, interpretation of the results was difficult because of changes in bubble shape caused by these additions. A study of this decay effect was not considered desirable, since long periods were required to wash out any surfactant materials added to the water-tunnel.

In this study the bubble, when formed, is probably fully circulating. The rapid accumulation of surfactant quickly changes the bubble behaviour to that of a noncirculating bubble, which, for theoretical studies, can be considered as a rigid sphere. The mass transfer rates recorded during the initial period for the carbon dioxide-monoethanolamine system are very high. The resulting surface flux is appreciable, and probably hinders the accumulation of surfactant to a much larger extent than for the no reaction case. Thus it would be expected that the decay period would be of longer duration in the carbon dioxide-monoethanolamine experiments. The erratic absorption rate measurements obtained at higher velocities (>5.8 cm) were probably the result of surfactant being swept from the interface periodically. Measurements under these high velocity

conditions usually exhibited several periods of rapidly decreasing absorption rates identical to the initial behaviour shown in Figure 15.

(ii) Linear Portion of Curve, Absorption Rate vs. Time: Beyond the initial period the absorption rate was almost constant with time. In about one-half the experiments reported, there was no significant* decrease in absorption rate over the linear part of the curve. Any decrease in absorption rate was probably a result of the accumulation of oxygen and nitrogen in the bubble. A de-gassing effect was confirmed by a simple experiment outlined in Appendix I. It was not possible to deaerate the distilled water used in this study, but the effect of inert gas accumulation which results is not considered to be critical. If the amount of oxygen and nitrogen transferred into the bubble were large, the apparent rate of carbon dioxide absorbed would be lowered, as the amount absorbed would have been partially replaced by the inert gases. In addition, the solubility and, consequently, the concentration driving force of the carbon dioxide in the liquid would be markedly reduced. A significant transfer of inerts into the bubble would then cause a large decrease in apparent absorption rate with an eventual approach to zero. The decreases in absorption rate in this study were, when significant, very small. It can, therefore, be concluded that only a small quantity of inert gas could have accumulated in the bubble during the absorption period.

(iii) Analysis of Data: Only the data points which appeared to be in the linear region were considered for each run. The small effect of the gradual accumulation of inerts was eliminated by putting the best least

* All statistical tests were carried out at the 95% confidence level.

squares straight line through the data, in the linear region, and extrapolating to zero time, as shown in Figure 15. The intercept then gives the absorption rate for a single, noncirculating gas bubble before the accumulation of inerts. Absorption rate measurements for 2 to 4 bubbles were combined in calculating the transfer rate for any one condition of flow rate and concentration level.

5.2 Calculation Procedure

The following expression may be written by way of definition of the liquid phase mass transfer coefficient:

$$N_{\text{CO}_2} = k_L A_b (c^S - c_\infty) \quad (5.1)$$

Where N_{CO_2} is the absorption rate and A_b is the bubble surface area. Equilibrium at the gas-liquid interface has been assumed, and c^S is therefore the solubility of carbon dioxide in the solutions. Clarke (C6) has shown that any change in carbon dioxide solubility due to the presence of monoethanolamine is unlikely. The concentration of carbon dioxide in the bulk was always negligible during the experiments and, therefore c_∞ was zero. Bubble surface areas were determined from photographs. The details are given in Appendix F.

The value of N_{CO_2} was calculated from the least squares analysis outlined in the previous section. Corrections were applied for the pressure at the test section location (5.2 p.s.i.g.) and "leakage rate". The latter, a measure of the rate at which carbon dioxide escaped from the gas syringe into the atmosphere, was determined with the aid of a sensitive differential pressure gauge (see Appendix G). This leakage correction, normally 0.016 c.c./min., when applied to the high absorption rate values obtained

for the CO₂-MEA system, amounted to only a small percentage of the observed rates. For the CO₂-water system, with its much lower transfer rates, the correction amounted to as much as 30% of the observed values.

From the corrected absorption rates the value of k_L could be calculated from equation (5.1), and the Sherwood number could be obtained from equation (3.14):

$$\text{Sh} = 2Rk_L/D_{\text{CO}_2} \quad (5.2)$$

where R was the radius of the gas bubble, and D_{CO_2} the diffusivity of carbon dioxide in water at 25°C. The radius was obtained by approximating the gas bubble by a sphere having the same surface area (Appendix F). The value for the carbon dioxide diffusivity was taken from the work of Davidson and Cullen (D4). Clarke (C6) has indicated that the presence of monoethanolamine in solution is unlikely to affect the diffusivity.

In order to correlate the data in terms of Reynolds and Schmidt numbers, additional information such as liquid velocities, viscosities, monoethanolamine concentrations and diffusivity was required.

The pipe Reynolds numbers based on the measured volume flow ranged from 300 to 1600. Since the flow was, therefore, always in the laminar region, and the test section is preceded by more than 20 feet of pipe containing no sharp elbows or other obstructions, a well developed parabolic velocity profile was obtained in the test section (K5). A knowledge of the total flow rates then readily permitted calculation of the centerline velocities. As the bubble diameter was only 6% of the test section diameter the center line velocity, rather

than the average velocity, was used.

A Cannon-Fenske calibrated viscometer was used to determine the viscosities of the monoethanolamine solutions.

Concentrations were determined by measuring the solution refractive index. Calibration curves are presented in Appendix E.

A wide range of values for the diffusivity of monoethanolamine in water has been reported in the literature (I1, T2). The interferometric technique used by Thomas and Furzer (T2) is quite accurate, and their experimentally determined diffusivity values are in reasonable agreement with theoretical predictions (I1). The results of Thomas and Furzer were used in this study. The effect of a different choice of diffusivity value on the theoretical results of this investigation will be discussed.

Values of the various parameters are listed in Table 5.1. It should be noted that a viscosity correction has not been applied to the diffusivity of carbon dioxide, since this correction would be smaller than the scatter in reported values (D4). Similarly, no viscosity correction was applied to the monoethanolamine diffusivity.

5.3 Results

(i) Experimental Correlations: The experimental results are shown in Table 5.2 and presented as a Sh vs. $Re^{1/2} Sc^{1/3}$ plot in Figure 16. The latter representation was used to facilitate comparison with previous mass transfer results and with the theoretical work of the previous section. In all cases the data were fitted with best least squares straight lines. The following relationships were obtained

$$\text{for 0 mole \% MEA} \quad Sh = 23 + 0.52 Re^{1/2} Sc^{1/3} \quad (5.3)$$

TABLE 5.1

Physical Properties at 25.0°C

Conc. of MEA mole %	Viscosity c.p.	Refractive Index	Diffusivity		Solubility of Carbon dioxide gm. moles/liter
			CO ₂ cm ² /sec	MEA cm ² /sec	
0	0.889	1.3339	1.95x10 ⁻⁵	1.07x10 ⁻⁵	0.0338
0.33	0.923	1.3352	1.95x10 ⁻⁵	1.07x10 ⁻⁵	0.0338
0.66	0.953	1.3366	1.95x10 ⁻⁵	1.07x10 ⁻⁵	0.0338
0.99	0.984	1.3379	1.95x10 ⁻⁵	1.07x10 ⁻⁵	0.0338

TABLE 5.2

Experimental Results -
Absorption from Carbon dioxide Bubbles
into Monoethanolamine Solutions

CONC. MEA mole %	Re	Sc _A	\bar{Sh} observed	\bar{Sh} corrected*
0.0	39.8	456	73.6	53.8
			60.8	41.0
			68.4	48.6
			66.8	47.0
			66.3	46.5
			60.3	40.5
	64.8	456	83.3	63.5
			69.0	49.2
			86.7	66.9
			86.6	66.8
			73.5	53.7
			70.8	51.0
	131	456	83.3	63.5
	150	456	80.6	60.8
			96.7	76.9
			101	81.0
			81.3	61.5
			87.3	67.5
	207	456	106	86.0
			98.3	78.5
92.3			72.5	
98.8			79.0	
108			88.0	
221	456	107	87.0	

TABLE 5.2 (Continued)

CONC. MEA mole %	Re	Sc _A	\bar{Sh} _{observed}	\bar{Sh} _{corrected*}
0.33	38.5	472	121	101
			114	94.0
	62.5	472	110	90.0
			142	122
	126	472	156	136
144	472	173	153	
	213	472	210	190
0.66	37.2	488	161	141
			173	153
	60.4	488	189	169
			183	163
	140	488	231	211
		242	222	
	193	488	269	249
			307	287
0.99	36.3	503	174	158
			178	154
	59.2	503	197	177
			239	219
	137	503	319	299
		312	292	
	189	503	367	347
			357	337

* corrected for leakage rate of 0.0156 cc/min

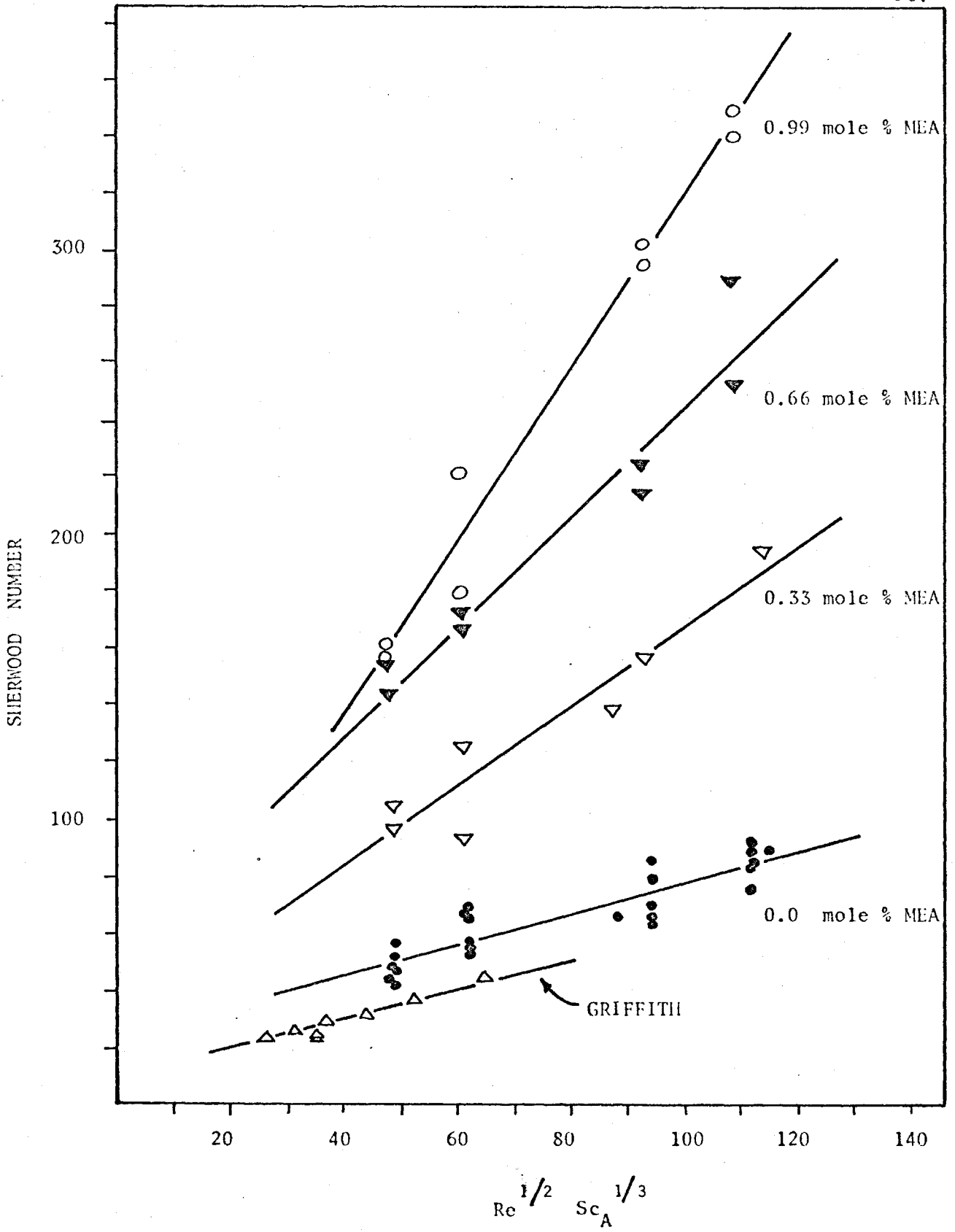


FIGURE 16. - EXPERIMENTAL RESULTS

$$\text{for 0.33 mole \% MEA} \quad \text{Sh} = 26 + 1.37 \text{Re}^{\frac{1}{2}} \text{Sc}^{\frac{1}{3}} \quad (5.4)$$

$$\text{for 0.66 mole \% MEA} \quad \text{Sh} = 52 + 1.90 \text{Re}^{\frac{1}{2}} \text{Sc}^{\frac{1}{3}} \quad (5.5)$$

$$\text{for 0.99 mole \% MEA} \quad \text{Sh} = 12 + 3.04 \text{Re}^{\frac{1}{2}} \text{Sc}^{\frac{1}{3}} \quad (5.6)$$

Figure 16 also includes the data obtained by Griffith (G9) for the carbon dioxide-water system. These data were fitted with the least squares straight line to obtain

$$\text{Sh} = 11 + 0.50 \text{Re}^{\frac{1}{2}} \text{Sc}^{\frac{1}{3}} \quad (5.7)$$

Griffith, on the other hand, correlated his data by forcing the straight line fit through the theoretical limit of $\text{Sh}=2$ at $\text{Re}^{\frac{1}{2}} \text{Sc}^{\frac{1}{3}} = 0$, and found

$$\text{Sh} = 2 + 0.72 \text{Re}^{\frac{1}{2}} \text{Sc}^{\frac{1}{3}} \quad (5.8)$$

If the data of this work are fitted by a straight line through the same limiting value (not necessarily a reasonable step since neither Griffith's data, nor the data obtained in this investigation, show any inclination to approach this value despite its theoretical significance) the correlation becomes:

$$\text{Sh} = 2 + 0.78 \text{Re}^{\frac{1}{2}} \text{Sc}^{\frac{1}{3}} \quad (5.9)$$

The results of this study are somewhat higher than those obtained by Griffith. A statistical evaluation showed that the slopes, as expressed by the coefficients 0.52 and 0.50 in equations (5.3) and (5.7), are not significantly different. This discrepancy is most likely due to some systematic error.

It should be emphasized that neither the discrepancy between

correlations, nor the scatter of the experimental data, was excessive or unusual. For example compare the several correlations for benzoic acid-water in Figure 9 and the variation in the heat transfer results of Ross (R3).

(ii) Sources of Error: The measurement of rates of gas leakage from the syringe is the most obvious source of error. The apparatus could not be tested for leakage rate without being partially dismantled and connected to a differential pressure gauge as detailed in Appendix G. Although test conditions were as close as possible to the conditions under which absorption measurements were taken, the possibility of a systematic error in this step cannot be dismissed.

A second possible reason for the observed discrepancy may have been the result of bubble support differences. Griffith used a support which covered less than 5% of the surface area of the equivalent sphere. In this investigation the support was somewhat larger and covered approximately 13% of the area. The presence of the bubble support, in effect, reduces the area available for mass transfer in the vortex region. Since local transfer rates in this region are expected to be lower than elsewhere on the surface, by removing a larger portion of this area, the resulting observed average transfer rates might be expected to be higher than in Griffith's case. An experimental study of the effect of bubble support size on observed mass transfer rates was not included as part of this study.

A third related factor to be considered is the hydrodynamic effect of the bubble support. It is conceivable that changes in the location of the separation point could result from the presence of

the bubble holder. Any effect of this nature would probably be more pronounced in this study since the support was larger than used by Griffith (G9). Velocity profiles would be affected over only a small area of the bubble, and the effect on overall absorption rates would be expected to be small. A theoretical investigation of the effect of an obstruction behind a sphere may now be possible utilizing the numerical procedures developed recently by Hamielec et al (H4, H5). It is likely that by a suitable alteration of the boundary conditions, which these equations are made to satisfy, it would be possible to obtain a reasonable representation of flow around a sphere attached to a support of arbitrary size and shape.

In general, it can be concluded that the discrepancy between the results of this work and Griffith's data can be explained in a qualitative manner. In view of the scatter in mass or heat transfer correlations reported in the literature, it is not possible to draw any firm conclusions regarding the accuracy of the physical mass transfer data of this investigation. If, as has been argued, the main source of error can be attributed to the gas leakage measurement, then the results obtained for the carbon-dioxide-monoethanolamine system should be more reliable, since the leakage corrections in this case were a much smaller percentage of the observed absorption rates.

(iii) Natural Convection: In the development of the mathematical model it had been assumed that natural convection effects were negligible. A check was made to determine whether natural convection could be expected under the experimental conditions of this work. The relationship developed

by Garner and Keey (G6) was employed. These authors stated that forced convection alone would be significant if

$$\text{Re} > 0.4 \text{Gr}^{1/2} / \text{Sc}^{1/6} \quad (5.10)$$

The right hand side of equation (5.10) was evaluated using the most extreme case, that of the highest monoethanolamine concentration in the bulk and pure water at the interface. It was found that forced convection alone should be significant for $\text{Re} > 10$. Since the Reynolds number of this study were greater than 35 no natural convection effects would be expected. This is reasonable when it is noted that the density of monoethanolamine solutions are not markedly different from the density of water over the range studied (T2). Thus the buoyancy forces would not be large.

Observations of refractive index patterns around the gas bubble, visible when absorption into monoethanolamine solutions was taking place, confirmed that natural convection could not be a major factor in this study. The straight line fitted through the physical mass transfer data did not pass through the limiting value of $\text{Sh} = 2$ at $\text{Re}^{1/2} \text{Sc}^{1/3} = 0$ (see equation 4.3). This does not mean that natural convection was a factor as this can be explained away on theoretical grounds. For creeping flow and high Schmidt numbers $\text{Sh} \propto \text{Re}^{1/3} \text{Sc}^{1/3}$ and the slope is a function of Reynolds number on the type of plot employed here (Figure 16). Thus a linear extrapolation is not valid and should not be expected to give an intercept value of 2.

(iv) Interfacial Phenomena: Interfacial activity, if present, would be expected to result in higher mass transfer rates over the whole flow

rate range. Such activity could be caused by surface tension gradients resulting from the concentration changes around the bubble. However, fluctuations of the gas-liquid interface were not visually apparent except during a short period following bubble formation. Apparently, the surfactant film which forms on the bubble surface, reducing interfacial movement, also proves very effective in suppressing interfacial activity. In the author's opinion the absorption rates on the linear portion of the curve (Figure 15) were unaffected by interfacial activity.

(v) Conclusions: It has been concluded that the experimental results obtained in this study are suitable for comparison with solutions to the model equations developed in Section 3.1.

It has not been possible to explain completely the deviation of the physical mass transfer correlation intercept from the theoretical value, although the gas leakage measurement may have been a contributing factor.

5.4 Auxiliary Studies

(i) Bubble Shape: All results reported herein were obtained with the bubble support facing down, as shown in Figure 12. Initially, experiments were carried out with the bubble facing upward, but results obtained were contrary to all previous mass transfer correlations. For the configuration of Figure 12 the bubble was ellipsoidal, whereas in the initial studies it was elongated in the vertical direction. An explanation for the differences in behaviour is given in Appendix I, where it has been concluded that bubble shape was the key factor. Indications are that a theoretical and experimental study of flow around, and transfer from, bubbles of different

shapes would be of considerable interest.

(ii) Shape of Bubble Support : Although the effect of bubble support size was not investigated, a preliminary look was taken at the effect of support shape. In order to do this the tapered Teflon tip was altered to cylindrical form without changing the dimensions in the vicinity of the nozzle. A series of experiments showed that, at least for this small change, there was no effect of tip shape on mass transfer. Results of this test are given in Appendix I.

(iii) Presence of Metals in Solution: As previously indicated the copper and brass material of the water tunnel restricted the choice of suitable gas-liquid reacting systems. There was a corrosion effect even for the monoethanolamine system chosen. This was evidenced by a solution color change, to a definite blue, after prolonged contact with copper and brass. Two separate tests, detailed in Appendix I, were carried out determining that the presence of these dissolved metals did not affect absorption rates, even up to copper concentrations of 0.3 gm./liter.

5.5 Comparison of Theoretical and Experimental Results

5.5.1 Preliminary Comparisons

The solution of the mathematical model, developed in Section 3.1, made it possible to compare the numerical results with previous experimental work on heat or physical mass transfer. For transfer from circulating gas bubbles, with first or second order reaction, the model results were compared with penetration theory. In both cases the agreement was very good and provided convincing evidence of the usefulness of the

model.

Clarke (C6) has shown for the carbon dioxide-monoethanolamine system that if the gas-liquid contact times exceed 10^{-3} seconds, second order reaction kinetics are applicable. The shortest possible contact time defined for this calculation as $2R/U$, was 50×10^{-3} seconds; thus for this study, second order behaviour was assured. Experimental conditions resulted in the gas bubble behaving like a rigid sphere, as the accumulation of surfactant on the surface prevented interfacial movement.

With the knowledge of the reaction rate constant and the diffusivities of both carbon dioxide and monoethanolamine, it is possible to calculate the concentration profiles around the sphere for any given reactant concentration and Reynolds number. It should be emphasized that the rigid sphere behaviour of the gas bubble required the use of velocity profiles for flow around solid spheres. This led once again, to the difficulties associated with the prediction of mass transfer rates in the vortex region. In purely physical mass transfer it was assumed that no transfer occurred in the vortex region, and the same assumption was made for the chemical reaction case. This may be quite reasonable under steady state conditions, as after the monoethanolamine initially present in the vortex region has been consumed further reaction will depend on the rather slow transfer of reactant from the main stream.

Solutions of the model equations for second order reaction conditions covering the range of the experimental study are shown in Table 5.3. These numerical values are compared in Figure 17 with

TABLE 5.3

THEORETICAL RESULTS - MASS TRANSFER FROM A
NON-CIRCULATING GAS BUBBLE WITH SECOND ORDER REACTION

Re	Sc _A	Sc _B	k _A ⁻⁶ x10 ⁻⁶	k _B ⁻⁶ x10 ⁻⁶	\bar{Sh}
20	456	832	0	0	27.7
	472	862	1.27	1.16	71.5
	488	890	2.54	1.16	110
	503	920	3.81	1.16	150
50	456	832	0	0	37.2
	472	862	1.27	1.16	95.9
	488	890	2.54	1.16	149
	503	920	3.81	1.16	202
100	456	832	0	0	50.4
	472	862	1.27	1.16	125
	488	890	2.54	1.16	194
	503	920	3.81	1.16	262
200	456	832	0	0	72.8
	472	862	1.27	1.16	176
	488	890	2.54	1.16	277
	503	920	3.81	1.16	378

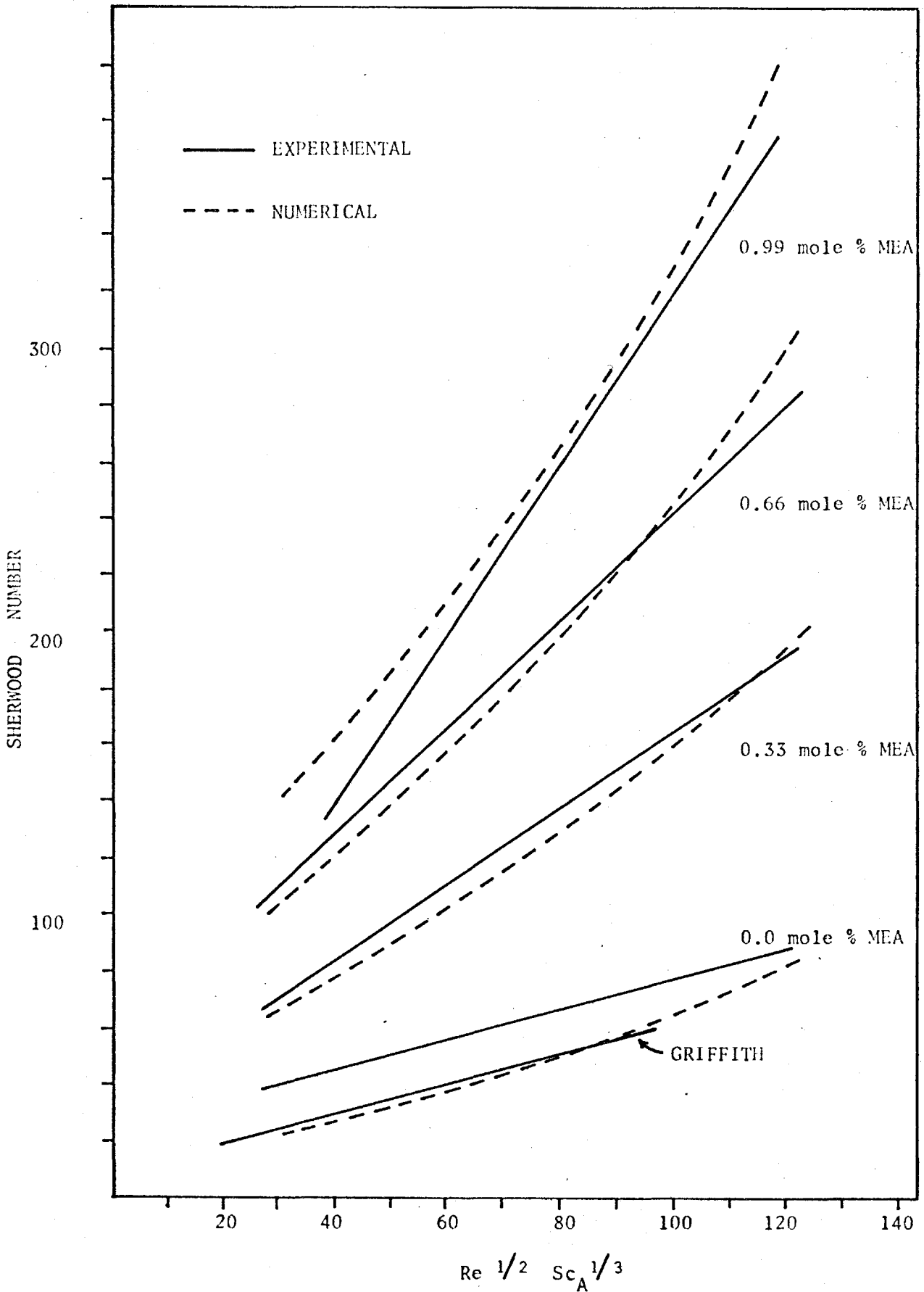


FIGURE 17. - COMPARISON BETWEEN THEORETICAL & EXPERIMENTAL RESULTS

the experimental correlations obtained. Griffith's data for equation (5.7) has been included as well.

In general, the agreement between the predicted and experimental values is excellent. For physical mass transfer, the numerical results agree more closely with Griffith's data than with the data of this study. Possible reasons for the discrepancy between the experimental correlations have been discussed previously.

The agreement between theoretical and experimental values is quite satisfactory for the reacting system. The greatest difference occurs at the highest monoethanolamine concentration. This is probably a reflection of the experimental difficulties at this concentration level where, due to the high absorption rates, it was more difficult to maintain a bubble of fixed size over the 4 to 6 minute time interval. In all cases, however, the numerically predicted results are within the confidence limits (at 95% level) of the experimental correlations.

The assumption of zero transfer in the vortex region, coupled with the experimental set-up where a considerable portion of this region was occupied by the bubble support, no doubt promoted the agreement between theory and experiment.

5.5.2 Convergence Tests

Extensive checks for convergence were carried out as discussed in Section 3.3.1. The results are shown in Table 5.4. It is obvious, once again, that the numerical solutions obtained are not affected appreciably by a halving of the mesh size. There was, however, one notable difference. A change in radial step size, while maintaining

TABLE 5.4

Convergence Tests -
Transfer from a Solid Sphere
with Second Order Reaction

Re	Sc _A	Sc _B	k _A x10 ⁻⁶	k _B x10 ⁻⁶	Δr ₀ x10 ⁻⁵	No. of Radial Steps	Δθ (deg.)	Position of Outer Boundary	Sherwood Number			AVG.	
									AT 0°	AT 45°	AT 90°		
50	472	862	1.27	1.16	5.0	30	3	1.44	174.3	160.9	100.0	96.3	
						60	1.5	1.44	174.6	160.5	100.4	*	
						40	3	7.02	174.4	160.9	100.0	97.0	
						40	3	1.37	174.6	171.5	93.6	95.9	
	488	890	2.54	1.16	5.0	30	3	1.44	273.5	252.5	155.0	149.1	
						60	1.5	1.44	273.8	252.1	155.3	*	
						40	3	1.44	273.8	268.7	145.9	149.3	
	503	920	3.81	1.16	5.0	30	3	1.44	373.1	345.9	208.2	201.3	
						60	1.5	1.44	373.6	345.6	207.6	*	
						40	3	1.44	373.4	366.7	199.2	202.4	
	100	488	890	2.54	1.16	5.0	30	3	1.44	415.1	375.6	204.1	194.3
							60	1.5	1.44	415.6	374.5	203.0	*
503		920	3.81	1.16	5.0	30	3	1.44	564.3	517.9	269.2	262.5	
						60	1.5	1.44	565.4	517.1	266.5	*	
200		472	862	1.27	1.16	5.0	30	3	1.44	406.0	361.0	186.4	176.5
							60	1.5	1.44	406.7	358.1	184.2	*
	40						3	7.02	405.9	360.9	186.3	176.4	

* Solutions obtained only up to $\theta=90^\circ$

$\Delta\theta$ constant, resulted in a significant change in the local Sherwood numbers. Previous convergence tests had indicated that a change in radial, or both radial and angular step sizes, had little effect on the resulting local and average Sherwood numbers. A possible reason for this behaviour may lie in the finite-difference approximations employed. In this case, since $k_A > 10^4$, it was necessary to use the DuFort-Frankel approximation for the second derivative in r (equation (3.44)). The standard form, equation (3.21), could not be used for reasons of stability as discussed in Section 3.2.2. The Du Fort-Frankel approximation contains concentrations from three different angular locations. Therefore it might be expected to be more susceptible to angular step size changes than the standard form which contains only concentrations at one angular location.

It has been concluded that convergence of the numerical solutions has been obtained. However, this does not allow the conclusion that the values obtained are accurate approximations of the exact analytic solution. This is simply a necessary condition which must be satisfied. Sufficient conditions are extremely difficult to obtain except in the trivial case where an analytic solution is available.

5.5.3 Effect of Diffusivity and Reaction Rate.

The uncertainty in the values reported for the diffusivity of monoethanolamine and in the value of the rate constant for the carbon dioxide-monoethanolamine reaction has been pointed out previously.

The value for the diffusivity of monoethanolamine used in this

work was taken from the results of Thomas and Furzer (T2). If, however, a different value had been chosen the numerical solutions would have been affected to some degree. In Table 5.5 results are presented for two different diffusivity values differing by about 12%. It can be concluded from a comparison of the two sets of results that a change of this order will introduce an uncertainty of only 5-6% in the calculated Sherwood numbers.

A similar variation in reported values exists for the reaction rate constant. In this work the value reported by Emmert and Pigford (E1) was used. Whereas, Astarita (A5) and Clarke (C6) reported a value about 30% higher at 25°C. In Table 5.6 results are reported using both these values. It can be safely concluded that the mass transfer rate is almost independent of the reaction rate at this high level. In other words, the kinetics are approaching those of an infinitely fast second order reaction where the transfer rate becomes entirely dependent on the diffusivities and hydrodynamic conditions (See Figure 18 for typical concentration profiles). Therefore, the accurate determination of reaction rate constants utilizing the experimental procedure of this study would not be possible for fast second order reactions. If, however, this reaction were slower there might be some merit in using this experimental method to obtain reaction rate values.

5.5.4 General Conclusions

The numerical solutions of the model equations are in agreement with all available results for mass transfer, with and without chemical reaction, from both circulating and noncirculating spheres. It would

TABLE 5.5

Effect of Monoethanolamine Diffusivity
on Calculated Sherwood Numbers

Sc_A	k_A $\times 10^{-6}$	D_B $\times 10^5$	Sc_B	k_B $\times 10^{-6}$	Re	\bar{Sh}
472	1.27	1.07	862	1.16	20	71.5
					50	95.9
					100	125
					200	177
472	1.27	1.20	819	1.03	20	75.7
					50	101
					100	131
					200	186

TABLE 5.6

Effect of Reaction
Rate Constant on Calculated
Sherwood Numbers

Sc_A	Sc_B	k_2 liters mole sec.	k_A $\times 10^{-6}$	k_B $\times 10^{-6}$	Re	\overline{Sh}
488	890	5400	2.54	1.16	50	149
					100	194
					200	277
488	890	7000	3.33	1.50	50	152
					100	197
					200	280

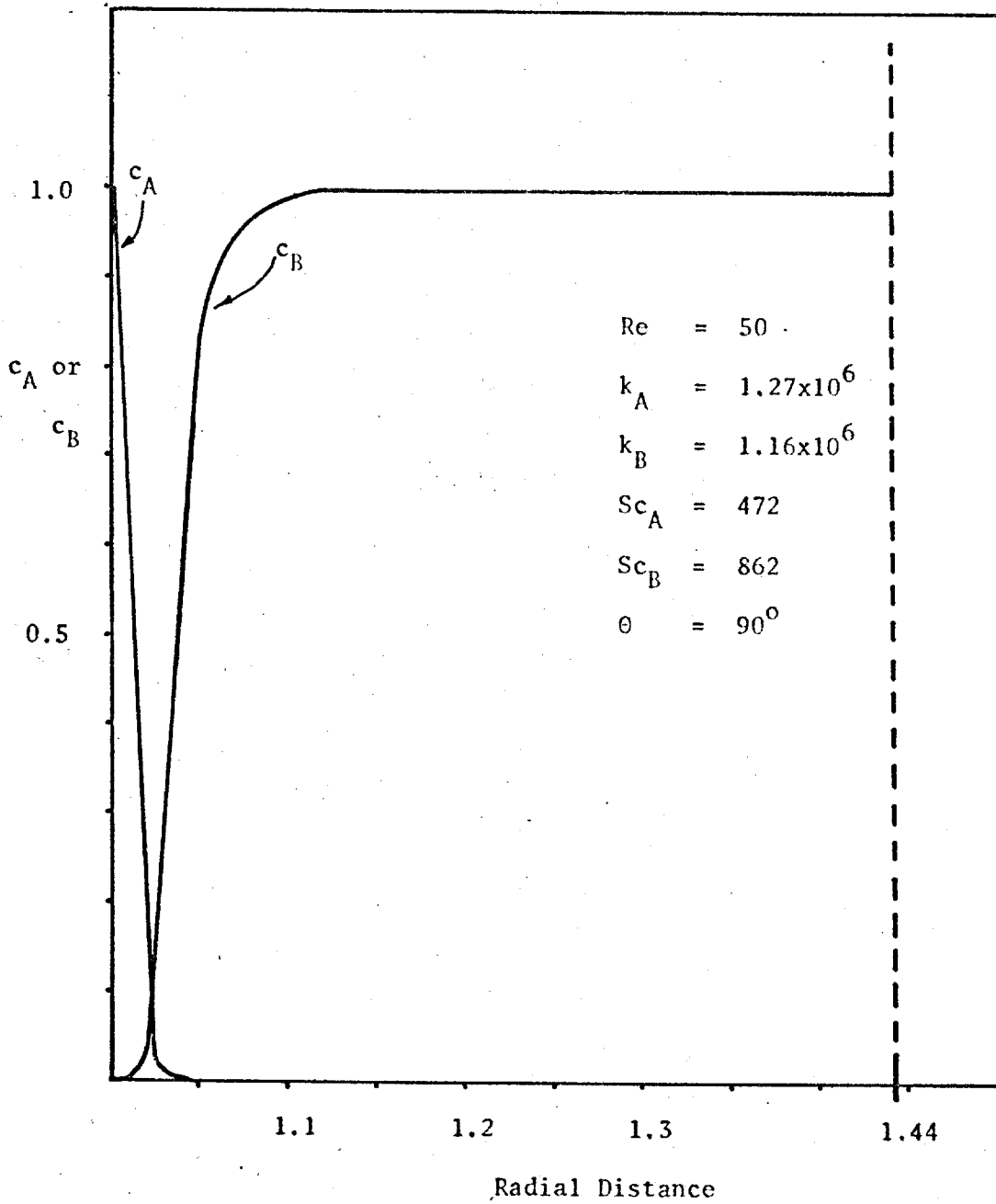


FIGURE 18. - CONCENTRATION PROFILES FOR CONDITIONS APPROACHING INFINITELY FAST SECOND ORDER REACTION

be expected that the model would be applicable to all gas-liquid or fluid-solid systems. Further confirmation of this applicability could be obtained from a study of several other gas-liquid systems.

This author believes that the model is applicable for spherical fluid bodies for all Reynolds numbers up to the point when vortex shedding begins. The velocity profiles used for the rigid sphere case, however, are known to be inaccurate below Reynolds numbers of 10, and also do not predict the proper shape for the vortex region at Reynolds numbers beyond 200. Thus the extrapolation of the numerical results beyond the range covered is not recommended. However, the numerical techniques, if supplied with the correct velocity profiles, should be applicable from $Re < 1$ up to the point where transient vortex behaviour begins.

The model developed in this work was used by Yau (Y1) to predict rates of transfer from a series of bubbles formed at a single orifice. The predicted and experimental values were in good agreement except where severe bubble deformation had occurred. Potential flow velocity profiles were used to describe the flow field. Bubble interaction was not significant in the study by Yau and the model in its present form would not be expected to handle oscillating or interacting bubbles.

In a commercial reactor a gas bubble would be circulating for a short period after formation, but would almost immediately become contaminated by surfactant material, thus preventing further interfacial movement. A suitable description of this transient behaviour might be obtained by employing the models developed using circulating sphere

hydrodynamics for the initial absorption period and rigid sphere hydrodynamics for the second absorption interval.

Bubble swarms dispersed in a stirred vessel have been considered by Gal-Or and co-workers (G1, G2, G3). The definition of a suitable bubble Reynolds number would be most difficult under these conditions. Since such a Reynolds number is required for the model developed here, it is suggested that the model developed by Gal-Or would be more suitable for dispersions in stirred vessels. The latter model, at present, will handle only the case of first order reaction. However, there should be no reason why it could not be extended to second and higher orders by resorting to numerical techniques.

6. CONCLUSIONS AND RECOMMENDATIONS

6.1 Conclusions

Numerical techniques have been extended to obtain solutions of the equations describing forced convection mass transfer from single circulating and non-circulating spheres with simultaneous first or second order reaction.

The numerical results for transfer from circulating gas bubbles are in excellent agreement with penetration theory.

Predicted physical transfer rates from rigid spheres compare favourably with the experimental correlations of other workers.

Mass transfer data, for the reacting systems carbon dioxide-monoethanolamine, have been obtained over the range $30 < Re < 200$. The rates of mass transfer predicted by the model for the case of second order reaction are in excellent agreement with these experimental results.

Indications are that the model would be useful in predicting rates of transfer in multiple bubble situations, providing that bubble distortion and interaction effects were small. The model would not be expected to be useful when considering oscillating bubbles.

6.2 Recommendations

An investigation into alternate means of solving the complete elliptic equation would be most useful since the successful solution of this equation would allow for the calculation of local mass transfer rates in the vortex region. The assumption of no mass transfer beyond

the separation point, made when dealing with rigid spheres, could then be evaluated.

A theoretical study of the effect of sphere support size and shape on the hydrodynamics and mass transfer would be desirable. The present water-tunnel would be suitable for a parallel experimental study of these factors.

Preliminary studies have shown the need for a theoretical and experimental study of the effect of sphere shape on transfer rates.

Further studies of mass transfer from gas bubbles should be preceded by the development of an improved, leak free, method of feeding gas to the bubble.

The general applicability of the models developed could be tested further by a study of other gas-liquid reacting systems. The present apparatus, because of the materials of construction, would not be suitable for most reacting systems. An alternate water tunnel, preferably of glass, would be desired.

APPENDICES

A. SOLUTION OF ELLIPTIC EQUATION FOR FIRST ORDER REACTION

Equation (3.2) can be written in finite-difference form using central differences for all derivatives. The resulting finite-difference equation may be written (replacing c_A by A) as

$$\begin{aligned}
 & A_{i,j-1} (-a_1 + a_2 - a_3) + A_{i,j+1} (a_1 - a_2 - a_3) \\
 & + A_{i-1,j} (-a_4 - ha_5 + a_6) + A_{i+1,j} (a_4 - a_5 - a_6) \\
 & + A_{i,j} (a_5 (1+h) + 2a_3 + 2k/Pe_A) = 0
 \end{aligned} \tag{A-1}$$

where

$$\begin{aligned}
 a_1 &= V_\theta / 2r_i \Delta\theta \\
 a_2 &= \cot\theta_j / r_i^2 \Delta\theta Pe_A \\
 a_3 &= 2 / r_i^2 \Delta\theta^2 Pe_A \\
 a_4 &= V_r / (1+h) (h^{i-1} \Delta r_o) \\
 a_5 &= 4 / (1+h) (h^{i-1} \Delta r_o)^2 Pe_A \\
 a_6 &= 4 / (1+h) (h^{i-1} \Delta r_o) r_i Pe_A
 \end{aligned} \tag{A-2}$$

Equation (A-1) was rearranged to facilitate solution by a relaxation technique.

$$\begin{aligned}
 A_{i,j}^{(n+1)} &= A_{i,j}^{(n)} + \omega [b_1 A_{i,j-1}^{(n)} + b_2 A_{i,j+1}^{(n)} \\
 &\quad + b_3 A_{i-1,j}^{(n)} + b_4 A_{i+1,j}^{(n)} - A_{i,j}^{(n)}]
 \end{aligned} \tag{A-3}$$

Where $b_1 = (-a_1 + a_2 - a_3) / (-a_5(1+h) - 2a_3 - 2k/Pe_A)$ and the remaining b_i are similar combinations of the a_i . The superscripts (n) and (n+1) represent the A values after the n^{th} and $(n+1)^{st}$ iterations. The

optimum value of the relaxation factor ω could only be determined by trial and error.

New values $(A_{i,j}^{(n+1)})$ were calculated at all mesh points using equation (A-3), and then compared with the previous values at these locations $(A_{i,j}^{(n)})$. The new values replaced the old values as soon as they became available. This was continued until the concentrations at all mesh points became constant within a specified tolerance. This solution procedure was successful only for $Pe_A < 10^2$. At the high Peclet numbers of interest in this study ($Pe_A > 10^4$) the solution became unstable and made it impossible to obtain useful results.

Some insight into the reasons for this instability may be obtained by studying equations (A-1) and (A-2). As the value of Pe_A is increased the coefficients a_2 , a_3 , a_5 , and a_6 approach zero, except very near the sphere surface. At a short distance away from the surface equation (A-1) approaches the form

$$a_1(A_{i,j+1} - A_{i,j-1}) + a_4(A_{i+1,j} - A_{i-1,j}) + (a_5(1+h) + 2a_3 + 2k/Pe_A) A_{i,j} = 0 \quad (A-4)$$

Since the concentration values do not change rapidly from one mesh point to the next, it is obvious that errors could be introduced when subtracting two values of the same order of magnitude resulting in an unavoidable loss of accuracy. A similar problem was encountered when dealing with the parabolic equations and has been discussed in Section 3.2.2. In the latter case it was possible to circumvent the source of inaccuracy by using alternate finite-difference approximations for some of the derivatives. A full investigation of the possibility of a

similar step has not been carried out for the elliptic equation case. However, the use of both a forward and a backward difference for the first derivative in θ , rather than the central difference employed here, did not offer any improvement.

One criterion for numerical stability is what Ames (A4) calls a "positive test". If the coefficients (i.e. the a_i above) are all positive, stability is assured; whereas the presence of some negative coefficients *may* lead to instability. In equation (A-4) both positive and negative values of a_1 and a_4 are present and instabilities did occur. On the other hand, the coefficients for the case of $Pe_A \leq 10$ were found to be always positive and, not surprisingly, stable solutions were obtained.

The usual procedure for eliminating negative coefficients is to make the mesh size smaller. A rough calculation, carried out with $Pe = 10^5$, indicated that all coefficients could be made positive only if the step sizes in both radial and angular directions were less than 10^{-4} dimensionless units. Since the mesh system must extend a distance as great as 3 or 4 dimensionless radii in order to include the vortex region, it is obvious that the number of mesh points required would be prohibitive.

The method described for obtaining solutions of equation (A-1) is impractical for $Pe > 10^2$ since excessive computer storage would be required. Alternate methods which would remove the source of instability and, at the same time, require only a reasonable number of mesh points must be developed.

B. FINITE DIFFERENCE APPROXIMATIONS

The approximation for the first derivative in r was developed from the Taylor series for a variable radial step size. It was not necessary to specify the type of variation beforehand. This general form was especially convenient for computation purposes, as alternate mesh systems could be tried with a minimum of program changes. The general form was developed from

$$c_{i+1,j} = c_{i,j} + (r_{i+1}-r_i) \frac{\partial c}{\partial r} + \frac{(r_{i+1}-r_i)^2}{2} \frac{\partial^2 c}{\partial r^2} + \quad (B-1)$$

$$c_{i-1,j} = c_{i,j} + (r_{i-1}-r_i) \frac{\partial c}{\partial r} + \frac{(r_{i-1}-r_i)^2}{2} \frac{\partial^2 c}{\partial r^2} + \quad (B-2)$$

In general $(r_{i+1}-r_i)$ does not equal $(r_{i-1}-r_i)$.

Equation (B-1) was multiplied by $(r_{i-1}-r_i)^2$ and equation (B-2) by $\{-(r_{i+1}-r_i)^2\}$, and the two equations added together. After rearranging, the following relationship was obtained:

$$\begin{aligned} \frac{\partial c}{\partial r} \quad i,j &= \frac{(r_{i-1}-r_i)}{(r_{i+1}-r_i)(r_{i-1}-r_{i+1})} c_{i+1,j} \\ &- \left[\frac{1}{(r_{i-1}-r_{i+1})} \frac{(r_{i-1}-r_i)}{(r_{i+1}-r_i)} - \frac{(r_{i+1}-r_i)}{(r_{i-1}-r_i)} \right] c_{i,j} \\ &- \frac{(r_{i+1}-r_i)}{(r_{i-1}-r_{i+1})(r_{i-1}-r_i)} c_{i-1,j} \end{aligned} \quad (B-3)$$

In the event that a uniform radial step size was employed, the above equation would reduce to the more familiar form

$$\frac{\partial c}{\partial r} \quad i,j = \frac{c_{i+1,j} - c_{i-1,j}}{(r_{i+1}-r_{i-1})} \quad (B-4)$$

The same procedure was followed in developing a form for the second

derivative with the following result:

$$\begin{aligned} \frac{\partial^2 c}{\partial r^2} \quad i,j &= \frac{2c_{i+1,j}}{(r_{i+1}-r_i)(r_{i+1}-r_{i-1})} - \frac{2c_{i,j}}{(r_i-r_{i-1})(r_{i+1}-r_i)} \\ &+ \frac{2c_{i-1,j}}{(r_i-r_{i-1})(r_{i+1}-r_{i-1})} \end{aligned} \quad (B-5)$$

This equation also reverted to the more familiar form when the radial step size was uniform, i.e.

$$\frac{\partial^2 c}{\partial r^2} \quad i,j = \frac{c_{i+1,j} - 2c_{i,j} + c_{i-1,j}}{(r_{i+1}-r_i)^2} \quad (B-6)$$

The difficulties with the use of equation (B-3) have been discussed in Section 3.2.2.

It was not necessary to develop a special form for the angular derivative as a uniform angular step size was employed throughout this study.

C. DIFFUSION FROM A SPHERE WITH SECOND ORDER REACTION

The boundary conditions of equation (3.4) and (3.5) required initial concentration estimates along the radial vector through the frontal stagnation point. These concentration estimates were obtained from solutions of the equations describing transfer from a sphere into a stagnant fluid: The equations may be written as

$$\frac{d^2 c_A}{dr^2} + \frac{2}{r} \frac{dc_A}{dr} - k_A c_A c_B = 0 \quad (C-1)$$

$$\frac{d^2 c_B}{dr^2} + \frac{2}{r} \frac{dc_B}{dr} - k_B c_A c_B = 0 \quad (C-2)$$

With boundary conditions:

$$c_A = 1, \quad dc_B/dr = 0 \quad \text{at } r = 1$$

$$c_A = 0, \quad c_B = 1 \quad \text{as } r \rightarrow \infty$$

These equations could be readily solved by Runge-Kutta methods, however, finite-difference techniques are similarly convenient and were used in this study. No difficulties were encountered in obtaining solutions.

If the initial concentration estimates were not sufficiently close to the correct values, convergence could not be obtained and a certain amount of trial and error became necessary. For example, if a solution for a Reynolds number of 200 and reaction rates of $k_A = 10^6$ and $k_B = 10^5$ were required, the estimates obtained by solving the stagnant fluid equations with these reaction rate values were unsuitable. Instead it was necessary to use the solutions of equations (C-1) and (C-2) with $k_A = 10^6$ and $k_B = 10^4$. These concentration values were reasonably close

to the correct values along the zero-angle line. Thus convergence was readily obtained, satisfying the zero slope criterion at $\theta=0^\circ$.

D. POLYNOMIAL REPRESENTATION OF BOUNDARY CONDITION $\partial c_B / \partial r = 0$ at $r = 1$

Using the Taylor series a representation of this boundary condition may be developed by writing

$$B_{i+1,j} = B_{i,j} + (r_{i+1}-r_i) \frac{\partial B}{\partial r} + \frac{(r_{i+1}-r_i)^2}{2} \frac{\partial^2 B}{\partial r^2} + \quad (D-1)$$

$$B_{i+2,j} = B_{i,j} + (r_{i+2}-r_i) \frac{\partial B}{\partial r} + \frac{(r_{i+2}-r_i)^2}{2} \frac{\partial^2 B}{\partial r^2} + \quad (D-2)$$

Equation (D-1) was multiplied by $(r_{i+2}-r_i)^2$, equation (D-2) by $\{-(r_{i+1}-r_i)^2\}$, and the two equations added. After some rearrangement the following relationship was obtained:

$$\begin{aligned} \frac{\partial B}{\partial r} \quad i,j &= \frac{(r_{i+2}-r_i)}{(r_{i+1}-r_i)(r_{i+2}-r_{i+1})} B_{i+1,j} \\ &- \left[\frac{(r_{i+2}-r_i)}{(r_{i+1}-r_i)(r_{i+2}-r_{i+1})} - \frac{(r_{i+1}-r_i)}{(r_{i+2}-r_i)(r_{i+2}-r_{i+1})} \right] B_{i,j} \\ &- \frac{(r_{i+1}-r_i)}{(r_{i+2}-r_i)(r_{i+2}-r_{i+1})} B_{i+2,j} \end{aligned} \quad (D-3)$$

At $r = 1$, i may be set equal to unity, and $\partial B / \partial r$ set equal to zero. The following relationship for the concentration at the interface could then be obtained:

$$B_{1,j} = \frac{(r_3-r_1)^2}{(r_3-r_1)^2-(r_2-r_1)^2} B_{2,j} - \frac{(r_2-r_1)^2}{(r_3-r_1)^2-(r_2-r_1)^2} B_{3,j} \quad (D-4)$$

Therefore the quantity $B_{1,j}$ never appeared explicitly as an unknown but only as a function of $B_{2,j}$ and $B_{3,j}$. This polynomial representation caused no difficulties in the matrix inversion step.

E. PHYSICAL DATA

(i) Viscosity of Monoethanolamine Solutions

Several solutions of known monoethanolamine concentration were prepared and their viscosities determined at $25 \pm .1^{\circ}\text{C}$, by means of a calibrated Cannon-Fenske viscometer (model 50, number B289). The results obtained, which are plotted in Figure 19, are in agreement with values reported by Thomas and Furzer (T2).

(ii) Rotameter Calibrations

Three Fisher-Porter glass rotameters were available for the measurement of the water-tunnel flow rates. These rotameters were:

FP $\frac{1}{2}$ - 17 - G - 10 with float $\frac{1}{2}$ GUSVT - 40

FP $\frac{3}{4}$ - 27 - G - 10 with float $\frac{3}{4}$ GSVT - 54

FP 1 - 35 - G - 10 with float 1 GNSVT - 64

Calibrations were carried out by weighing the quantity of water passed through for a given float reading over a timed interval. The calibration curves are shown in Figure 20.

(iii) Monoethanolamine Concentration

The concentration of monoethanolamine in aqueous solution was conveniently determined from a measure of the solution refraction index. A series of solutions of known concentrations were prepared and the refractive indices determined, at $25 \pm .1^{\circ}\text{C}$, using a Officine Galileo refractometer. The calibration curve obtained is shown in Figure 21.

During actual experiments the solution samples were normally taken about 20 minutes after the monoethanolamine had been added to the system. Repeated samples indicated that there was no refractive index

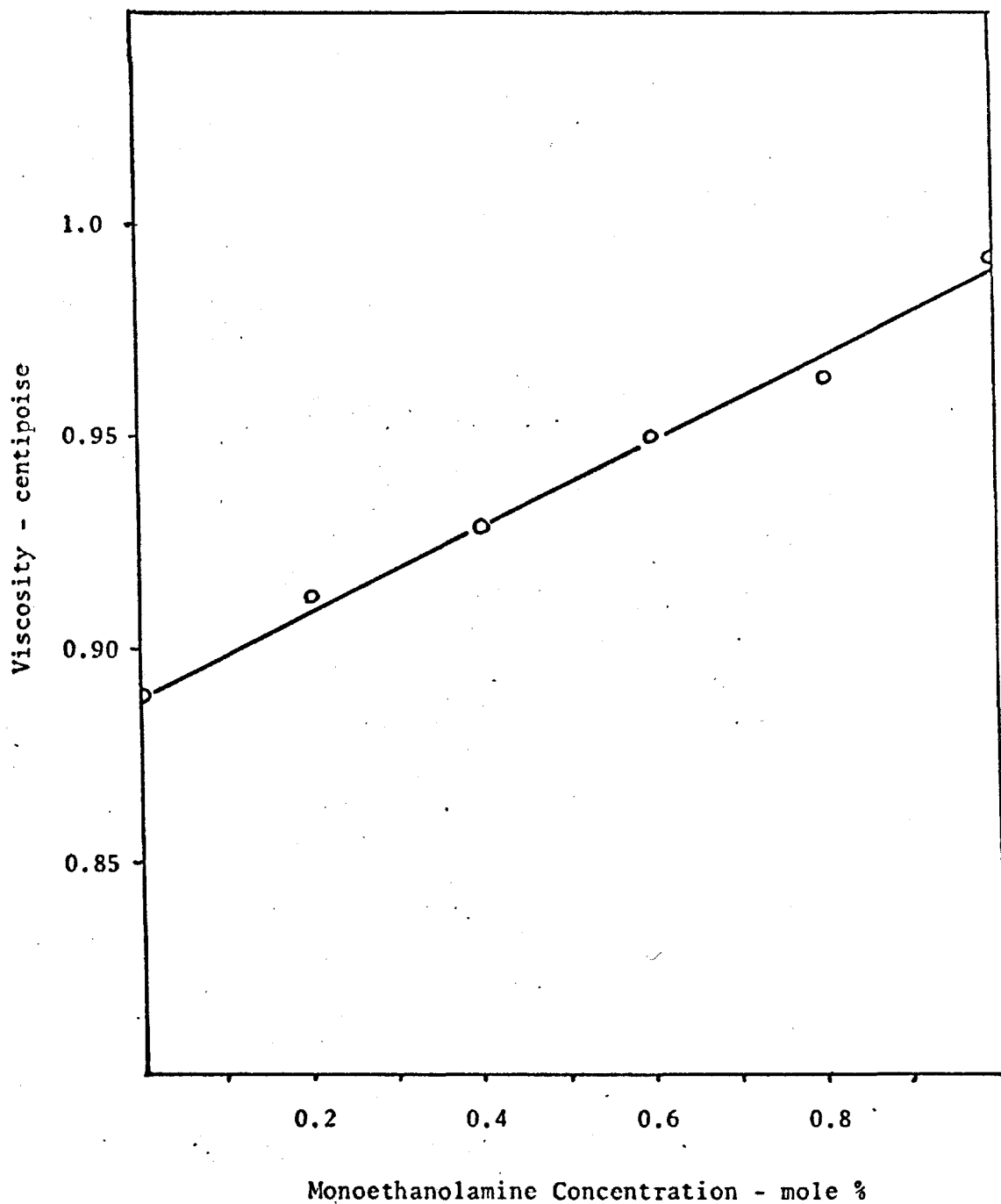


FIGURE 19. - VISCOSITY OF MONOETHANOLAMINE SOLUTIONS
at 25°C

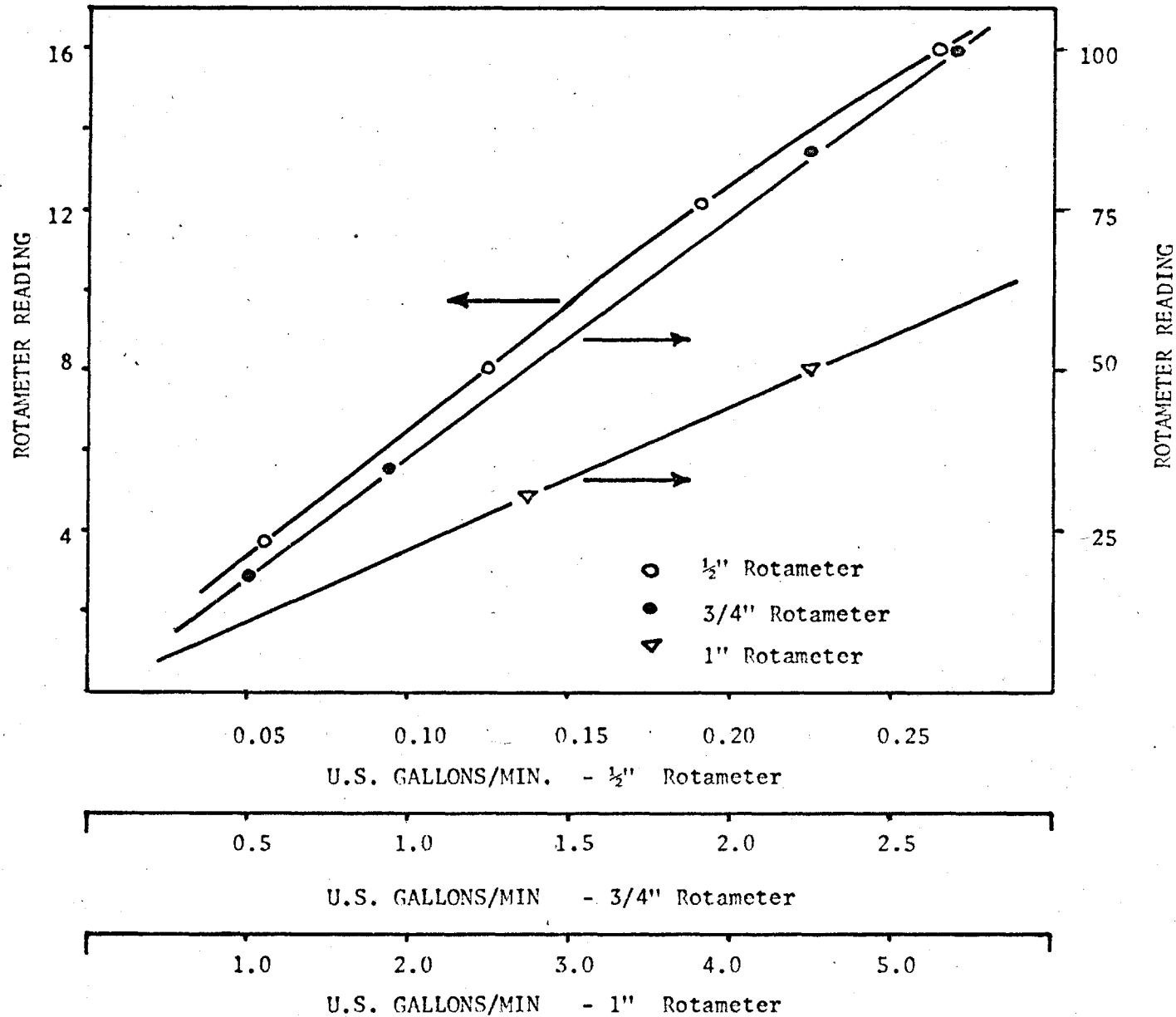


FIGURE 20. - ROTAMETER CALIBRATION CURVES

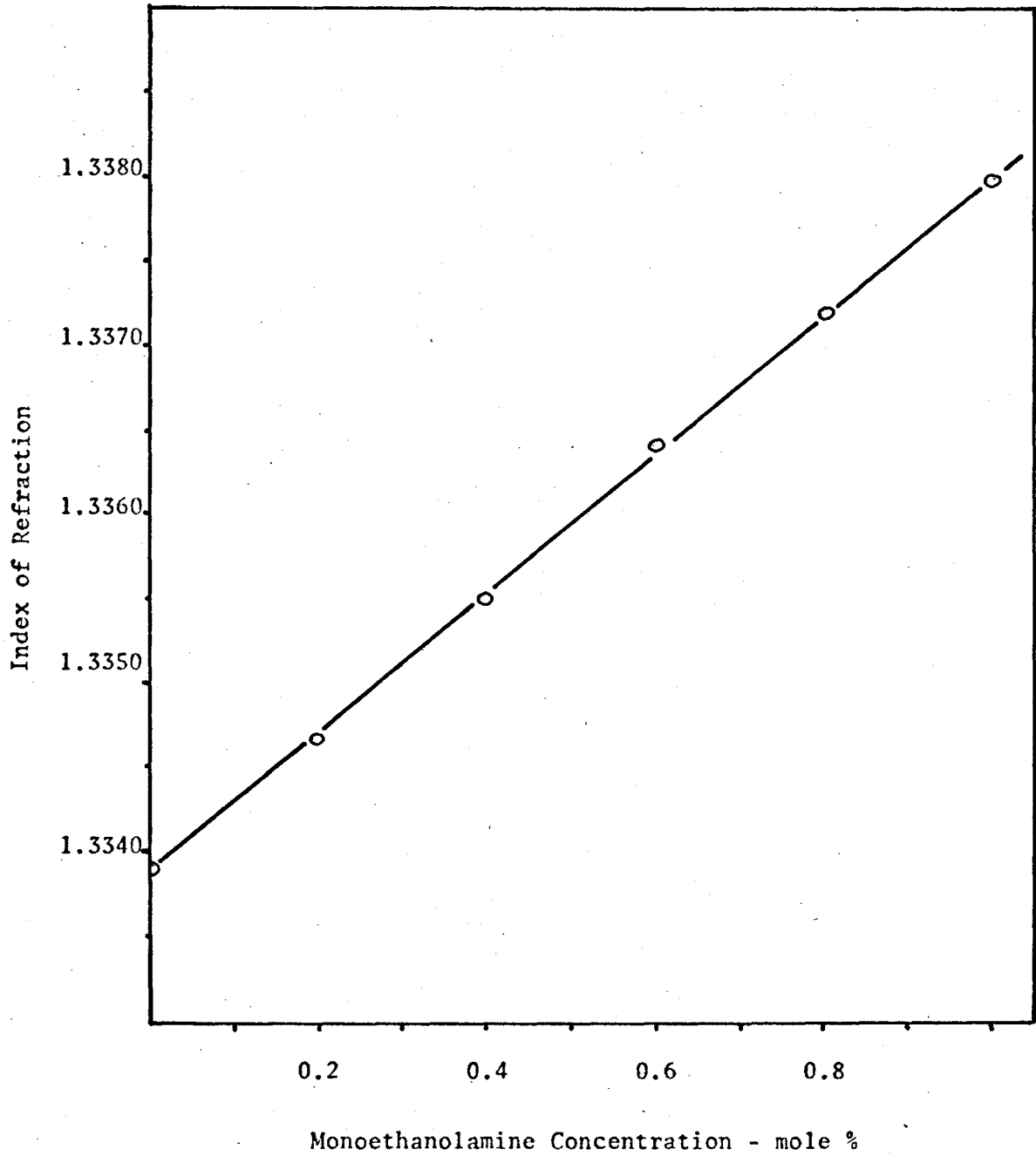


FIGURE 21. - INDEX OF REFRACTION OF MONOETHANOLAMINE SOLUTIONS

change over a two hour period, despite a marked color change in the solution.

(iv) Carbon Dioxide Solubility

The solubility of carbon dioxide in water at 1 atmosphere and 25°C has been reported as 0.0338 gm-moles/liter (D6). This value, adjusted linearly for the pressure in the test bubble (5.2 p.s.i.g.), was used throughout this study as the solubility in both water and monoethanolamine solutions. The latter solubility is impossible to measure because of the very fast reaction. Clarke (C6) however has shown that any solubility change due to the presence of the amine is unlikely. This conclusion was based on the results of tests with nitrous oxide which is similar to carbon dioxide in many of its mass and molecular properties. It was found that the solubility of nitrous oxide was unaffected by monoethanolamine concentration and Clarke concluded that the same should be true of the carbon dioxide solubility.

(v) Diffusivities

The diffusivity of carbon dioxide in water at 25°C was taken as 1.95×10^{-5} cm²/sec from the work of Davidson and Cullen (D4). Other reported values are within ±15% of this value. In view of the scatter in the reported values, corrections for viscosity, which would have been of the same order as the experimental scatter, were not applied.

The effect of the presence of monoethanolamine on the carbon dioxide diffusivity cannot be determined, but again, Clarke (C6) has shown from studies with nitrous oxide that little change would be expected.

A wide range of values for the diffusivity of monoethanolamine

in water has been reported (I1, T2). The agreement between the experimental results of different workers is poor. Values predicted from semi-theoretical equations also scatter significantly. In the opinion of this author the values obtained in the recent experimental work of Thomas and Furzer (T2) are the most reliable. These authors found that the diffusivity was a function of monoethanolamine concentration. However, over the concentration range covered in this study the variation was slight and an average value of $1.07 \times 10^{-5} \text{ cm}^2/\text{sec}$ was used throughout. The effect of the uncertainty of the amine diffusivity on the theoretical results of this investigation has been discussed in Section 5.5.3.

F. MEASUREMENT OF BUBBLE SURFACE AREA

The surface area of the bubble available for mass transfer was determined via measurements taken from bubble photographs. These photographs (Figure 22) were taken with an Asahi Pentax camera at f/22 and 1/500 seconds exposure time, using a photoflood lamp and Kodak Panatomic-X film. Two levels of flow rates and monoethanolamine concentration were used. There was no significant effect of these variables on bubble shape.

The top of the bubble was maintained at a distance of 0.25 cm from the top of the bubble support as was the case when absorption rate measurements were being taken. The various distances measured on the negatives are shown schematically in Figure 23. A measuring scale on the photographs was established by setting (b+c) equal to 0.25 cm and the remaining distances obtained on this basis. The results of these measurements are listed in Table F-1.

The bubble shape was, for all practical purposes, ellipsoidal. The surface area exposed could be obtained by integrating the formula for the surface area of an ellipsoid between the appropriate limits.

The equation for the surface area may be written

$$A_b = 2\pi \int_b^c \left[a^2 + \frac{a^2}{b^2} \left(\frac{a^2}{b^2} - 1 \right) y^2 \right]^{1/2} dy \quad (F-1)$$

The total area available for mass transfer was calculated as 0.257 cm². This was the figure used when calculating the liquid phase mass transfer coefficients.

The equivalent sphere diameter used in calculating Reynolds and



ABSORPTION OF CARBON DIOXIDE
INTO WATER



ABSORPTION OF CARBON DIOXIDE
INTO 0.66 mole % MONOETHANOLAMINE

FIGURE 22 - PHOTOGRAPHS OF GAS BUBBLE

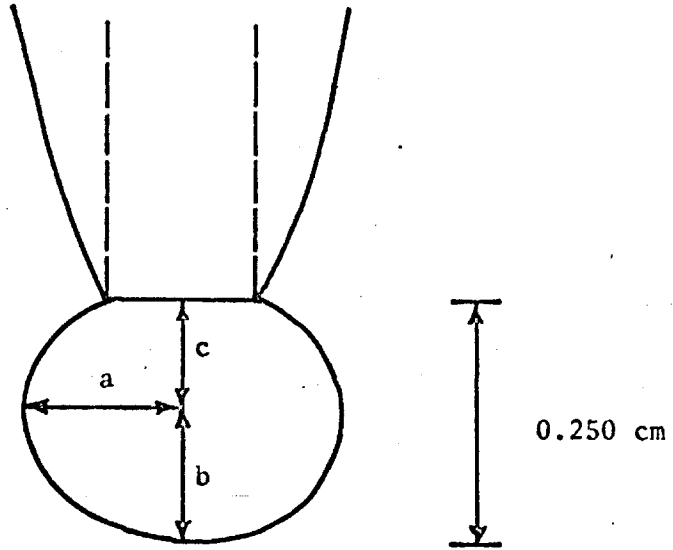


FIGURE 23. - DISTANCES MEASURED ON BUBBLE PHOTOGRAPHS

TABLE F.1

Measurements from Bubble Photographs

Frame Number	Bubble Height (a+c) cm.	Half Height (a) cm.	Bubble Width (2b) cm.
1.	0.250	0.153	0.323
2.	0.250	0.150	0.317
3.	0.250	0.151	0.319
4.	0.250	0.153	0.326
5.	0.250	0.150	0.320
6.	0.250	0.154	0.325
7.	0.250	0.151	0.327
8.	0.250	0.153	0.325
9.	0.250	0.157	0.329
10.	0.250	0.154	0.324
	-----	-----	-----
Average Values	0.250	0.153	0.323

Sherwood numbers was based on the diameter of a sphere having the same surface area as the ellipsoid. In this case the total area, including that covered by the bubble support, was employed. The total area was calculated as 0.316 cm^2 resulting in an equivalent diameter of 0.317 cm.

G. MEASUREMENT OF GAS LEAKAGE

The leakage rate from the syringe was determined with the aid of a sensitive differential pressure gauge (Industrial Instrument Corporation) having a range of ± 1.08 p.s.i., graduated in steps of 0.05. The gas syringe was connected as shown in Figure 24. The end of the stainless steel tubing, the normal location of the bubble support, was sealed off for the tests.

Carbon dioxide was admitted into the system from the gas cylinder until the pressure reached 5.2 p.s.i.g., the normal operating pressure during absorption rate determinations. The pressure was then equalized on both sides of the differential gauge; the valve between the two sides closed; and the system allowed to stand at 25°C for a measured period of time. At the end of this time interval the pressure on the syringe side of the system would have dropped as a result of gas escaping from the syringe into the atmosphere. The volume escaped was determined by moving the syringe plunger until the pressure returned to its initial value, and recording the decrease in system volume from the syringe counter.

The results of the several tests carried out are listed in Table G-1. The leakage rate was found to be independent of plunger position, as indicated by volume counter readings, and thus the same leakage correction was applied to all observed absorption rates. The leakage tests were not carried out for each absorption rate experiment but only in the middle and at the end of the series of experiments. There was no significant difference between the results

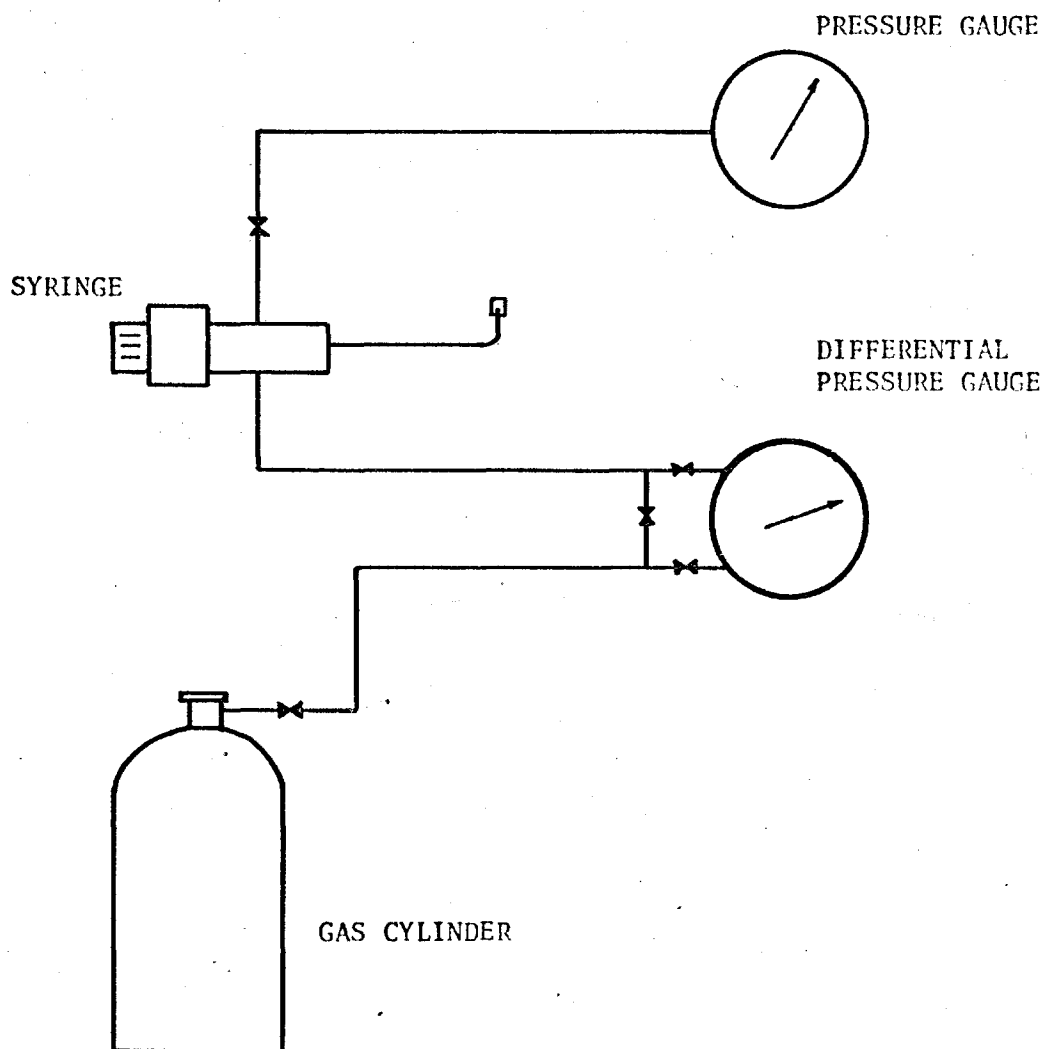


FIGURE 24. - EQUIPMENT ARRANGEMENT - DETERMINATION OF LEAKAGE RATE FROM GAS SYRINGE

TABLE G.1

Measurement of Carbon Dioxide
Leakage Rate

Run No.	Time min.	Volume Change c.c.	Leakage cc/min.
1	125	1.866	0.0149
2.	630	9.330	0.0148
3.	60	0.902	0.0148
4.	30	0.458	0.0153
5.	30	0.715	0.0238
6.	30	0.420	0.0140
7.	35	0.452	0.0129
8.	30	0.338	0.0113
9.	34	0.696	0.0204
10.	39	0.604	0.0155
11.	30	0.440	0.0147
12.	50	0.756	0.0151

AVG RATE = 0.0156 ± 0.0065 cc/min

at 95% confidence level

of the two sets of data.

Later in this study, when a series of absorption rate experiments was carried out with a cylindrical rather than a tapered bubble support, another set of leakage determinations were made. These results did show a variation with plunger position. The leakage rates are plotted in Figure 25. It is obvious, in this case, that it was necessary to use a correction which depended on the counter reading.

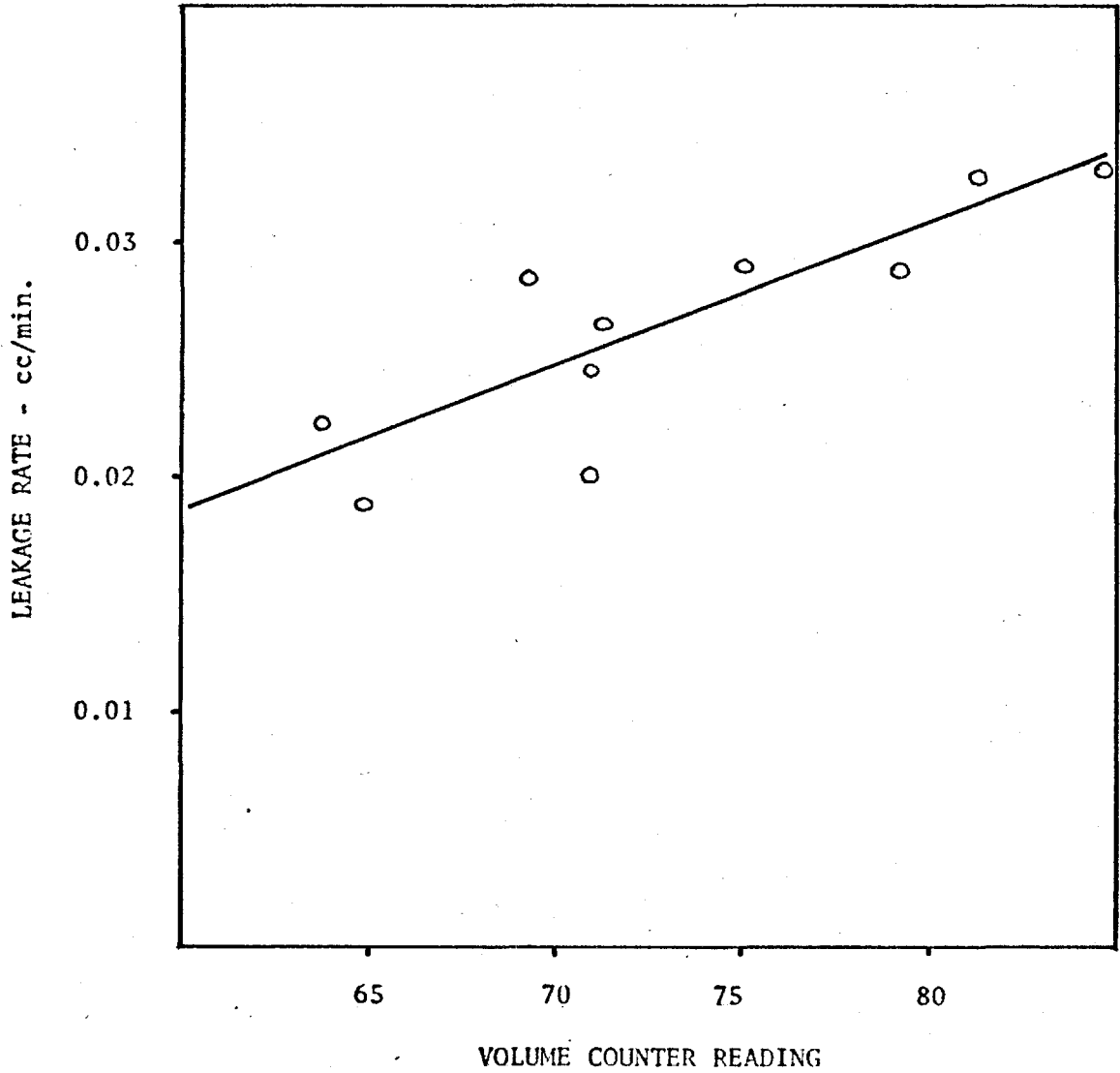


FIGURE 25. - LEAKAGE RATES - APPLIED TO EXPERIMENTS WITH CYLINDRICAL BUBBLE SUPPORT

H. SAMPLE CALCULATION

The relationship defining the liquid phase mass transfer coefficient may be written as

$$N_{\text{CO}_2} = k_L A_b (c^S - c_\infty) \quad (\text{H-1})$$

where c^S is the solubility of carbon dioxide at 1 atmosphere and c_∞ is the concentration of carbon dioxide in the bulk of the liquid, taken as zero. If the value of N_{CO_2} is not corrected to atmospheric conditions the value of c^S need not be adjusted for the pressure in the bubble as the two corrections would cancel one another. The Sherwood number is defined as

$$\text{Sh} = \frac{dk_L}{D_{\text{CO}_2}} = \frac{N_{\text{CO}_2} d}{A_b c^S D_{\text{CO}_2}} \quad (\text{H-2})$$

Values used in this study were

$$d = 0.317 \text{ cm}$$

$$A_b = 0.257 \text{ cm}^2$$

$$c^S = 0.0338 \text{ gm-moles/liter}$$

$$D_{\text{CO}_2} = 1.95 \times 10^{-5} \text{ cm}^2/\text{sec.}$$

After using suitable unit conversion factors the following final relationship was obtained:

$$\text{Sh} = 1270 \left[\text{corrected Absorption Rate} \right] \quad (\text{H-3})$$

Where the units of the absorption rate are cc./min. This "corrected absorption rate" is the value of the intercept of a plot of absorption rate versus time (Figure 15) corrected for leakage rate. The method of analysis used to obtain the intercept value has been discussed in

Section 5.1.

Calculations are outlined for the experiment carried out with a centerline velocity of 4.2 cm/sec and a monoethanolamine concentration of 0.33 mole %.

$$\begin{aligned} \text{Corrected Absorption Rate} &= \text{Intercept Value} - \text{Leakage Correction} \\ &= 0.1366 - 0.0156 = 0.121 \text{ cc/min} \end{aligned}$$

$$\text{Sh} = 1270 (0.121) = 153$$

$$\text{Re} = \frac{dU\rho}{\mu} = \frac{0.317(4.2)(0.998)}{(0.922 \times 10^{-2})}$$

$$\text{Re} = 144$$

$$\text{Sc}_A = \frac{\mu}{\rho D_{\text{CO}_2}} = \frac{0.922 \times 10^{-2}}{(0.998)(1.95 \times 10^{-5})}$$

$$\text{Sc}_A = 472$$

$$\text{Re}^{1/2} \text{Sc}_A^{1/3} = (144)^{1/2} (472)^{1/3}$$

$$\text{Re}^{1/2} \text{Sc}_A^{1/3} = 92.3$$

I. AUXILIARY EXPERIMENTAL STUDIES

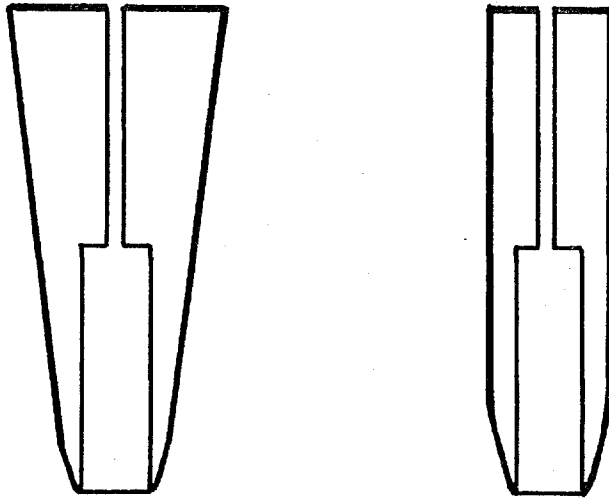
(i) Shape of Bubble Support

The tapered Teflon tip used throughout the study was later altered to cylindrical form, as illustrated in Figure 26. Using the cylindrical tip a series of experiments was carried out covering the same flow rate range as previously, but only three instead of four concentration levels.

The results obtained using the cylindrical bubble support are shown in Table I-1. A statistical test to determine whether this new data differed from that obtained with the tapered tip (Table 5.2) was carried out following the procedure outlined in (V3). At all concentration levels the tests showed that there was no significant difference between the two data sets. It could be concluded therefore that this change in bubble support shape had no effect on the absorption rate.

(ii) Bubble Shape

The diagram illustrating the water-tunnel details (Figure 12) shows the test bubble facing downward with the liquid flow in the upward direction. All results reported herein were obtained with this configuration. Initially, however, a series of experiments was carried out with the test section located on the right hand side of the apparatus (See Figure 11) so that the bubble could be faced upward with the flow in the opposite direction. The results obtained with this arrangement were contrary to all previous mass transfer correlations, as the absorption rates were only slightly affected by changes in liquid flow rate. Photographs of the bubbles taken under both conditions showed



TAPERED

CYLINDRICAL

FIGURE 26. - SCHEMATIC OF TAPERED AND CYLINDRICAL BUBBLE SUPPORT

TABLE I.1

Absorption Rate Results -
Cylindrically Shaped Bubble Support

Conc MEA mole %	Re	Sc _A	ABS RATE cc/min	Corrected ABS. RATE cc/min	\bar{Sh} corrected
0	39.8	456	0.0590	0.0385	48.8
			0.0521	0.0319	40.6
	64.8	456	0.0725	0.0382	48.5
			0.0630	0.0403	51.2
	131	456	0.0891	0.0606	76.8
150	456	0.0853	0.0598	76.0	
0.33	38.5	472	0.103	0.079	101
			0.122	0.089	113
	62.5	472	0.122	0.089	113
	126	472	0.152	0.127	162
	199	472	0.184	0.155	196
0.66	37.2	488	0.134	0.111	142
	60.4	488	0.145	0.121	153
	140	488	0.202	0.177	224
	193	488	0.286	0.260	330

that there was a marked difference in bubble shape. Figure 27 illustrates a bubble facing upward with opposing liquid flow. There is a pronounced elongation in the vertical direction. As a result the surface area below the horizontal line (shaded in diagram) was almost twice the surface area of the front portion of the bubble. A spherical bubble would have identical areas in the front and rear portions.. This excessively large percentage of the surface was in a region where the liquid velocities near the gas-liquid interface, and consequently the mass transfer rates in the region, would be little affected by changes in the main stream velocity.

This method of obtaining a single gas bubble was discontinued, since it was obvious that the shape obtained was not a reasonable approximation of the spherical shape dealt with theoretically.

With the bubble formation equipment as shown in Figure 12, an ellipsoidally shaped bubble was obtained (Figures 22 and 23). The ellipsoidal form was a very reasonable approximation of a spherical bubble and had the proper percentage of surface and in the front and rear portions.

(iii) Contact Between Copper Metal and Monoethanolamine Solutions

It has been noted that the monoethanolamine solutions turned blue on prolonged contact with the copper and brass materials of the water-tunnel. Tests were performed during the initial part of this work to determine whether the presence of these dissolved metals affected the carbon dioxide absorption rates.

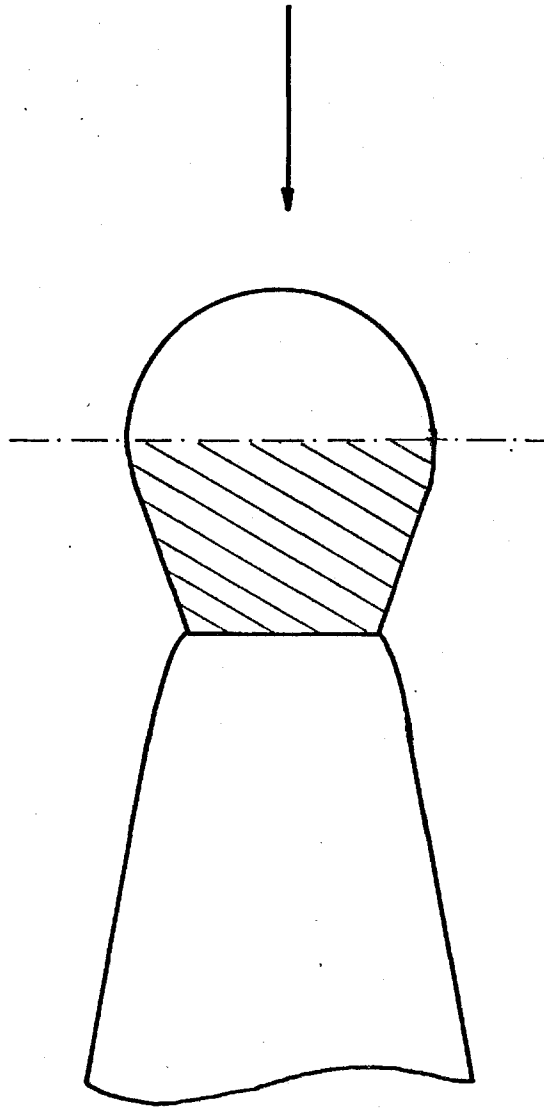


FIGURE 27. - - VERTICALLY ELONGATED GAS BUBBLE

The first test utilized a small glass apparatus, illustrated in Figure 28, which served as a rather crude water-tunnel. Several solutions of equal monoethanolamine concentration were prepared. One-half of these were placed in contact with copper and brass for an extended period. Absorption rates were then determined with solutions containing no dissolved metals and with those which had been exposed to copper and brass. The results obtained are in Table I-2. The application of a Student t test (V4) indicated that there was no significant difference between the two sets of data at the 95% confidence level. The presence of dissolved metals had therefore not affected the absorption rate of carbon dioxide into monoethanolamine solutions.

A second test was carried out in the regular water-tunnel with its copper pipes and brass flanges.

Absorption rates were determined shortly after a quantity of monoethanolamine had been added to the system, i.e., after the system was well mixed. Another series of absorption rate measurements were performed after about 1½ hours had elapsed. The results obtained are given in Table I-3. Once again a Student t test was applied and showed that there was no significant difference between the two sets of data.

As a result of the two separate tests, it was concluded that the presence of dissolved copper and brass in monoethanolamine solutions did not have a significant effect on the absorption rate of carbon dioxide.

(iv) Transfer of Inerts into the Gas Bubble

To confirm that oxygen and nitrogen dissolved in the distilled

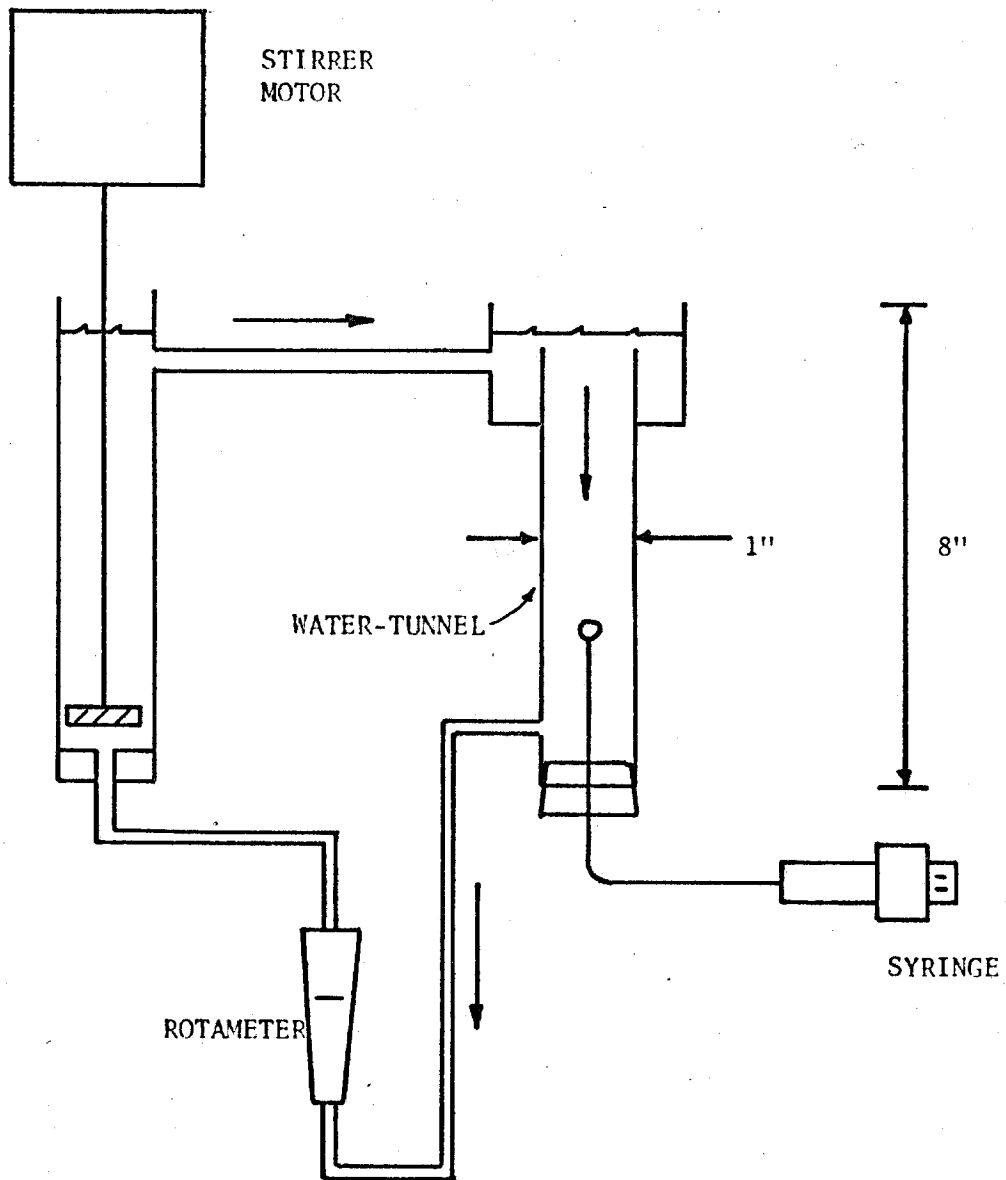


FIGURE 28. - GLASS WATER-TUNNEL USED FOR PRELIMINARY EXPERIMENTS

TABLE 1.2

Effect of Dissolved Metals on Rate
of Absorption of Carbon Dioxide
into Monoethanolamine Solutions

ABSORPTION RATES

MEA SOL ^N CONTAINING NO DISSOLVED METAL	MEA SOL ^N EXPOSED TO COPPER AND BRASS
cc/min.	cc/min.
0.0893	0.0903
0.0891	0.0882
0.0914	0.0868
0.0963	0.0938
0.115	0.114
0.101	0.123
0.0974	0.0988
0.0983	0.0970
0.119	0.100
	0.0948
	0.0930
	0.0946
$\bar{x}_1 =$ 0.0995	$\bar{x}_2 =$ 0.0979

$$t = 0.349$$

calc.

$$t_{0.95} = 2.093$$

∴ Cannot reject $\bar{x}_1 = \bar{x}_2$

TABLE I.3

Effect of Contact Time between
Monoethanolamine and Water-tunnel
Materials - Absorption of Carbon Dioxide

TIME AFTER MEA ADDED min	ABS. RATE cc/min
15 - 60	0.340
	0.362
	0.346
	0.335
	0.360
	0.349
90 - 120	0.321
	0.338
	0.334
	0.338
	0.348
	0.337

$$\bar{x}_1 = 0.349 \quad \bar{x}_2 = 0.336$$

$$t = 1.17$$

calc.

$$t_{0.95} = 2.228$$

\therefore Cannot reject $\bar{x}_1 = \bar{x}_2$

water would transfer into the carbon dioxide bubble, the following experiment was carried out. A beaker was filled with monoethanolamine solution and inverted in a bath containing the same solution. Carbon dioxide was bubbled into the inverted beaker for a short period. The absorption proceeded very rapidly, up to a point where a small volume of gas remained. This residual volume did not become absorbed, even on prolonged standing. A typical chromatographic analysis showed that the gas contained 31% oxygen, and 69% nitrogen. Since the carbon dioxide used contained less than 0.01% inerts, the oxygen and nitrogen must have been desorbed from the distilled water. The observed composition reflects the fact that oxygen is more soluble in water than nitrogen.

J. SOLUTION OF NAVIER-STOKES EQUATION

A finite-difference technique was used by Jenson (J2) to solve the Navier-Stokes equation for flow around a solid sphere for Reynolds numbers of 5, 10, 20 and 40. Jenson used a relaxation technique and a desk calculator. In the present study the work of Jenson was closely followed, except that solutions were obtained using an iterative procedure on an IBM-7040 computer.

(i) Equations and Finite Difference Approximations

The Navier-Stokes equation for viscous, incompressible, axisymmetric flow in terms of the stream function (Ψ) in spherical co-ordinates may be written as

$$\frac{\text{Re}}{2} \left[\frac{\partial \Psi}{\partial r} \cdot \frac{\partial}{\partial \theta} \left(\frac{E^2 \Psi}{r^2 \sin^2 \theta} \right) - \frac{\partial \Psi}{\partial \theta} \cdot \frac{\partial}{\partial r} \left(\frac{E^2 \Psi}{r^2 \sin^2 \theta} \right) \right] \sin \theta = E^4 \Psi \quad (\text{J-1})$$

where

$$E^2 = \frac{\partial^2}{\partial r^2} + \frac{\sin \theta}{r^2} \frac{\partial}{\partial \theta} \left(\frac{1}{\sin \theta} \frac{\partial}{\partial \theta} \right)$$

Equation (J-1) may be split into two simultaneous second-order equations by introducing the vorticity (ζ) as follows:

$$E^2 \Psi = \zeta r \sin \theta \quad (\text{J-2})$$

$$\frac{\text{Re}}{2} \left[\frac{\partial \Psi}{\partial r} \cdot \frac{\partial}{\partial \theta} \left(\frac{\zeta}{r \sin \theta} \right) - \frac{\partial \Psi}{\partial \theta} \cdot \frac{\partial}{\partial r} \left(\frac{\zeta}{r \sin \theta} \right) \right] \sin \theta = E^2 (\zeta r \sin \theta) \quad (\text{J-3})$$

The co-ordinate system employed is shown in Figure 29. Note that the locations are identified in a manner consistent with (H4, H5) and are not consistent with Figure 4. The velocity components are related to

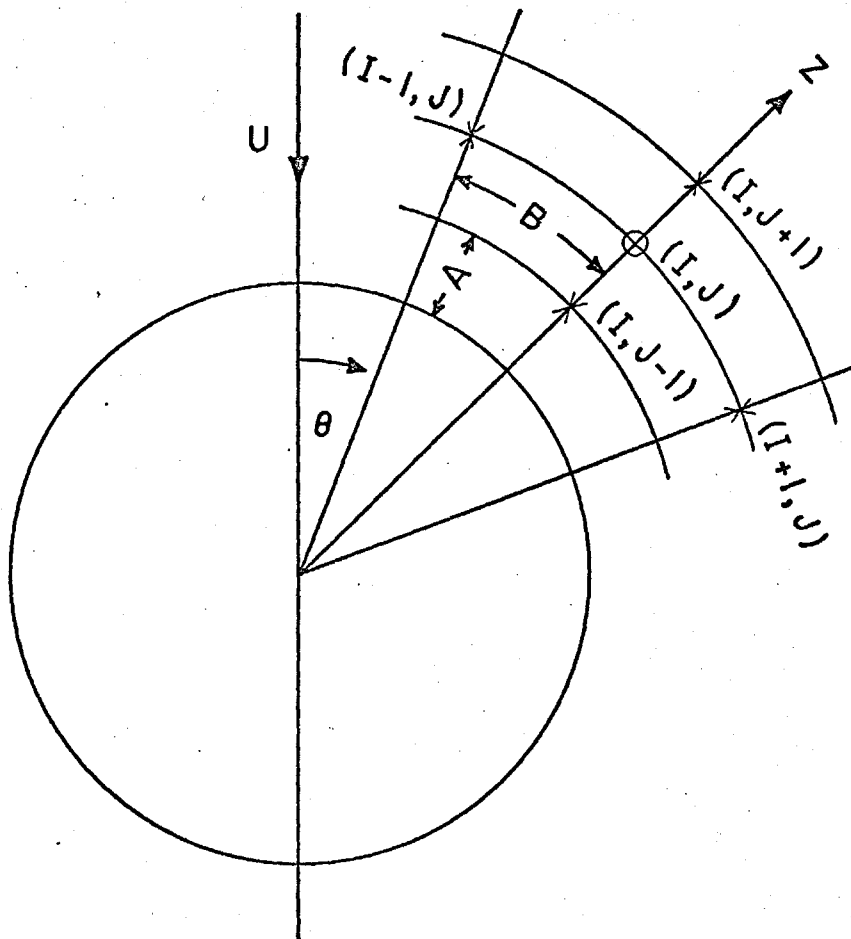


FIGURE 29. - FINITE-DIFFERENCE MESH SYSTEM
- SOLUTION OF NAVIER-STOKES EQUATION

the stream function as follows:

$$V_{\theta} = \frac{1}{r \sin \theta} \frac{\partial \Psi}{\partial r}; \quad V_r = \frac{-1}{r^2 \sin \theta} \frac{\partial \Psi}{\partial \theta}$$

All quantities have been made dimensionless by putting

$$r = \frac{r'}{A} \quad \Psi = \frac{\Psi'}{UA^2}, \quad \zeta = \frac{\zeta' A}{U}, \quad V_r = \frac{V'_r}{U}, \quad V_{\theta} = \frac{V'_{\theta}}{U}, \quad Re = \frac{2UA}{\nu}$$

The present investigation was aimed at repeating and extending Jenson's work to higher Reynolds numbers. The finite-difference equations accurate to second order derived by Jenson were used with an exponential step size in the radial direction and a constant angular step size. The stream function and vorticity vary most rapidly near the sphere surface, thus requiring a small step size there, while a larger step size far from the surface is adequate. This was achieved by using the substitution $r = e^Z$ and taking equal intervals in Z , viz. equations (J-2) and (J-3) became

$$e^{2Z} E^2 \Psi - \zeta e^{3Z} \sin \theta = 0 \quad (J-4)$$

$$\frac{Re}{2} \left[\frac{\partial \Psi}{\partial Z} \frac{\partial F}{\partial \theta} - \frac{\partial \Psi}{\partial \theta} \frac{\partial F}{\partial Z} \right] e^Z \sin \theta - e^{2Z} E^2 G = 0 \quad (J-5)$$

where

$$e^{2Z} E^2 = \frac{\partial^2}{\partial Z^2} - \frac{\partial}{\partial Z} + \sin \theta \frac{\partial}{\partial \theta} \left(\frac{1}{\sin \theta} \frac{\partial}{\partial \theta} \right)$$

$$F = \frac{\zeta}{e^Z \sin \theta}, \quad G = \zeta E^Z \sin \theta$$

Considering lattice spacing A in the Z - direction and B in the θ - direction, equations (J-4) and (J-5) were written in finite-difference form as

$$\begin{aligned} & \Psi(I, J+1) \left(\frac{2-A}{2A^2} \right) + \Psi(I, J-1) \left(\frac{2+A}{2A^2} \right) + \Psi(I+1, J) \left(\frac{2-B \cot \theta(I)}{2B^2} \right) \\ & + \Psi(I-1, J) \left(\frac{2+B \cot \theta(I)}{2B^2} \right) - \Psi(I, J) \left(\frac{2}{A^2} + \frac{2}{B^2} \right) - G(I, J) e^{2Z} = 0 \end{aligned} \quad (J-6)$$

$$\begin{aligned} & G(I, J+1) \left(\frac{2-A}{2A^2} \right) + G(I, J-1) \left(\frac{2+A}{2A^2} \right) + G(I+1, J) \left(\frac{2-B \cot \theta(I)}{2B^2} \right) \\ & + G(I-1, J) \left(\frac{2+B \cot \theta(I)}{2B^2} \right) - G(I, J) \left(\frac{2}{A^2} + \frac{2}{B^2} \right) \\ & - \frac{\text{Re } Z(J)}{4} \sin \theta(I) \left[\left(\frac{\Psi(I, J+1) - \Psi(I, J-1)}{2A} \right) \left(\frac{F(I+1, J) - F(I-1, J)}{B} \right) \right. \\ & \left. - \left(\frac{\Psi(I+1, J) - \Psi(I-1, J)}{B} \right) \left(\frac{F(I, J+1) - F(I, J-1)}{A} \right) \right] = 0 \end{aligned} \quad (J-7)$$

(ii) Boundary Conditions

Both the stream function and vorticity (or their derivatives) must be specified on a boundary completely enclosing the region of flow.

For flow around a solid sphere these conditions are:

Along the axis of symmetry

$$\Psi = 0 \quad ; \quad \frac{\partial \Psi}{\partial r} = 0 \quad ; \quad \zeta = 0 \quad \text{at} \quad \theta = 0, \pi$$

On the sphere surface

$$\Psi = 0 \quad ; \quad \zeta = \frac{E^2 \Psi}{\sin \theta} \quad \text{at} \quad r=1$$

Far from the sphere where there is undisturbed parallel flow

$$\Psi = \frac{1}{2} r^2 \sin^2 \theta \quad ; \quad \zeta = 0 \quad \text{as} \quad r \rightarrow \infty$$

(iii) Method of Solution

Initial estimates of the stream function and vorticity values, obtained from the work of Hamielec (H2, H3), were inserted at all mesh locations. The calculations were started by using these initial values of Ψ and G to calculate an improved Ψ from equation (J-6). The

new Ψ found were substituted into equation (J-7) to find improved G values. The new G found were then substituted into equation (J-6) and this procedure was repeated until Ψ and G changed by less than a specified tolerance per iteration. The tolerance chosen for all calculations was 0.0001 for both Ψ and G.

In the iterative procedure to solve equation (J-6) and (J-7) relaxation factors were used to stabilize the computations. They were introduced as follows:

$$\Psi_n(I,J) = \Psi_{n-1}(I,J) + WW(\Psi_n(I,J) - \Psi_{n-1}(I,J)) \quad (J-8)$$

$$G_n(I,J) = G_{n-1}(I,J) + W(G_n(I,J) - G_{n-1}(I,J)) \quad (J-9)$$

where subscript "n" denotes the nth value calculated. The relaxation factors, WW and W, had to be found by trial and error.

This solution procedure was stable as long as a suitable choice of relaxation factors and position of the outer boundary had been made. Computation times were lengthy, requiring as long as two hours on an IBM-7040.

(iv) Summary

Since this author was instrumental only in the development of suitable computer programs to provide solutions of equations (J-6) and (J-7), the voluminous results obtained, and their interpretation, are not included as part of this study. The interested reader is referred to publications (H4) and (H5).

One conclusion reached as a result of this extension of Jenson's work was pertinent to this theoretical study; it was found that the

velocity profiles used here (H2, H3) allowed reasonable descriptions of the flow field. This indicates that the use of the presumably more accurate finite-difference solutions to describe the flow, rather than the Kawaguti-type profiles, would not alter the mass transfer solutions of this work.

K. PROGRAM LISTINGS AND PROCEDURE OUTLINES

(i) Diffusion from a Sphere into a Stagnant Fluid with Second Order Reaction

The solution of equations (C-1) and (C-2) was obtained using finite-difference techniques. The solution proceeded as follows:

1. Initial estimates of c_A and c_B were inserted at all radial mesh points.
2. New values of c_A were obtained by solving equation (C-1)
3. These c_A values were introduced into equation (C-2) which was then solved for new c_B values.
4. If the new c_A and c_B values differed from the previous ones the procedure was repeated. This iteration continued until the concentration values no longer changed within a specified tolerance.

The solution was usually punched on cards in binary form so that it could be included as input for the forced convection transfer problem.

```

C   DIFFUSION FROM A SPHERE INTO A STAGNANT FLUID ACCOMPANIED BY A
C   SECOND ORDER CHEMICAL REACTION
C   REQUIRES THE SOLUTION OF TWO SECOND ORDER NONLINEAR ORDINARY
C   DIFFERENTIAL EQUATIONS ** USED FINITE DIFFERENCE METHODS
C
C   RKA,RKB ** REACTION RATE CONSTANTS
C   H,DRAD ** RADIAL MESH PARAMETERS
C   EPS ** TOLERANCE TO DETERMINE CONVERGENCE
C   M ** NUMBER OF RADIAL STEPS
C
C   DIMENSION TRI(3,70),RHS(70),COA(70),COB(70),COE(70)
C   DIMENSION A(70),B(70),RAD(70)
C   READ (5,1000) RKA,RKB
C   READ(5,1000) H,DRAD
C   READ(5,1002) EPS
C   READ(5,1003)M
C   READ(5,1003) JPUNCH
C   WRITE (6,1004) RKA,RKB
C   WRITE (6,1005) H,DRAD
C   WRITE (6,1006) EPS,M
C
C   RADIAL MESH SYSTEM
C
C   MM=M+1
C   DO 555 J=1,MM
C   MJ=J-1
555  RAD(J)=1.+DRAD*(H**MJ-1.)/(H-1.)
C
C   DDR1=RAD(2)-RAD(1)
C   DDR2=RAD(3)-RAD(1)
C   DDR3=RAD(3)-RAD(2)
C   RATIO1=DDR2*DDR2/(DDR2*DDR2-DDR1*DDR1)
C   RATIO2=DDR1*DDR1/(DDR2*DDR2-DDR1*DDR1)
C
C   INITIAL CONCENTRATION DISTRIBUTION
C
C   DO 10 J=1,M
C   A(J)=0.50
10  B(J)=0.10
C   A(1)=1.0
C   A(MM)=0.0
C   B(MM)=1.0
C   WRITE (6,1007) (RAD(J),A(J),B(J),J=1,MM)
C
C   EVALUATION OF COEFFICIENTS
C
C   DO 20 J=2,M
C   DR1=RAD(J)-RAD(J-1)
C   DR2=RAD(J+1)-RAD(J)
C   DR3=RAD(J+1)-RAD(J-1)
C   F1=1./DR3
C   F4=2./(DR2*DR3)
C   F5=2./(DR1*DR2)

```

```

F6=2./(DR1*DR3)
ODD=2.*F1/RAD(J)
COA(J)=F4+ODD
COB(J)=F6-ODD
20 COE(J)=-F5

```

```

C
C SOLUTION BY MATRIX INVERSION AND ITERATION
C

```

```

300 JN=0
DO 30 J=2,M
CE=COE(J)-RKA*B(J)
CA=COA(J)/CE
CB=COB(J)/CE
TRI(2,J-1)=1.0
IF (J.EQ.2) GO TO 310
TRI(1,J-1)=CB
IF (J.EQ.M) GO TO 320
310 TRI(3,J-1)=CA
320 RHS(J-1)=0.0
IF (J.EQ.2) RHS(J-1)=-CB*A(1)
30 CONTINUE
MMINUS=M-1

```

```

C
C CALL BND SOL (TRI,RHS,2,1,MMINUS)
C

```

```

DO 40 J=2,M
DIFF=ABS(A(J))-ABS(RHS(J-1))
IF (ABS(DIFF).GT.EPS) JN=1
40 A(J)=RHS(J-1)

```

```

C
C
DO 50 J=2,M
CE=COE(J)-RKB*A(J)
CA=COA(J)/CE
CB=COB(J)/CE
TRI(2,J-1)=1.0
IF (J.EQ.2) TRI(2,1)=1.0+RATIO1*CB
IF (J.EQ.2) GO TO 510
TRI(1,J-1)=CB
IF (J.EQ.M) GO TO 520
510 TRI(3,J-1)=CA
IF (J.EQ.2) TRI(3,1)=(CA-RATIO2*CB)
520 RHS(J-1)=0.0
IF (J.EQ.M) RHS(J-1)=-CA*B(J+1)
50 CONTINUE

```

```

C
C CALL BND SOL (TRI,RHS,3,1,MMINUS)
C

```

```

DO 60 J=2,M
DIFF=ABS(B(J))-ABS(RHS(J-1))
IF (ABS(DIFF).GT.EPS) JN=1
60 B(J)=RHS(J-1)
B(1)=RATIO1*B(2)-RATIO2*B(3)

```

```

JJ=JJ+1
JMAX=3000
IF (JJ.EQ.JMAX) GO TO 70
IF (JN.EQ.1) GO TO 300

```

```

C
C SOLUTION ON CARDS IN BINARY FORM IF JPUNCH = 1
C

```

```

IF (JPUNCH.EQ.1) WRITE (7) (RAD(J),A(J),B(J),J=1,MM)
GO TO 80
70 WRITE (6,1008) JMAX
80 WRITE (6,1007) (RAD(J),A(J),B(J),J=1,MM)
1000 FORMAT (2F12.6)
1002 FORMAT (F12.6)
1003 FORMAT (I5)
1004 FORMAT (1H-,6HRKA = F15.4,10X,6HRKB = F15.4)
1005 FORMAT (1H-,4HH = F15.4,3X,7HDRAD = F10.6)
1006 FORMAT (1H-,6HEPS = F15.6,10X,26HNO OF RADIAL INCREMENTS = I5)
1007 FORMAT (3X,3F15.6,/)
1008 FORMAT (1H-,24HHAS NOT CONVERGED AFTER I5,2X,10HITERATIONS)
END

```

```

$ENTRY
  10000.0      1000.0
  1.30        0.00005
  0.00001
    30
    1
$IBSYS

```

CD TOT 0147

- (ii) Mass Transfer from a Circulating or Non-circulating Sphere with First Order Chemical Reaction.

The Reynolds number, Schmidt numbers, reaction rate constant, and mesh size details must be specified as program input.

The program has been written to allow convergence tests by doubling the number of radial steps while leaving the position of the outer boundary unchanged. This is accomplished by setting ICHEK = 1. Initial concentration estimates are either taken from the analytic solution for diffusion into a stagnant fluid (if IBNRY = 0), or from previous results available on punched cards in binary form (if IBNRY = 1).

Velocity profiles for flow around solid spheres or circulating gas bubbles may be utilized. For the latter case profiles are available from Hamielec (H2, H3) only up to $Re = 80$. At higher values the potential flow profiles may be used.

Output is in printed form and includes local and average Sherwood numbers, as well as concentration values at each angular and radial position.

C CALCULATION OF LOCAL AND AVERAGE MASS TRANSFER RATES AROUND SPHERES
 C DIFFUSION AND FIRST ORDER CHEMICAL REACTION
 C CRANK NICHOLSON METHOD

C RE ** REYNOLDS NUMBER
 C A1,B1 ** VALUE OF CONSTANTS IN HAMIELEC VELOCITY PROFILES
 C SC ** SCHMIDT NUMBER
 C RK ** REACTION RATE CONSTANT
 C H,DRAD ** RADIAL MESH PARAMETERS
 C EPS ** TOLERANCE ON ZERO SLOPE CRITERION
 C N ** NUMBER OF ANGULAR STEPS
 C NNN ** NUMBER OF EXTRA ANGULAR STEPS AT THETA = 0
 C M ** NUMBER OF RADIAL STEPS

C DIMENSION C(75,62),THETA(75),RAD(62),GRAD(75),RATIO(75)
 C DIMENSION A(62),B(62),D(62),E(62)
 C DIMENSION DTHT(5)
 C DIMENSION VT(75,62),VR(75,62)
 C DIMENSION TRI(3,62),RHS(62)

C
 C READ (5,1000) RE,A1,B1
 C READ (5,1001) SC
 C READ (5,1001) RK
 C READ (5,1000) DRAD,H,EPS
 C READ (5,1002) N,NNN,M
 C READ (5,1003) IBNRY,IBNOUT
 C READ (5,1004) ICHEK

C
 C PROCEDURE FOR CONVERGENCE TEST ** TAKE 1/2 RADIAL STEP SIZE
 C THETA INCREMENT UNCHANGED ** PROCEDURE FOLLOWED IF ICHEK=1
 C

C IF (ICHEK.EQ.0) GO TO 155
 C M=2*M
 C R3=1.00005
 C R5=1.000115
 C H=SQRT((R5-1.)/(R3-1.))-1.
 C DRAD=(R3-1.)/(H+1.)

C
 C PRELIMINARY CALCULATIONS
 C

155 DTHT =3.1416/(FLOAT(N))
 N=N+NNN
 NN=N+1
 MM=M+1
 PE=RE*SC
 DENOM=SC**0.333*RE**0.5
 IF (H.EQ.1.) WRITE (6,333)
 IF (H.GT.1.) WRITE (6,222)
 DTHT(1)=DTHT/(FLOAT(NNN))
 DTHT(2)=DTHT
 RAD(1)=1.0
 THETA(1)=3.1416
 IF (H.EQ.1.) GO TO 21

```

GO TO 13
21 DO 14 J=2,MM
14 RAD(J)=RAD(J-1)+DRAD
GO TO 114
13 DO 17 J=2,MM
MN=J-1
17 RAD(J)=1.0+DRAD*(H**MN-1.)/(H-1.)

```

C
C
C
C

INITIAL CONC DISTRIBUTION OBTAINED FROM PREVIOUS PROGRAM
USING COARSER MESH ** USE THESE VALUES IF IBNRY =1

```

IF (IBNRY.EQ.0) GO TO 114
READ (5) NJN
READ (5) ((C(I,J),I=1,NJN),J=1,MM,2)
DO 175 I=1,NJN
DO 175 J=2,M,2
175 C(I,J)=C(I,J-1)-(C(I,J-1)-C(I,J+1))*(RAD(J)-RAD(J-1))/
1(RAD(J+1)-RAD(J-1))
WRITE (6,4) ((RAD(J),C(1,J)),J=1,MM)
GO TO 180

```

C
C
C
C
C

INITIAL CONCENTRATIONS FROM ANALYTIC SOLUTION OF EQUATION
DESCRIBING DIFFUSION FROM A SPHERE WITH FIRST ORDER REACTION
USE THESE VALUES IF IBNRY = 0

```

114 DUM=SQRT(RK)
111 DO 11 J=1,M
C(1,J)=EXP(DUM*(1.-RAD(J)))/RAD(J)
DO 22 I=1,NN
22 C(I,J)=C(1,J)
11 WRITE (6,4) RAD(J),C(1,J)
DO 33 I=2,NN
33 C(I,MM)=0.0
WRITE (6,4) RAD(MM),C(1,MM)
180 CONTINUE

```

C
C
C

CALC OF VELOCITY PROFILES

```

DO 23 I=1,N
DTHET=DTHT(2)
DD=3.1416-DTHET
IF (THETA(I).GT.DD) DTHET=DTHT(1)
THETA(I+1)=THETA(I)-DTHET
DUM1=COS(THETA(I))
DUM2=COS(THETA(I+1))
DUM3=SIN(THETA(I))
DUM4=SIN(THETA(I+1))
DO 23 J=2,M

```

C
C
C

VELOCITY PROFILES ** SOLID SPHERE

```

A2=-((120.+75.*A1)/29.
A3=((153.+63.*A1)/29.

```

```

A4=- (47.5+17.*A1)/29.
B2=-69.*B1/27.
B3=57.*B1/27.
B4=-15.*B1/27.
R1=RAD(J)
R2=RAD(J)*R1
R3=RAD(J)*R2
DMM1=(R3-A1-2.*A2/R1-3.*A3/R2-4.*A4/R3)/R3
DMM2=(-B1-2.*B2/R1-3.*B3/R2-4.*B4/R3)/R3
DMM3=(R3+2.*A1+2.*A2/R1+2.*A3/R2+2.*A4/R3)/R3
DMM4=(B1+B2/R1+B3/R2+B4/R3)/R3
VT(I,J)=DMM1*(DUM3+DUM4)/2.+DMM2*(DUM1*DUM3+DUM2*DUM4)/2.
DMM5=((2.*(DUM1)**2-(DUM3)**2)+(2.*(DUM2)**2-(DUM4)**2))/2.
23 VR(I,J)=DMM3*(DUM1+DUM2)/2.+DMM4*DMM5

```

C
C
C
PRELIMINARY CALCULATIONS

```

NI=NNN-1
43 CONTINUE
DO 44 I=1,N
  NJN=I+1
  DTHET=DTHT(2)
  DD=3.1416-DTHET
  IF (THETA(I).GT.DD) DTHET=DTHT(1)
  THETA(I+1)=THETA(I)-DTHET
  DO 55 J=2,M
    IF (H.EQ.1.) GO TO 51
    MN=J-1
    ODD=H**MN*DRAD*(1.+1./H)
    ODDSQ=(H**MN*DRAD)**2*(1.+1./H)/2.
    GO TO 52
51 ODD=RAD(J+1)-RAD(J-1)
    ODDSQ=ODD*ODD/4.
52 ODD1=DTHET/(PE*ODDSQ)
    ODD2=DTHET/(PE*ODD)
    ODD3=DTHET/(4.*ODD)
    ODD4=((1.+H)+RK*ODDSQ)
    A(J)=ODD1*RAD(J)/VT(I,J)
    B(J)=2.*(ODD2/VT(I,J)-ODD3*VR(I,J)*RAD(J)/VT(I,J))
    D(J)=1.+A(J)*ODD4
55 E(J)=A(J)*ODD4-1.

```

C
C
C
CALC OF CONCENTRATION PROFILES

```

DO 5000 J=2,M
  DM1 = (A(J) + B(J))/D(J)
  DM2 = (H * A(J) - B(J))/D(J)
  DM3 = E(J)/D(J)
  TRI(2, J-1) = 1.0
  IF (J.EQ.2) GO TO 501
  TRI (1, J-1) = -DM2
  IF (J.EQ.M) GO TO 502
501 TRI(3, J-1) = -DM1

```

```

502 RHS (J-1) = DM1 * C(I,J+1) + DM2 * C(I,J-1) -DM3 * C(I,J)
IF (J.EQ.2) RHS(J-1)= RHS (J-1)+ DM2 * C(I+1,J-1)
IF (J.EQ.M) RHS (J-1) = RHS(J-1) + DM1 * C(I+1,J+1)
5000 CONTINUE
MMINUS = M-1
C
CALL BNDSOL (TRI, RHS, 3, 1, MMINUS)
C
DO 503 J=2,M
503 C(I+1,J) = RHS(J-1)
C
CHECK ON CONDITION THAT DC/DTHETA =0 AT THETA = 3.1416
C
IF (I.GE.2) GO TO 45
DIFF=C(1,2)-C(2,2)
IF (ABS(DIFF).LT.EPS) GO TO 45
WRITE (6,1006) C(1,2),C(2,2)
DO 24 II=1,N
DO 24 J=2,M
IF (C(2,J).LT.0.0) C(2,J)=0.0
24 C(II,J)=C(2,J)
GO TO 43
45 GRAD(I)=2.*(C(I,1)-C(I,2))/DRAD
RATIO(I)=GRAD(I)/DENOM
IF (I.EQ.1) GO TO 44
DUM=1.20*GRAD(I-1)
IF (GRAD(I).GT.DUM.OR.GRAD(I).LT.0.0) GO TO 70
44 WRITE (6,2) I,C(I,10)
70 WRITE (6,9) SC,RE,PE,RK
WRITE (6,7) DRAD,DTHET
C
CALC OF OVERALL SHERWOOD NO
C
515 SUM=0.0
NNJ=NNJ-1
DO 600 I=2,NNJ
SUM=SUM-(THETA(I)-THETA(I-1))*(GRAD(I)*SIN(THETA(I))+GRAD(I-1)
1*SIN(THETA(I-1)))/2.
600 CONTINUE
SUM=SUM/(1.+COS(THETA(NNJ)))
DO 88 I=1,NNJ
ANGLE=THETA(I)*180./3.1416
WRITE (6,6) ANGLE
WRITE (6,555) GRAD(I),RATIO(I)
88 WRITE (6,5) (C(I,J),J=1,MM)
WRITE (6,444) SUM
C
PUNCH OUT BINARY DECK ** IF IBNOUT = 1
C
IF (IBNOUT.EQ.0) GO TO 150
WRITE (7) NJN
WRITE (7) ((C(I,J),I=1,NNJ),J=1,MM)
150 CONTINUE

```

```

1007 FORMAT (3X,10F10.4)
1006 FORMAT (2F15.6)
1005 FORMAT (6F10.4)
1004 FORMAT (I5)
1003 FORMAT (2I5)
1002 FORMAT (3I5)
1001 FORMAT (F15.4)
1000 FORMAT (3F12.4)
  999 FORMAT (1H-,7HRADIUS=F10.6)
  995 FORMAT (3X,5F10.6)
   9  FORMAT (1H-,3HSC=F10.3,3X,3HRE=F10.3,3X,3HPE=F20.3,3X,3HRK=F15.4)
  888 FORMAT (1H-,26H THETA      VTHETA      VRAD)
   8  FORMAT (1H-,2HW=F10.6,3X,4HEPS=F12.8)
  777 FORMAT (1X,3F10.6)
   7  FORMAT (1H-,5HDRAD=F10.6,3X,6HDTHET=F10.6)
   6  FORMAT (1H-,9HANGLE IS F10.4)
  555 FORMAT (1H0,15HLOCAL SH NO IS F10.4,3X,15HLOCAL RATIO IS F10.4)
   5  FORMAT (1H0,10F10.6)
  444 FORMAT (1H-,17HAVERAGE SH NO IS F15.4)
   4  FORMAT (3X,2F10.6)
  333 FORMAT (1H-,15HMESH IS UNIFORM)
   3  FORMAT (6F12.6)
  222 FORMAT (1H-,18HMESH IS NONUNIFORM)
   2  FORMAT (3X,I4,F10.6)
      END

```

```

$ENTRY
  200.0      0.1829      -20.6800
  500.0
 10000.0
  0.00005   1.30      0.00005
   60   10   30
   0    0
   0
$IBSYS

```

CD TOT 0270

C VELOCITY PROFILES ** POTENTIAL FLOW

C
 VR(I,J)=-(-1.+1./R3)*(DUM1+DUM2)/2.
 VT(I,J)=(1.+1./(2.*R3))*(DUM3+DUM4)/2.

C VELOCITY PROFILES ** CIRCULATING GAS BUBBLES

C
 C
 DO 23 J=2,M
 A2=-1.25-1.75*A1
 A3=0.75+0.75*A1
 B2=-1.75*B1
 B3=0.75*B1
 R1=RAD(J)
 R2=RAD(J)*R1
 R3=RAD(J)*R2
 DMM1=(R3-A1-2.*A2/R1-3.*A3/R2)/R3
 DMM2=(-B1-2.*B2/R1-3.*B3/R2)/R3
 DMM3=(R3+2.*A1+2.*A2/R1+2.*A3/R2)/R3
 DMM4=(B1+B2/R1+B3/R2)/R3
 VT(I,J)=DMM1*(DUM3+DUM4)/2.+DMM2*(DUM1*DUM3+DUM2*DUM4)/2.
 DMM5=((2.*(DUM1)**2-(DUM3)**2)+(2.*(DUM2)**2-(DUM4)**2))/2.
 23 VR(I,J)=DMM3*(DUM1+DUM2)/2.+DMM4*DMM5

- (iii) Mass Transfer from a Circulating or Non-circulating Sphere with Second Order Chemical Reaction.

The Reynolds number, Schmidt numbers, reaction rate constants, and mesh size details must be specified as program input.

Arbitrary initial concentration estimates may be put in directly or read in on cards from solutions obtained in part (i) of this Appendix. The latter values are read in by setting JREAD = 1.

Convergence tests are performed by setting JCHECK = 1. This doubles the number of radial steps, while leaving the position of the outer boundary unchanged. Angular step size must be handled separately through the definition of DTHET.

The quantity JMOD must be set equal to 1 when dealing with transfer from solid spheres at $k_A > 10^4$. By setting JMOD = 1 the DuFort-Frankel modifications discussed in Section 3.2.2 are utilized.

Velocity profiles are as in the first order reaction case, with only the storage of these values handled in a different manner.

Output is in printed form. It includes local and average Sherwood numbers, along with concentration values of both materials A and B at each angular and radial position.

```

C MASS TRANSFER FROM A SINGLE SPHERE AT INTERMEDIATE RE NUMBERS
C FOR THE CASE OF SECOND ORDER CHEMICAL REACTION
C CRANK NICHOLSON METHOD
C A *** CONC OF MATERIAL DIFFUSING FROM SPHERE SURFACE
C B *** CONC OF MATERIAL DIFFUSING FROM MAIN STREAM
C VR *** RADIAL VELOCITY COMPONENT
C VT *** TANGENTIAL VELOCITY COMPONENT
C THETA *** ANGLE IN RADIANS
C RAD *** DIMENSIONLESS RADIUS
C SH *** SHERWOOD NUMBER
C AA,BA,DA,EA,AB,BB,DB,EBARE COEFFICIENTS IN FINITE DIFF EQN
C RE *** REYNOLDS NUMBER
C SCA,SCB *** SCHMIDT NUMBERS
C PEA,PEB *** PECLET NUMBERS
C RKA,RKB *** REACTION RATE CONSTANTS FOR SECOND ORDER REACTION
C EPS *** TOLERANCE ON CALCULATED VALUES
C N *** NUMBER OF ANGULAR INCREMENTS
C NEXTRA *** NO OF SMALLER ANGULAR STEPS NEAR FRONTAL STAG POINT
C
C JMOD MUST EQUAL 1 FOR TRANSFER FROM SOLID SPHERES AND RKA.GT.10000
C
C DIMENSION A(75,70),B(75,70)
C DIMENSION THETA(80),RAD(70),SH(80)
C DIMENSION VT(70),VR(70),VTEXP(70),VREXP(70)
C DIMENSION AAA(70),ABB(70),BAA(70),BBB(70)
C DIMENSION DAA(70),DAB(70)
C DIMENSION DUMAB(70),DUMBB(70),DUMDB(70),DUMAA(70),DUMBA(70),
1 DUMDA(70),E(70)
C DIMENSION DTHT(20)
C DIMENSION AHALF(70),BHALF(70)
C DIMENSION TRI(3,70),RHS(70)
C DIMENSION AA(70),BA(70),DA(70),EA(70),AB(70),BB(70),DB(70),EB(70)
C DIMENSION AAX(70),BAX(70),DAX(70),EAX(70),ABX(70),BBX(70)
1,DBX(70),EBX(70),RAX(70),RBX(70)
C
C READ (5,1000) RE,A1,B1
C READ (5,1001) SCA,SCB
C READ (5,1001) RKA,RKB
C READ(5,1001) H,DRAD
C READ (5,1002) EPS
C READ (5,1003) N,NEXTRA,M,JREAD,JCHECK
C READ (5,1016) JMOD
C
C WRITE (6,1005) RE,A1,B1
C WRITE (6,1006) SCA,SCB,RKA,RKB
C WRITE (6,1007) EPS,H
C WRITE (6,1008) N,M
C RESCA=SQRT(RE)*SCA**0.333
C WRITE (6,1002) RESCA
C
C RADIAL MESH SYSTEM
C
C MM=M+1

```

```

DO 555 J=2,MM
MJ=J-1
555 RAD(J)=1.+DRAD*(H**MJ-1.)/(H-1.)
C
C INITIAL CONC DISTRIBUTIONS AND BOUNDARY CONDITIONS
C
IF (JREAD.EQ.1) GO TO 22
DSQRT=SQRT(RKA)
DO 15 J=1,MM
A(1,J)=EXP(DSQRT*(1.-RAD(J)))/RAD(J)
DO 15 I=2,N
15 A(I,J)=A(1,J)
DO 20 J=1,MM
B(1,J)=0.50
DO 20 I=2,N
20 B(I,J)=B(1,J)
GO TO 23
22 IF (JCHECK.EQ.0) GO TO 222
M=2*M
MM=M+1
R3=1.00005
R5=1.000115
H=SQRT((R5-1.)/(R3-1.)-1.)
DRAD=(R3-1.)/(H+1.)
READ(5)(RAD(J),A(1,J),B(1,J),J=1,MM,2)
DO 800 J=1,MM
MN=J-1
800 RAD(J)=1.0+DRAD*(H**MN-1.)/(H-1.)
DO 801 J=2,M,2
A(1,J)=A(1,J-1)-(A(1,J-1)-A(1,J+1))*(RAD(J)-RAD(J-1))/(RAD(J+1)-
1RAD(J-1))
801 B(1,J)=B(1,J-1)-(B(1,J-1)-B(1,J+1))*(RAD(J)-RAD(J-1))/(RAD(J+1)-
1RAD(J-1))
GO TO 802
C
C INITIAL CONCENTRATION ESTIMATES FROM EQUATIONS DESCRIBING
C DIFFUSION FROM A SPHERE WITH SECOND ORDER REACTION
C THESE VALUES READ IN IN BINARY FORM *** IF JREAD = 1
C
222 READ(5) (RAD(J),A(1,J),B(1,J),J=1,MM)
802 DO 24 I=1,N
DO 24 J=1,MM
A(I,J)=A(1,J)
24 B(I,J)=B(1,J)
23 DO 21 I=1,N
A(I,1)=1.0
A(I,MM)=0.0
21 B(I,MM)=1.0
WRITE (6,1000) (RAD(J),A(1,J),B(1,J),J=1,MM)
C
C PRELIMINARY CALCULATIONS
C
DDR1=RAD(2)-RAD(1)

```

```

DDR2=RAD(3)-RAD(1)
DDR3=RAD(3)-RAD(2)
RATIO1=DDR2/(DDR1*DDR3)
RATIO2=DDR1/(DDR2*DDR3)
RATIO3=DDR2*DDR2/(DDR2*DDR2-DDR1*DDR1)
RATIO4=DDR1*DDR1/(DDR2*DDR2-DDR1*DDR1)
DTHET=3.1416/(FLOAT(N))
WRITE (6,1009) DRAD,DTHET
N=N+NEXTRA
PEA=RE*SCA
PEB=RE*SCB
WRITE (6,1010) PEA,PEB
DTHT(1)=DTHET/(FLOAT(NEXTRA))
DTHT(2)=DTHET
THETA(1)=3.1416

```

C
C

```

JCONV=0
CMAX=2.0
JTURN=0
DO 45 I=1,N
ICOUNT=I-1
DTHET=DTHT(2)
DD=3.1416-DTHET
IF (THETA(I).GT.DD) DTHET=DTHT(1)
THETA(I+1)=THETA(I)-DTHET
DUM1=COS(THETA(I))
DUM2=COS(THETA(I+1))
DUM3=SIN(THETA(I))
DUM4=SIN(THETA(I+1))
DO 35 J=2,M

```

C
C
C

CALCULATION OF VELOCITY PROFILES *** SOLID SPHERES

```

A2=- (120.+75.*A1)/29.
A3=(153.+63.*A1)/29.
A4=- (47.5+17.*A1)/29.
B2=-69.*B1/27.
B3=57.*B1/27.
B4=-15.*B1/27.
R1=RAD(J)
R2=RAD(J)*R1
R3=RAD(J)*R2
DMM1=(R3-A1-2.*A2/R1-3.*A3/R2-4.*A4/R3)/R3
DMM2=(-B1-2.*B2/R1-3.*B3/R2-4.*B4/R3)/R3
DMM3=(R3+2.*A1+2.*A2/R1+2.*A3/R2+2.*A4/R3)/R3
DMM4=(B1+B2/R1+B3/R2+B4/R3)/R3
VT(J)=DMM1*(DUM3+DUM4)/2.+DMM2*(DUM1*DUM3+DUM2*DUM4)/2.
VTEP(J)=DMM1*DUM3+DMM2*DUM1*DUM3
DMM5=((2.*(DUM1)**2-(DUM3)**2)+(2.*(DUM2)**2-(DUM4)**2))/2.
VR(J)=DMM3*(DUM1+DUM2)/2.+DMM4*DMM5
VREXP(J)=DMM3*DUM1+DMM4*(2.*DUM1**2-DUM3**2)

```

C

```

C      CALCULATION OF COEFFICIENTS FOR FINITE DIFFERENCE EQUATION
C
344  DR1=RAD(J)-RAD(J-1)
      DR2=RAD(J+1)-RAD(J)
      DR3=RAD(J+1)-RAD(J-1)
      F1=1./DR3
      F4=2./(DR2*DR3)
      F5=2./(DR1*DR2)
      F6=2./(DR1*DR3)
      ODD1=VR(J)*F1/2.
      ODD2A=F4/PEA
      ODD2B=F4/PEB
      ODD3A=2.*F1/(RAD(J)*PEA)
      ODD3B=2.*F1/(RAD(J)*PEB)
      ODD4=VT(J)/(RAD(J)*DTHET)
      ODD2AA=F6/PEA
      ODD2BB=F6/PEB
34  AA(J)=ODD1-ODD2A-ODD3A
      AB(J)=ODD1-ODD2B-ODD3B
      BA(J)=-ODD1-ODD2AA+ODD3A
      BB(J)=-ODD1-ODD2BB+ODD3B
C
C      IF JMOD = 1 *** USE DUFORT FRANKEL MODIFICATION IN IMPLICIT AS
C      WELL AS EXPLICIT STEP
C
      IF (I.EQ.1.OR.JMOD.EQ.0) GO TO 345
C
C      DUFORT FRANKEL MODIFICATION
C
      DA(J)=          -ODD4
      DB(J)=          -ODD4
      DAA(J)=         F5/(2.*PEA)
      DAB(J)=         F5/(2.*PEB)
      EA(J)=          ODD4  +  1.5*F5/PEA
      EB(J)=          ODD4  +  1.5*F5/PEB
      GO TO 346
C
C      USING STANDARD FORM FOR SECOND DERIVATIVE IN RADIAL DIRECTION
C
345  DA(J)=-ODD4+F5/PEA
      DB(J)=-ODD4+F5/PEB
      EA(J)=ODD4+F5/PEA
      EB(J)=ODD4+F5/PEB
C
346  ODDX=VREXP(J)*F1/2.
      ODDXX=VTEXP(J)/(RAD(J)*DTHET)
      AAX(J)=ODDX-ODD2A-ODD3A
      ABX(J)=ODDX-ODD2B-ODD3B
      BAX(J)=-ODDX-ODD2AA+ODD3A
      BBX(J)=-ODDX-ODD2BB+ODD3B
      DAX(J)=-ODDXX+F5/PEA
      DBX(J)=-ODDXX+F5/PEB
      EAX(J)=ODDXX+F5/PEA

```

```

    EBX(J)=ODDXX+F5/PEB
    RAX(J)=-ODDXX/2.+F5/(2.*PEA)
35  RBX(J)=-ODDXX/2.+F5/(2.*PEB)

```

```

C
C   EXPLICIT PORTION OF FINITE DIFFERENCE SOLUTION
C

```

```

400  IF (JTURN.EQ.1) GO TO 405
     DO 410 J=2,M
     JMIN=J
     IF (I.EQ.1) GO TO 404
     RBJAY=RBX(J)+2.*RKB*A(I,J)/PEB
     BHALF(J)=(-2.*ABX(J)*B(I,J+1)-2.*BBX(J)*B(I,J-1)-RBX(J)*B(I-1,J)
1-RBJAY*B(I,J))/EBX(J)
     IF (BHALF(J).GT.1.0) GO TO 411
     GO TO 410
404  BHALF(J)=B(I+1,J)
410  CONTINUE
     GO TO 420
411  DO 412 J=JMIN,M
412  BHALF(J)=1.0
     GO TO 420
405  DO 415 J=2,M
     JMIN=J
     IF (I.EQ.1) GO TO 406
     RAJAY=RAX(J)+2.*RKA*B(I,J)/PEA
     AHALF(J)=(-2.*AAX(J)*A(I,J+1)-2.*BAX(J)*A(I,J-1)-RAX(J)*A(I-1,J)
1-RAJAY*A(I,J))/EAX(J)
     IF (AHALF(J).LT.0.0) GO TO 416
     GO TO 415
406  AHALF(J)=A(I+1,J)
415  CONTINUE
     GO TO 440
416  DO 417 J=JMIN,M
417  AHALF(J)=0.0
     GO TO 440

```

```

C
C   SOLUTION OF SIMULTANEOUS EQUATIONS BY INVERSION OF
C   TRIDIAGONAL MATRIX
C

```

```

420  DO 430 J=2,M
     IF (JTURN.EQ.1) BHALF(J)=(B(I,J)+B(I+1,J))/2.
     ODD5A=RKA*BHALF(J)/PEA
     DAJAY=DA(J)+ODD5A
     EAJAY=EA(J)+ODD5A
     TRI(2,J-1)=1.0
     IF (J.EQ.2) GO TO 421
     TRI(1,J-1)=BA(J)/EAJAY
     IF (J.EQ.M) GO TO 422
421  TRI(3,J-1)=AA(J)/EAJAY
422  IF (I.EQ.1.OR.JMOD.EQ.0) GO TO 424

```

```

C
C   DUFORT FRANKEL MODIFICATION
C

```

```

RHS(J-1)=(-AA(J)*A(I,J+1)-BA(J)*A(I,J-1)-DAJAY*A(I,J)-DAA(J)
1*A(I-1,J))/EAJAY
GO TO 423

```

```

C
C USING STANDARD FORM FOR SECOND DERIVATIVE IN RADIAL DIRECTION
424 RHS(J-1)=(-AA(J)*A(I,J+1)-BA(J)*A(I,J-1)-DAJAY*A(I,J))/EAJAY

```

```

C
423 IF (J.EQ.2) RHS(J-1)=RHS(J-1)-BA(J)*A(I+1,J-1)/EAJAY
IF (J.EQ.M) RHS(J-1)=RHS(J-1)-AA(J)*A(I+1,J+1)/EAJAY
430 CONTINUE
MMINUS=M-1

```

```

C
CALL BNDSOL (TRI,RHS,3,1,MMINUS)

```

```

C
DO 433 J=2,M
JMIN=J
A(I+1,J)=RHS(J-1)
IF (A(I+1,J).LT.0.0) GO TO 434

```

```

433 CONTINUE
GO TO 437

```

```

434 DO 436 J=JMIN,M

```

```

436 A(I+1,J)=0.0

```

```

437 IF (JTURN.EQ.1) GO TO 435

```

```

440 DO 445 J=2,M

```

```
IF (J.EQ.2) GO TO 50
```

```
GO TO 55
```

```
50 B(I,1)=RATIO3*B(I,2)-RATIO4*B(I,3)
```

```
B(I+1,1)=RATIO3*B(I+1,2)-RATIO4*B(I+1,3)
```

```
55 IF (JTURN.EQ.0) AHALF(J)=(A(I,J)+A(I+1,J))/2.
```

```
ODD5B=RKB*AHALF(J)/PEB
```

```
DBJAY=DB(J)+ODD5B
```

```
EBJAY=EB(J)+ODD5B
```

```
TRI(2,J-1)=1.0
```

```
IF (J.EQ.2) TRI(2,1)=1.0+(BB(2)*RATIO3)/EBJAY
```

```
IF (J.EQ.2) GO TO 441
```

```
TRI(1,J-1)=BB(J)/EBJAY
```

```
IF (J.EQ.M) GO TO 442
```

```
441 TRI(3,J-1)=AB(J)/EBJAY
```

```
IF (J.EQ.2) TRI(3,1)=(AB(2)-RATIO4*BB(2))/EBJAY
```

```
442 IF (I.EQ.1.OR.JMOD.EQ.0) GO TO 444

```

```

C
C DUFORT FRANKEL MODIFICATION

```

```

RHS(J-1)=(-AB(J)*B(I,J+1)-BB(J)*B(I,J-1)-DBJAY*B(I,J)-DAB(J)*
1B(I-1,J))/EBJAY
GO TO 443

```

```

C
C USING STANDARD FORM FOR SECOND DERIVATIVE IN RADIAL DIRECTION

```

```

444 RHS(J-1)=(-AB(J)*B(I,J+1)-BB(J)*B(I,J-1)-DBJAY*B(I,J))/EBJAY

```

```

443 IF (J.EQ.M) RHS(J-1)=RHS(J-1)-AB(J)*B(I+1,J+1)/EBJAY

```

```

445 CONTINUE

```

```

C      CALL BNDSOL (TRI,RHS,3,1,MMINUS)
C
      DO 446 J=2,M
      JMIN=J
      B(I+1,J)=RHS(J-1)
      IF (B(I+1,J).GT.1.0) GO TO 447
446  CONTINUE
      GO TO 449
447  DO 448 J=JMIN,M
448  B(I+1,J)=1.0
449  B(I+1,1)=RATIO3*B(I+1,2)-RATIO4*B(I+1,3)
      IF (JTURN.EQ.0) GO TO 435
      GO TO 420
C
C      CHECK ON BOUNDARY CONDITION DC/DTHETA=0 AT THEIA=3.1416
C
435  IF (I.GE.2) GO TO 80
      DIFFA=ABS(A(1,2))-ABS(A(2,2))
      DIFFB=ABS(B(1,2))-ABS(B(2,2))
      WRITE (6,1025) A(1,2),A(2,2),B(1,2),B(2,2)
      JJJ=JJJ+1
      IF (DIFFA.LT.EPS.AND.DIFFB.LT.EPS.AND.JJJ.GI.3) GO TO 80
      IF (JJJ.GT.150) GO TO 349
      DO 65 JI=1,M
      IF (A(2,JI).LT.0.0) A(2,JI)=0.0
      IF (B(2,JI).LT.0.0) B(2,JI)=0.0
      IF (B(2,JI).GT.1.0) B(2,JI)=1.0
65  CONTINUE
      DO 70 II=1,N
      DO 70 JL=1,M
      A(II,JL)=(A(1,JL)+A(2,JL))/2.
70  B(II,JL)=(B(1,JL)+B(2,JL))/2.
      GO TO 400
C
C      CALCULATION OF LOCAL SHERWOOD NUMBERS
C
80  GRAD=(A(I,1)-A(I,2))/(RAD(1)-RAD(2))
      JCONV=1
      SH(I)=-2.*GRAD
      ANGLE=THETA(I)*180./3.1416
      WRITE (6,1012) ANGLE,SH(I)
      WRITE(6,1013)
      WRITE(6,1014) (A(I,J),J=1,MM)
      WRITE(6,1015)
      WRITE (6,1014) (B(I,J),J=1,MM)
      IF (I.EQ.1) GO TO 42
      DO 41 J=1,MM
      IF (B(I,J).LT.(-0.05)) GO TO 200
41  CONTINUE
      DUMS=1.2*SH(I-1)
      IF (SH(I).GT.DUMS.OR.SH(I).LT.0.0) GO TO 200
      JJ=JJ+1
42  IF (JTURN.EQ.1) GO TO 43

```

```

      JTURN=1
      GO TO 45
43  JTURN=0
45  CONTINUE

```

```

C
C   CALCULATION OF AVERAGE SHERWOOD NUMBER
C

```

```

200 SUM=0.0
    SH(1)=SH(2)
    DO 300 I=2,ICOUNT
      SUM=SUM-(THETA(I)-THETA(I-1))*(SH(I)*SIN(THETA(I))+SH(I-1)
1    *SIN(THETA(I-1)))/2.

```

```

300 CONTINUE
    SUMX=SUM/2.
    SUM=SUM/(1.+COS(THETA(ICOUNT)))
    WRITE(6,1017) SUM
    WRITE (6,1020) SUMX
    GO TO 350

```

```

349 WRITE (6,1019)

```

```

350 CONTINUE

```

```

1000 FORMAT (3F12.6)

```

```

1001 FORMAT (2F12.4)

```

```

1002 FORMAT (F12.4)

```

```

1003 FORMAT (5I5)

```

```

1004 FORMAT (5F12.4)

```

```

1005 FORMAT (1H-,9HRE NO IS F10.2,10X,5HA1 = F10.4,10X,5HB1 = F10.4)

```

```

1006 FORMAT (1H-,6HSCA = F10.2,10X,6HSCB = F10.2,10X,6HRKA = F15.2,10X,
16HRKB = ,F15.2)

```

```

1007 FORMAT (1H-,6HEPS = F10.6,10X,4HH = F10.3)

```

```

1008 FORMAT (1H-,25HNO OF THETA INCREMENTIS = I5,10X,26HNO OF RADIAL INC
1REMENTS = I5)

```

```

1009 FORMAT (1H-,7HDRAD = F10.6,10X,9HDIHEIA = F10.6)

```

```

1010 FORMAT (1H-,12HPECLET(A) = F10.2,10X,12HPECLET(B) = F10.2)

```

```

1011 FORMAT (5X,2F10.6)

```

```

1012 FORMAT (1H-,9HANGLE IS F10.3,10X,18HSHERWOOD NUMBER = F14.4)

```

```

1013 FORMAT (1H-,33HCONCENTRATIONS OF SUBSIANCE A ARE)

```

```

1014 FORMAT (5X,10F10.6)

```

```

1015 FORMAT (1H-,33HCONCENTRATIONS OF SUBSIANCE B ARE)

```

```

1016 FORMAT (I5)

```

```

1017 FORMAT (1H-,26HAVERAGE SHERWOOD NUMBER = F14.4)

```

```

1019 FORMAT (1H-,54HUNABLE TO OBTAIN ZERO SLOPE AT THETA EQUAL 180 DEGR
1EES)

```

```

1020 FORMAT (1H-,42HAVG SH NO BASED ON TOTAL AREA OF SPHERE = F14.4)

```

```

1025 FORMAT (3X,4F15.7)

```

```

      END

```

```

$ENTRY

```

```

200.0      0.1829      -20.6800

```

```

500.0      800.0

```

```

1000000.0  100000.0

```

```

1.3        0.00005

```

```

0.00001

```

```

60  10  30  1  0

```

```

1

```

```

$IBSYS

```

C VELOCITY PROFILES ** POTENTIAL FLOW

C

```

R3=RAD(J)*RAD(J)*RAD(J)
VT(J)=(1.+1./(2.*R3))*(DUM3+DUM4)/2.
VTEXP(J)=(1.+1./(2.*R3))*(DUM3)
VR(J)=-(-1.+1./R3)*(DUM1+DUM2)/2.
VREXP(J)=-(-1.+1./R3)*(DUM1)

```

C VELOCITY PROFILES ** CIRCULATING GAS BUBBLES

C

```

A2=-1.25-1.75*A1
A3=0.75+0.75*A1
B2=-1.75*B1
B3=0.75*B1
R1=RAD(J)
R2=RAD(J)*R1
R3=RAD(J)*R2
DMM1=(R3-A1-2.*A2/R1-3.*A3/R2)/R3
DMM2=(-B1-2.*B2/R1-3.*B3/R2)/R3
DMM3=(R3+2.*A1+2.*A2/R1+2.*A3/R2)/R3
DMM4=(B1+B2/R1+B3/R2)/R3
VT(J) =DMM1*(DUM3+DUM4)/2.+DMM2*(DUM1*DUM3+DUM2*DUM4)/2.
VTEXP(J)=DMM1*DUM3+DMM2*DUM1*DUM3
DMM5=((2.*(DUM1)**2-(DUM3)**2)+(2.*(DUM2)**2-(DUM4)**2))/2.
VR(J) =DMM3*(DUM1+DUM2)/2.+DMM4*DMM5
VREXP(J)=DMM3*DUM1+DMM4*(2.*DUM1**2-DUM3**2)

```

L. EXPERIMENTAL DATA AND CORRELATIONS

The new data are presented in Table L.1 along with confidence limits on the absorption rates. The latter were determined from the statistical analysis procedure discussed in Section 5.1

Experimental correlations, along with pertinent statistical parameters, are presented in Table L.2.

TABLE L.1

Experimental Data - Absorption of Carbon Dioxide into
Monoethanolamine Solutions
(Leakage Correction was 0.0156 cc/min in all cases)

Conc. of MEA mole %	Rotameter Reading	Absorption Rate cc/min	Corrected Absorption Rate cc/min	Corrected Sherwood Number
0	12 ⁺	0.0579 ± 0.0039*	0.0423	53.8
		0.0479 ± 0.0046	0.0323	41.0
		0.0539 ± 0.0034	0.0383	48.6
		0.0526 ± 0.0039	0.0370	47.0
		0.0522 ± 0.0057	0.0366	46.5
		0.0476 ± 0.0031	0.0320	40.5
	11	0.0656 ± 0.0058	0.0500	63.5
		0.0543 ± 0.0052	0.0387	49.2
		0.0683 ± 0.0060	0.0527	66.9
		0.0682 ± 0.0035	0.0526	66.8
		0.0579 ± 0.0069	0.0423	53.7
		0.0558 ± 0.0041	0.0402	51.0
	22	0.0656 ± 0.0039	0.0500	63.5
	25	0.0634 ± 0.0057	0.0478	60.8
		0.0761 ± 0.0049	0.0605	76.9
		0.0797 ± 0.0031	0.0641	81.0
		0.0641 ± 0.0037	0.0485	61.5
		0.0687 ± 0.0052	0.0531	67.5
	35	0.0837 ± 0.0067	0.0681	86.0
		0.0774 ± 0.0047	0.0618	78.5
		0.0727 ± 0.0034	0.0571	72.5
		0.0779 ± 0.0045	0.0623	79.0
		0.0854 ± 0.0067	0.0698	88.0
	37	0.0841 ± 0.0064	0.0685	87.0

* Confidence limits at 95% level

+ $\frac{1}{2}$ inch rotameter, all others refer to $\frac{3}{4}$ inch rotameter

TABLE L.1 (Continued)

Conc. of MEA mole %	Rotameter Reading	Absorption Rate cc/min.	Corrected Absorption Rate cc/min.	Corrected Sherwood Number
0.33	12 ⁺	0.0954 ± 0.0072	0.0798	101
		0.0900 ± 0.0030	0.0744	94.0
	11	0.0867 ± 0.0063	0.0711 1	90.0
		0.1118 ± 0.0055	0.0962	122
	22	0.1223 ± 0.0067	0.1067	136
25	0.1366 ± 0.0053	0.1210	153	
0.66	12 ⁺	0.1267 ± 0.0031	0.1111	141
		0.1360 ± 0.0074	0.1204	153
	11	0.1494 ± 0.0045	0.1338	169
		0.1443 ± 0.0064	0.1287	163
	25	0.1824 ± 0.0084	0.1668	211
0.1909 ± 0.0054		0.1753	222	
35	0.2117 ± 0.0062	0.1961	249	
	0.2419 ± 0.0117	0.2263	287	
0.99	12 ⁺	0.1376 ± 0.0096	0.1220	158
		0.1403 ± 0.0093	0.1247	154
	11	0.1552 ± 0.0071	0.1396	177
		0.1881 ± 0.0119	0.1725	219
	25	0.2513 ± 0.0077	0.2357	299
0.2457 ± 0.0157		0.2301	292	
35	0.2886 ± 0.0122	0.2730	347	
	0.2807 ± 0.0233	0.2651	337	

* Confidence limits at 95% level

+ ½ inch rotameter, all others refer to 3/4 inch rotameter

TABLE L.2

Experimental Correlations

$$\text{Sh} = A + B \text{Re}^{1/2} \text{Sc}^{1/3}$$

Concentration MEA mole %	A	B
0	23.1 ± 3.3*	0.518 ± 0.12
0.33	25.9 ± 15.2	1.37 ± 0.53
0.66	51.5 ± 15.8	1.90 ± 0.53
0.99	11.7 ± 13.3	3.04 ± 0.45

* Confidence Limits at 95% level

BIBLIOGRAPHY

- A1 Acrivos, A., Taylor, T.D.,
Phys. Fluids, 5, 387 (1962)
- A2 Akehata, T., Johnson, A.I.,
Can. J. Chem. Eng., 43, 262 (1965)
- A3 Aksel'rud, G.A.,
Zh. Fiz. khim., 27, 1445 (1953)
- A4 Ames, W.F.,
"Nonlinear Partial Differential Equations in Engineering"
p.327, Academic Press, New York (1965)
- A5 Astarita, G.,
Chem. Eng. Sci., 16, 202 (1961)
- A6 Astarita, G., Marrucci, G., Gioia, F.,
Chem. Eng. Sci., 19, 95 (1964)
- B1 Baird, M.H.I., Hamielec, A.E.,
Can. J. Chem. Eng., 40, 119 (1962)
- B2 Bird, R.B., Stewart, W.E., Lightfoot, E.N.,
"Transport Phenomena", p.559, John Wiley & Sons, New York (1960)
- B3 Boussinesq, J.,
J. Math. Pures Appl., 11, 285 (1905)
- B4 Bowman, C.W.,
Ph.D. Thesis, University of Toronto (1960)
- B5 Bowman, C.W., Ward, D.M., Johnson, A.I., Trass, O.,
Can. J. Chem. Eng., 39, 9 (1961)
- B6 Boye-Christensen, G., Terjesen, S.G.,
Chem. Eng. Sci., 7, 222 (1958)
- B7 *ibid.*, 9, 225 (1959)
- B8 Breiman, L.,
Norman Bridge Laboratory, Calif. Inst. Tech., Rept. No. 2F-2 (1952)

- B9 Brian, P.L.T. Hurley, J.F., Hasseltine, E.H.,
A.I.Ch.E. Journal, 7, 226 (1961)
- B10 Brian, P.L.T.,
A.I.Ch.E. Journal, 10, 5 (1964)
- B11 Brian, P.L.T., Baddour, R.F., Matiatos, D.C.,
A.I.Ch.E. Journal, 10, 727 (1964)
- B12 Brian, P.L.T., Beaverstock, M.C.,
Chem. Eng. Sci., 20, 47 (1965)
- C1 Calderbank, P.H.,
Trans. Instn. Chem. Engrs., 36, 443 (1958)
- C2 Calderbank, P.H.,
Trans. Instn. Chem. Engrs., 37, 174 (1959)
- C3 Calderbank, P.H., Moo-Young, M.B.,
Chem. Eng. Sci., 16, 39 (1961)
- C4 Calderbank, P.H., Rennie, J.,
Trans. Instn. Chem. Engrs., 40, 3 (1962)
- C5 Calderbank, P.H., Lochiel, A.C.,
Chem. Eng. Sci., 19, 485 (1964)
- C6 Clarke, J.K.A.,
Ind. Eng. Chem. Fundamentals, 3, 239 (1964)
- C7 Collatz, L.,
"The Numerical Treatment of Differential Equations",
p.31, Springer-Verlag, Berlin (1960)
- D1 Danckwerts, P.V.,
Trans. Faraday Soc., 46, 300 (1950)
- D2 *ibid.*, 46, 701 (1950)
- D3 Danckwerts, P.V., Kennedy, A.M.,
Chem. Eng. Sci., 8, 201 (1958)
- D4 Davidson, J.F., Cullen, E.J.,
Trans. Instn. Chem. Engrs., 35, 51 (1957)
- D5 Douglas, J., Jr.,
Trans. Am. Math. Soc., 89, 484 (1958)

- D6 Dodds, W.S., Stutzman, L.F., Sollami, B.J.,
Chem. Eng. Data, 1, 92 (1956)
- D7 Duda, J.L., Vrentas, J.S.,
Ind. Eng. Chem. Fundamentals, 5, 69 (1966)
- E1 Emmert, R.E., Pigford, R.L.,
A.I.Ch.E. Journal, 8, 171 (1962)
- E2 Emmert, R.E.,
Ph.D. Thesis, University of Delaware (1954)
- F1 Fox, L., Ed.,
"The Numerical Solution of Ordinary and Partial Differential
Equations," p.237, Pergamon Press, London (1962)
- F2 Friedlander, S.K.,
A.I.Ch.E. Journal, 3, 43 (1957)
- F3 Friedlander, S.K.,
A.I.Ch.E. Journal, 7, 347 (1961)
- F4 Frossling, N.,
Gerlands Beitr. Geophys., 52, 170 (1938)
- F5 Frossling, N.,
Lunds Univ. Arsskr. N.F. AVD., 36, #4 (1940)
- G1 Gal-Or, B., Resnick, W.,
Chem. Eng. Sci., 19, 653 (1964)
- G2 Gal-Or, B., Resnick, W.,
Ind. Eng. Chem. Proc. Des. Devel., 5, 15 (1966)
- G3 Gal-Or, B., Hoelscher, H.E.
A.I.Ch.E. Journal, 12, 499 (1966)
- G4 Garner, F.H., Grafton, R.W.,
Proc. Roy. Soc., A224, 64 (1954)
- G5 Garner, F.H., Suckling, R.D.
A.I.Ch.E. Journal, 4, 114 (1958)
- G6 Garner, F.H., Keey, R.B.,
Chem. Eng. Sci., 9, 119 (1958)
- G7 Goodridge, F., Robb, I.D.,
Ind. Eng. Chem. Fundamentals, 4, 49 (1965)

- G8 Grafton, R.W.,
Chem. Eng. Sci., 18, 457 (1963)
- G9 Griffith, R.M.,
Chem. Eng. Sci., 12, 198 (1960)
- H1 Hadamard, J.,
Compt. Rend., 152, 1735 (1911)
- H2 Hamielec, A.E., Johnson, A.I.,
Can. J. Chem. Eng., 40, 41 (1962)
- H3 Hamielec, A.E., Storey, S.H., Whitehead, J.M.,
Can. J. Chem. Eng., 41, 246 (1963)
- H4 Hamielec, A.E., Johnson, A.I., Houghton, W.T.,
A.I.Ch.E. Journal, to be published
- H5 Hamielec, A.E., Hoffman, T.W., Ross, L.L.,
A.I.Ch.E. Journal, to be published
- H6 Harriot, P.,
Can. J. Chem. Eng., 40, 60 (1962)
- H7 Higbie, R.,
Trans. Am. Inst. Chem. Eng., 31, 365 (1935)
- H8 Hikita, H., Asai, S.,
Int. Chem. Eng., 4, 332 (1964)
- I1 Ibrahim, S.H.I., Kuloor, N.T.,
Chem. Eng. Sci., 17, 1087 (1962)
- J1 Jensen, M.B., Jorgensen, E., Faurholt, C.,
Acta Chem. Scand., 8, 1137 (1954).
- J2 Jenson, V.G.,
Proc. Roy. Soc., A249, 346 (1959)
- J3 Johnson, A.I., Akehata, T.,
Can. J. Chem. Eng., 43, 10 (1965)
- J4 Johnson, A.I., Hamielec, A.E., Houghton, W.T.
A.I.Ch.E. Journal, to be published

- K1 Kawaguti, M.,
Rept. Inst. Sci., Tokyo, 2 (5/6), 66 (1948)
- K2 Keey, R.B., Glen, J.B.,
Can. J. Chem. Eng., 42, 227 (1964)
- K3 Kramers, H.,
Physica's Grav., 12, 61 (1946)
- K4 Kronig, R., Bruijsten, J.,
Appl. Sci. Res. Sect. A, 2, 439 (1951)
- K5 Knudsen, J.G., Katz, D.L.,
"Fluid Dynamics and Heat Transfer", p.228, McGraw-Hill,
New York (1958)
- L1 Lapidus, L.,
"Digital Computation for Chemical Engineers", pp. 158-166,
McGraw-Hill, New York (1962).
- L2 *ibid.*, p.164
- L3 Lee, K., Barrow, H.,
Int. J. Heat Mass Transfer, 8, 403 (1965)
- L4 Levich, V.G.,
Dokl. Akad. Nauk, 78, 1105 (1951)
- L5 Levich, V.G.,
"Physicochemical Hydrodynamics",
Prentice-Hall, Inc. (1962)
- L6 Lewis, J.B.,
Trans. Instn. Chem. Engrs., 31, 323 (1953)
- L7 Linton, M., Sutherland, K.L.,
Chem. Eng. Sci., 12, 214 (1960)
- M1 Marangozis, J.,
Ph.D. Thesis, University of Toronto (1960)
- N1 Nijssing, R.A.T.O., Hendriksz, R.H., Kramers, H.,
Chem. Eng. Sci., 10, 88 (1959)
- N2 Nunge, R.J., Gill, W.N.,
A.I.Ch.E. Journal, 4, 469 (1963)

- O1 Orell, A., Westwater, J.W.,
A.I.Ch.E. Journal, 5, 514 (1959)
- P1 Pang, Kwok-Hing,
M.Eng. Thesis, McMaster University (1965)
- P2 Pearson, J.R.A.,
Appl. Sci. Res. Sect. A, 11, 321 (1963)
- P3 Perry, R.H., Pigford, R.L.,
Ind. Eng. Chem., 45, 1247 (1953)
- P4 Plevan, R.E., Quinn, J.A.,
Presented at 58th Annual Meeting of the A.I.Ch.E.,
Philadelphia (1965)
- R1 Ranz, W.E., Marshall, W.R., Jr.,
Chem. Eng. Progr., 48, 141, 173 (1952)
- R2 Roberts, D., Danckwerts, P.V.,
Chem. Eng. Sci., 17, 961 (1962)
- R3 Ross, L.L.,
Ph.D. Thesis, McMaster University (1966)
- R4 Rowe, P.N., Claxton, K.T., Lewis, J.B.,
Trans. Inst. Chem. Engrs., 43, T 14 (1965)
- R5 Ruckenstein, E.,
Chem. Eng. Sci., 19, 131 (1964)
- R6 *ibid.*, p.505
- R7 Ruckenstein, E., Berbente, C.,
Chem. Eng. Sci., 19, 329 (1964)
- R8 Rybczynski, W.,
Bull. Acad. Sci. Cracow, A:40 (1911)
- S1 Seto, P.,
M. Eng. Thesis, McMaster University (1963)
- S2 Sharma, M.M., Danckwerts, P.V.,
Chem. Eng. Sci., 18, 729 (1963)
- S3 Sherwood, T.K., Pigford, R.L.,
"Absorption and Extraction", pp. 332-337, 2nd Edition, McGraw-Hill, New York (1952)

- S4 Sherwood, T.K., Wei, J.C.,
Ind. Eng. Chem., 49, 1030 (1957)
- S5 Sibulkin, M.,
J. Aero. Sci., 19, 570 (1952)
- S6 Sideman, S.,
Ind. Eng. Chem., 58, 54 (1966)
- S7 Steinberger, R.L., Treybal, R.E.,
A.I.Ch.E. Journal, 6, 227 (1960)
- S8 Sternling, C.V., Scriven, L.E.,
A.I.Ch.E. Journal, 5, 514 (1959)
- S9 Stokes, G.G.,
Trans. Camb. Phil. Soc., 9, part 2:51 (1851)
- T1 Torobin, L.B., Gauvin, W.H.,
Can. J. Chem. Eng., 37, 129 (1959)
- T2 Thomas, W.J., Furzer, J.A.,
Chem. Eng. Sci., 17, 115 (1962)
- T3 Tsubouchi, T., Masuda, H.,
Rept. Inst. High Sp. Mech., Japan, 16, 119 (1964/1965)
- V1 Vassilatos, G., Trass, O., Johnson, A.I.,
Can. J. Chem. Eng., 40, 210 (1962)
- V2 Vliet, G.C., Leppert, G.,
Trans. A.S.M.E., Series C, 83, 163 (1961)
- V3 Volk, W.,
"Applied Statistics for Engineers", pp. 246-252,
McGraw-Hill, New York (1958)
- V4 *ibid.*, pp 115-117
- W1 Ward, D.M. Trass, O., Johnson, A.I.,
Can. J. Chem. Eng., 40, 164 (1962)
- W2 Ward, W.J., Quinn, J.A.,
A.I.Ch.E. Journal, 10, 155 (1964)
- W3 Wellek, R.M.,
Ph.D. Thesis, Illinois Institute of Technology (1963)

- W4 Westerterp, K.R., von Dierondonck, L.L., de Kraa, J.A.,
Chem. Eng. Sci., 18, 157 (1963)
- W5 Wilke, C.R., Prausnitz, J.M., Acrivos, A.,
Ind. Eng. Chem., 52, 441 (1960)
- Y1 Yau, A.Y.,
M.Eng. Thesis, McMaster University (1966)
- Y2 Yuge, T.,
Rept. Inst. High Sp. Mech., Tokoku University,
57, 143 (1956).
- Y3 Yuge, T.,
Trans. A.S.M.E., Series C, 82, 214 (1960)